Dissertations   Theses and Dissertations

1992

The Physiology and Morphology of Canine Intracardiac Ganglion Cells

Xiaohe Xi
Loyola University Chicago

Recommended Citation

THE PHYSIOLOGY AND MORPHOLOGY OF

CANINE INTRACARDIAC GANGLION CELLS

BY

Xiaohe Xi, M.D.

A Dissertation Submitted to

the Faculty of the Graduate School

of Loyola University of Chicago in Partial Fulfillment

of the Requirements for the Degree of

Doctor of Philosophy

January

1992

謹以此書

獻給

敬愛的父親

您对我永恒的关爱

激励我不断求索

女兒：小和

ACKNOWLEDGEMENTS

I would like to express my most sincere appreciation to my advisor, Dr. Robert Wurster, for his continuous help, extraordinary encouragement and selfless time and effort. His invaluable guidance and instruction were primarily responsible for my development as a physiologist.

I would also like to thank my committee members, Drs. Walter Randall, Nae Dun, John Thomas and Zeljko Bosnjak, for their ceaseless interest, excellent technical suggestions and valuable criticism of manuscripts; and thank Drs. David Euler, Kurt Jacobs, John Thomas, Christopher Joyce and John McNulty, for their kindly experimental cooperation and for providing facilities for part of this work.

In particular, I wish to acknowledge Marge Duff and Maria Weber for their skilfull technical assistance in my experiments, posters and photography and, most of all, for their deep friendship.

I am grateful to the entire faculty, graduate students and all the other members in the Department of Physiology, who have provided a stimulating and friendly atmosphere and helped me in many ways.

Enormous thanks are extended to all my teachers, colleagues and friends in China for their help, friendship and concern during these years.

Finally, my deepest appreciation goes to my mother for her sustained love and encouragement, and to my sister and brother-in-law for their understanding and never-failing support.

VITA

The author Xiaohe Xi is the daughter of Si-jing Chen and Shu-min Xi. She was born on October 16, 1954 in Hebei province, People's Republic of China (P.R.C.).

She graduated from Shi-Yi High School in Beijing, P.R.C. in 1970. In September, 1973, she enrolled in the First P.L.A. Medical University in Guangzhou, P.R.C.. In March of 1977, she received her Doctor of Medicine degree. From April 1977 to July 1980, Dr. Xi worked as a resident in Nan Fang Hospital in Guangzhou and completed her clinical practice in Internal Medicine.

In September 1980, Dr. Xi entered the graduate program in the Guangdong Provincial Cardiovascular Institute and received her Master of Science degree in Cardiology at the end of March 1984. From April 1984 to January 1986, she worked as a clinical doctor and completed her clinical practice in Cardiology in Guangdong Provincial People's Hospital.

In February 1986, Dr. Xi came to the United States and worked as a visiting scientist in the Division of Echocardiography, Department of Cardiology, Northwestern Memorial Hospital in Chicago, Illinois. In January 1987, she enrolled in the graduate program in the Department of Physiology at Loyola University Stritch School of Medicine. Her dissertation work was completed under the direction of Dr. Robert D. Wurster. Dr. Xi is a member of the Society for Neuroscience.

PUBLICATIONS AND ABSTRACTS

1. Duan, C-H., F. Zhao, L. Zhang, and X. Xi. Measuring of mechanocardiography in normal subjects and patients with coronary artery disease. Medical Journal of P.L.A. 6:68-71, 1981.

2. Xi, X., and J-Z. Feng. Diagnostic value of ambulatory electrocardiography in coronary artery disease. Guangdong Medical Journal 4:32-34, 1983.

3. Xi, X., and J-Z. Feng. The use of cardiac catheterization and angiocardiography for the measurement of left ventricular function. Guangdong Provincial People's Hospital Compilation p230-238, 1983.

4. Feng, J-Z., G. Ou, X. Xi, and T. Yin. Analyzing the efficacy of Captopril in 21 patients with moderate or severe hypertension. Guangdong Medical Journal 5:22-24, 1984.

5. Xi, X., and J-Z. Feng. Angiographic ejection fraction for predicting the prognosis of valve replacement. Chinese Journal of Internal Medicine 24:409-411, 1985.

6. Xi, X., J-Z. Feng, X. Xie, and C. Jin. Left ventricular functional indexes for predicting the prognosis of valve replacement --- A study by M-mode UCG. Chinese Journal of Physical Medicine 7:211-213, 1985.

7. Xi, X., and J-Z. Feng. Valve replacement and left ventricular function. Translations in Cardiology 6:32-35, 1985.

8. Xi, X., and J-Z. Feng. Left ventricular functional measurements predict the prognosis of valve replacement in patients with aortic and/or mitral valve insufficiency --- A study by cineangiography. Chinese Journal of Cardiovascular Disease 14:277-279, 1986.

9. Xi, X., and W. Zhang. The progress of echocardiography. Journal of Clinical Medicine 3:145-148, 1987.

10. Xi, X., J. X. Thomas,Jr, W. C. Randall, and R. D. Wurster. Intracellular recordings from canine intracardiac ganglion cells. Journal of Autonomic Nervous System 32:177-182, 1991.

11. Xi, X., Randall, W. C., Wurster, R.D. Intracellular recording of spontaneous activity of *in situ* canine intracardiac ganglion cells. Neuroscience Letter, 1991. (in press)

12. Xi, X., Randall, W.C., Wurster, R.D. Electrophysiological properties of canine intracardiac ganglion cells. Brain Research, 1991. (submitted)

13. Xi, X., Randall, W.C., Wurster, R. D. Morphology of canine intracardiac ganglion cells. Journal of Comparative Neurology, 1991. (submitted)

14. Xi, X., Randall, W. C., Wurster, R. D. The presence, effects and possible mechanisms of CGRP on canine intracardiac ganglia; in vivo and in vitro studies. American Journal of Physiology, 1991. (in preparation)

15. Xi, X., M. J. Duff, M. Webber, R. R. Fiscus, J. X. Thomas, M. F. O'Toole, W. C. Randall, and R. D. Wurster. *In vivo* effects of CGRP on intracardiac vagal ganglia. FASEB Journal 3:A413, 1989.

16. Wurster, R. D., X. Xi, J. X. Thomas, and W. C. Randall. Electrical properties of mammalian intracardiac ganglion cells. FASEB Journal 4:A707, 1990.

17. Xi, X., J. X.Thomas, R. D. Wurster, and W. C. Randall. *In vivo* cardiac inotropic effects of CGRP are dependent on vagal afferents. FASEB Journal 4:A957, 1990.

18. Wurster, R.D., X. Xi, and W. C. Randall. Morphological organization of ganglion cells and small intensely fluorescent (SIF) cells of the canine intracardiac ganglia. Society for Neuroscience Abstracts 16:860, 1990.

19. Xi, X., W. C. Randall, and R. D. Wurster. Excitatory and inhibitory synaptic transmissions on canine intracardiac ganglion cells. Society for Neuroscience Abstracts 16:675, 1990.

20. Mostafa, M.H., X. Xi, R. D. Wurster, F. LaVelle, and E. F. Neafsey. Light and electron microscopic study of neurons in cardiac ganglia of the rat and dog. Society for Neuroscience Abstracts 16:860, 1990.

21. Xi, X., Randall, W. C., Wurster, R. D. Intracellular recording of spontaneous activity of *in situ* canine intracardiac ganglion cells. FASEB Journal 5:A1493, 1991.

22. Xi, X., Randall, W. C., Wurster, R. D. Slow excitatory and inhibitory synaptic potentials and their differential muscarinic mechanisms in canine intracardiac ganglia. submitted to International Symposium: The physiology, pharmacology and biophysics of ganglionic transmission, 1991.

TABLE OF CONTENTS

LIST OF TABLES

LIST OF ILLUSTRATIONS

CHAPTER I

INTRODUCTION

Vagal control of the automaticity, conductivity and contractility has long been recognized as an very important mechanism for the regulation of cardiac function. Generally, the vagal cardiac efferent limb is composed of preganglionic neurons located in the central nervous system and postganglionic neurons located in the intracardiac ganglia. Hence, intracardiac ganglia are the essential pathway through which vagal efferent signals modulate cardiac function. However, up to date, most of our understanding of the intracardiac ganglia is from amphibian. In the canine heart, Randall and coworkers have recently provided the precise and reproducible locations of the intracardiac ganglia which innervate different cardiac tissue (see Chapter II). Studies indicated that the negative chronotropic effect of vagal stimulation was abolished by blocking the ganglionic plexus situated in the pulmonary vein fat pad (PVFP) of right atrium. The SA node in canine heart is directly innervated by the neurons located in PVFP region.

Based on the above results, a new tissue preparation of canine intracardiac ganglia innervating SA node was developed in this dissertation. This *in vitro* preparation contains ganglia with intact capsule and interganglionic nerves, which are suitable for the consequent, intracellular studies.

The first study in this dissertation proposed to examine the morphological

characteristics of the neurons in the PVFP region. Conventional microelectrode techniques were employed for intracellular horseradish peroxidase (HRP) iontophoresis. Following the development of HRP reaction products, the structural features of the neurons were observed using microscopy. Glyoxylic acid fluorescent staining was also used to examine the presence of the small intensely fluorescent (SIF) cells. The organization of different types of neurons in the ganglion were analyzed and discussed.

The second study determined the membrane electrophysiological properties of individual ganglion cells. Standard intracellular stimulation and recording techniques were applied. The passive and active membrane properties were characterized and analyzed. Attention was particularly paid to testing the hypothesis that the ganglion contains heterogenous cell types; different cell types are distinguished not only by their membrane properties but also by their morphological features.

Many of the characteristics of ganglionic transmission in the canine intracardiac ganglia were investigated in the last study. First, the types and possible mechanisms of the spontaneous neuronal activity were elucidated. Second, the fast synaptic potential including the responsible receptor and ions was analyzed. Third, the presence and mechanisms of the slow synaptic potentials were examined. A suction electrode was used to stimulate the interganglionic nerve. The excitatory slow synaptic potential was analyzed electrophysiologically and pharmacologically to determine ionic mechanisms and the receptor subtype.

Unlike the sympathetic ganglia which have been well studied as a prototype for autonomic ganglionic activities, the electrophysiology and morphology of parasympathetic

ganglia have been less studied, in part, because the parasympathetic ganglia are usually located within the walls of the organ they innervate. It is hoped that the work presented in this dissertation will enrich our understanding of vagal cardiac control as well as the functions of the parasympathetic division of the autonomic nervous system.

CHAPTER II

GENERAL LITERATURE REVIEW

A.   PARASYMPATHETIC INNERVATION OF THE SINOATRIAL (SA) NODAL

REGION IN CANINE HEART

The function of the vagus nerves in the control of the heart, especially heart rate,

has been recognized for more than three centuries [80].   Acetylcholine (ACh), as a marker

of the density of parasympathetic innervation in cardiac tissue, has been found in the

greatest concentration in the SA node [14,27].   The SA node is more responsive to

parasympathetic regulation than the atrio-ventricular (AV) node which is preferentially

sensitive to sympathetic regulation [117,170,186]. Undoubtedly, vagal innervation of SA node

plays one of the most significant roles in vagal control of cardiac function.

1. Preganglionic Vagal Pathway

Preganglionic cardiac vagal motor neurons are mainly located in the medullary

regions of the nucleus ambiguous and the dorsal motor nucleus in the dog [71,192].   The

somata innervating different intracardiac ganglia in canine heart are indistinguishably

distributed in these medullary areas [157].   After exiting from the skull, the axons course

caudally in the neck to form the vagosympathetic trunk.   Then these efferent vagal fibers

form the cardiac neural plexus with sympathetic nerves in the thorax [117].

Although the anatomical descriptions of paracardiac and cardiac autonomic nerve

pathways in the dog have been published by Mizeres [137,138] in 1950's and Cooper et al.[35]

in 1960's, the precise intrapericardial distribution of preganglionic parasympathetic nerves remained obscure until about twenty years ago. A detailed description of the differential intrapericardial pathway of individual preganglionic parasympathetic nerves from thoracic cardiac neural plexus to SA and atrio-ventricular (AV) node and the exact sites of projection of these nerves onto the heart was provided by Randall and coworkers in 1973 [66]. These investigators stimulated individual cardiac nerves before and after surgical ablation of their pathways as they enter the atrium while observing the functional responses to the stimulation.   They reported that parasympathetic preganglionic innervation to the SA nodal region courses along the superior vena cava, superior left atrium and interatrial groove; parasympathetic preganglionic fibers to the AV nodal region course along the superior left atrium and at the junction of left atrium with the inferior vena cava. These observations have been confirmed by a number of subsequent studies [167,168,170].

2. Intracardiac Ganglia and the Postganglionic Pathway

Similar to other parasympathetic ganglia, the synapses between pre- and postganglionic vagal cardiac neurons occur in the intracardiac ganglia. Early histological studies have revealed that intracardiac ganglia of mammals and man were situated in the superior vena cava near its opening, along the interatrial groove and the septum, and along the coronary sinus [56,100,127,148]. Considerable species differences in the general location of intracardiac ganglia were noted [100].

The presence of intracardiac ganglia was further confirmed functionally by Priola and colleagues [159,161,162]. In their chronically denervated canine heart, both ACh and

nicotine elicited negative chronotropic and inotropic responses. The effects of nicotine were diminished by ganglionic blockers d-tubocurarine and low concentration tetrodotoxin. The actions of ACh were not affacted by the two agents. These experiments suggested that nicotine inhibited cardiac tissue indirectly through intrinsic nervous system which survive the vagal and sympathetic denervation in canine heart.

The exact location and differential postganglionic innervation of canine intracardiac ganglia were first systematically demonstrated by Randall and coworkers [55,59,157,167,169-172]. Canine intracardiac neurons with small myelinated and unmyelinated nerve fibers were histologically identified in several epicardial fat pads [160,169]. The anatomical feature of the fat pad will be described in more detail in Chapters IV and V. Surgical excision or chemical (phenol) destruction or nicotinic cholinergic blocking (hexamethonium) of the fat pad overlying the right pulmonary vein fat pad (PVFP) specifically interrupts vagally induced asystole or bradycardia, but does not affect vagal influences to AV conduction [59,171,172]. Similarly, vagal AV nodal control can be affected by interference with conduction through a fat pad located at the junction of the inferior vena cava and inferior left atrium (IVC-ILA), approximating the entry of the coronary sinus into the inferior, posterior interatrial septum [59,169,172]. However, blockade of conduction in this latter region did not alter vagal control of the SA nodal region. In addition, this latter region has also been associated with vagal control of contractility [167]. Therefore, both histological and functional observations suggest that different vagal ganglia selectively innervate SA node or AV node region in the canine heart.

As studied above, the ganglia located in the PVFP serve as synaptic stations mediating vagal control of SA nodal function in the dog. A more conventional view was that vagal regulation of SA node function is mediated via ganglia located on the posterior superior vena cava and posterior right atrium [17,89,100]. However, these conventional observations are not supported by studies of Furukawa and Levy [63] and Lazzara et al.[114]. Recently, the postganglionic pathway of vagal innervation of the canine SA node has also been verified [15]. Systematic stimulation of the epicardial region between the PVFP and the SA node evoked decrease in SA nodal rate, which was not blocked by hexamethonium. Authors suggested that the primary vagal postganglionic pathway to the SA node region is subepicardial and adjacent to the SA nodal artery along the sulcus terminalis.

3. Postganglionic Terminal Distribution in SA Nodal Region

Cardiac vagal activation can dramatically alter the pacemaker activity within the same cardiac cycle [87,88,117]. Hence, the time course required for transduction of the electrical signal from the nerve terminal to acetylcholine release, diffusion, activation of muscarinic receptors in the active pacemaker cells, and their subsequent effector response is incredibly short. It would appear essential that the pacemaker cells be richly supplied with cholinergic terminals [166]. The rich vagal innervation of the SA node area has been reported in different species [14,15,18,27,100,117,152]. Relatively little is known about the vagal neuromyal junction or the precise distribution of parasympathetic terminals around the effector cardiac cells [166]. Roberts et al.[175] described a complex pattern of nerves and fine nerve processes in the rabbit SA node region by combined techniques of microelectrode

recording of pacemaker cells and cholinesterase staining of nervous tissue. They found two or three nerve bundles traversing the SA node parallel to the crista terminalis. The distribution of the fine nerves in the central SA node was non-uniform. The sites of initial depolarization were usually constituted with a cluster of SA node cells enclosed in a nest of fine nerves. On the other hand, the sites of latent pacemaker potentials were located in some cell clusters in the peripheral area of SA node, which were distinguished by the absence of fine nerve processes. It is not clear yet whether the latter areas become sites of beat initiation during vagal stimulation-induced pacemaker shifts [23,87,88,117].

4. Muscarinic Regulation of SA Nodal Automaticity

In mammalian heart, acetylcholine (ACh) is known to be a potent neurotransmitter that causes slowing of the heart rate. The inhibitory effects of ACh on automaticity is mainly mediated by activation of muscarinic receptors in nodal pacemaker cells, which results in shortening of the action potential and membrane hyperpolarization [11,83]. It has been conclusively demonstrated that the action of ACh on nodal pacemaker cells is due to an increased potassium conductance [23,67,124]. Stimulation of muscarinic receptors could activate a membrane bound G_K-protein [57,181] that may be directly coupled to the ACh activated potassium channels (I_{K-ACh}), without involving adenylate cyclase and cAMP [30,125,155,180,197]. Some studies have shown that the I_{K-ACh} is a time and voltage dependent current [144,149] and the G_K-protein is pertussis toxin sensitive [16,57,155,181].

Stimulation of muscarinic receptors is also known to reduce a calcium current (I_{Ca}) in atrial cells under basal conditions, i.e. myocytes have not been previously stimulated with catecholamines [83,183]. This action is mediated via the receptor-activated and pertussis

toxin sensitive G_i-protein [12]. Experiments were designed to test whether cytosolic cAMP

is the mediator of the effect [78,98]. Under the condition that the I_{Ca} was increased and

saturated, ACh no longer depressed I_{Ca}, that is, the inhibitory effects of ACh were

completely prevented when cytosolic cAMP was buffered [12]. It has been suggested that,

in contrast to I_{K-ACh}, a decreased cytosolic adenylate cyclase and consequently a decreased

cAMP is related to the ACh reduction of I_{Ca} [6,78,98]. Furthermore, ACh has been shown

to inhibit the pacemaker current (I_f) in nodal cells by shifting its activation voltage to

more negative levels [42-44]. As well, the decreased cAMP level is involved in this

effect [78,98].

In general, the regulatory effects of ACh on cardiac myocytes can be classified

into two categories, namely cAMP-independent and cAMP-dependent effects [12]. Both

mechanisms of action are operative in nodal cells. Therefore, if the amount of ACh

released by parasympathetic nerve endings is sufficient to activate the muscarinic

receptors, it could potentially regulate pacemaker activity and other cardiac activities [12].

In addition to the postsynaptic actions, ACh has also been reported to act presynaptically

to inhibit the release of norepinephrine from the sympathetic nerve terminals [116,117].

Hence, ACh could inhibit SA nodal automaticity directly via alteration of I_{K-ACh}, I_{Ca} and

I_f and /or indirectly via reduction of sympathetic activity.

B.   STRUCTURE AND FUNCTION OF AUTONOMIC GANGLIA

Although the term "ganglia" began to be used in the 18th century [133] on the basis

of earlier studies, the morphological insight into the ganglia was first generated by the

work of Gaskell [65] and Langley (1852 - 1925) [111,112]. Their description of the autonomic nervous system and the following investigations of the pertinent neurotransmitter mechanisms have generated the essential understanding of the morphological and functional aspects of the autonomic system [95].

1. Sympathetic Ganglia

Sympathetic ganglion cells are situated in three locations throughout the body: paravertebral, prevertebral, and previsceral. The present concept of the structure and function of sympathetic ganglia is derived in large measure from studies on the superior cervical sympathetic ganglion (SCG). Its large size and accessibility and the similarity between chain ganglia make it a suitable model for morphological study. The histological, immunohistochemical and electrophysiological studies have revealed a variety of components in SCG. The main cell types of the SCG are principal neurons, SIF cells, vascular cells, fibroblasts, mast cells and glial cells (either satellite cell, wrapping up nerve cell bodies, or Schwann cells, associated with myelinated and nonmyelinated axons) [115]. All cells are enclosed by a capsule which consists of several layers of fibroblasts and dense collagen bundles [190].

a. Principal ganglion cells

Sympathetic principal cells are multipolar neurons with a complex array of processes and a wide range of soma sizes [39]. The cell body and its processes are enclosed by satellite cells. The Schwann cell investment is deficient at the sites of incoming synapses and is absent sporadically along dendrites [37]. In the SCG of the guinea pig, each neurons has an average of 13 multibranched dendrites [39]. Intracellular

labelling with horseradish peroxidase (HRP) reveals a variety of dendritic patterns of sympathetic neurons. Some dendrites are found to enclose the adjacent neurons or to run parallel to the surrounding nerve fibers. Purves and Hume [164] demonstrated that the number of different preganglionic axons converging on the postganglionic neurons is positively correlated with the number of dendrites. Hence, cells with more dendrites receive more preganglionic synapses.

Conflicting views have been expressed about the presence of recurrent axon collaterals [37]. An early silver impregnation study [39] and an intracellular dye injection study [130] showed a single unbranched axon for each ganglion cell. On the other hand, Norberg et al.[145,146] and Jacobowitz and Woodward [85] found varicose fibers in sympathetic ganglia by catecholamine histofluorescent techniques, which resemble the terminal ramifications of axons in sympathetic innervated tissues. They suggested the existence of not only the small intensely fluorescent (SIF) cell processes and dendritic branchings but also axon collaterals of ganglion cells in the varicose fiber networks. In a recent electrophysiological study, Prigioni and Russo [158] reported that some of the neurons in the caudal part of the SCG of the rat could be antidromically activated following stimulation of both of the cervical sympathetic trunk and the external carotid nerve. They indicated that these axons divided into collaterals which project not only to the preganglionic trunk but also to a postganglionic nerve. Apparently, further evidence is needed to resolve this controversy.

Although unlike the central nervous system in which subpopulation of neurons are well organized in different levels, the sympathetic ganglia could be roughly subdivided

into regions of neurons that project to specific targets. Both catecholamine histofluorescence [85] and electrophysiological studies [163] have shown that in SCG neurons were located at the pole of the ganglion near the origin of the efferent nerve. These studies also suggest that there are territories within sympathetic ganglia in which neurons to a specific organ may be found [37,122]. For example, in the SCG of the guinea pig, neurons that innervate the iris are predominantly located in the rostral part of the ganglion, while neurons which innervate the pinna are largely found in the caudal pole [122]. Hence, the organization of the sympathetic ganglion provides further insights on the heterogeneity of autonomic neurons.

b. SIF cells

In addition to principal cells, autonomic ganglia are noted to contain groups of small cells (SIF cells). These SIF cells were first mentioned and named by Eränkó and Harkónen [58] and Norberg et al. [145,146], respectively, in 1960's. To date, all sympathetic ganglia studied have a variable number of SIF cells.

Because these cells contained monoamines, they emitted considerable fluorescence when catecholamine histofluorescence techniques were utilized. Hence, they were called small intensely fluorescent cells or SIF cells. These cells were also called small granule-containing cells [129] when revealed with the electron microscope, or chromaffin cells if the chromate reaction was studied [70,178].

The SIF cells appeared as oval, spherical or elongated cell bodies with a central nucleus [194]. The size of SIF cells is in all case small compared to principal neurons. The mean diameter varied from 6 to 25 μm according to the species and ganglion

preparations [182]. In most species studied it is possible to distinguish, on the basis of morphological characteristics of the fluorescence method, two categories of SIF cells in the SCG [195]. One kind of SIF cell has processes [145] which are usually 30 - 40 μm, or occasionally longer than several hundred μm [84,182] in length. These cells are believed to be functional interneurons [193,195]. Another kind of SIF cell has no process [30] and is suggested to be a paraneuron [193,195].

Although some SIF cells are solitary, many SIF cells are found in clusters. The cluster of SIF cell range from a few to more than several dozen cells per section depending on species. In the majority of the species studied, namely cow, cat, monkey and rabbit, SIF cells are rather sparse - in the order of 2 to 7 cells per mg of tissue. However, in the rat SCG is significantly rich in SIF cells with 280 cells per mg of tissue [193]. These observations may suggest different mechanisms for intraganglionic modulation of ganglion transmission among different species [193].

In electron micrographs, the most conspicuous feature of the SIF cells is the large number of dense-cored (or granular) vesicles in the cell body. The dense-cored vesicles may vary significantly in size, shape and electron density according to species, fixation and different physiological states [182]. In the rat SCG, these vesicles were found to contain different chemical compounds, namely serotonin [187], dopamine [13], noradrenaline and adrenaline [36]. Processes also contained the same organelles as the cell body but in different proportions [182].

Demonstration of efferent and afferent synapses provided morphological evidence that the SIF cells may be adrenergic interneurons in the sympathetic ganglia. Yokota [198]

made a three-dimensional analysis of a cluster of four SIF cells in rat SCG. All four cells received afferent synapses and two of them made efferent somatodendritic synapses with postganglionic neurons. SIF cell efferent terminals synapse with dendrites; dendritic spines of the postganglionic neurons have also been observed in rabbit and monkey SCG [29,92]. Generally, the electron microscopic evidence that there are monoaminergic interneurons in the rat SCG has now become well accepted [193].

As described previously, one kind of SIF cell which has no processes is suggested not to be an interneuron but rather a paraneuron. Paraneurons are cells of neuroectodermal origin, produce peptide hormones and /or substances related to or identical with a monoamine transmitter, and form neurosecretory-like granules which are released in response to membrane depolarization [61]. The paraneuron kind of SIF cell presumably releases its transmitter into the capillaries which then transport the transmitters to ganglionic neurons. The vascular path (portal system) for the transportation of the SIF cell transmitters to principal cells has been observed [79]. The SIF cells often lack a Schwann cell sheath where they approach the basal membrane of blood capillary endothelium, an arrangement that could facilitate the transportation of monoamines into the blood vessel [193].

The electrophysiological role of the SIF cells on monoaminergic transmission in the SCG has been reviewed by Libet [120]. Release of a non-cholinergic transmitter is required to elicit the slow inhibitory postsynaptic potential (s-IPSP) response in principal neurons of the rabbit ganglia. Libet et al. found that muscarinic agonist elicit an initial s-IPSP followed by a slow excitatory postsynaptic potential (s-EPSP). When they

blocked presynaptic release of transmitters by lowering the Ca^{2+}/Mg^{2+} ratio, the s-IPSP was no longer evoked by muscarinic agonist. Therefore, the s-IPSP was elicited by muscarinic agonist via an interneuron which releases the neurotransmitter directly responsible for the s-IPSP. The neurotransmitter for s-IPSP in rabbit SCG is dopamine [121] presumably from the vesicles of SIF cells [193].

Taken together, SIF cells are groups of small, monoaminergic cells which act as interneurons or paraneurons in the autonomic ganglia. Their functional role is not quite clear presently. Some evidence suggested that SIF cells are responsible for the slow inhibitory transmission in the sympathetic ganglia.

c. Interneurons

In addition to the extensively studied monoaminergic interneurons (SIF cells) in sympathetic ganglia, less information is available about another possible type of interneuron which has been electrophysiologically and morphologically suggested in stellate ganglion of the cat [22]. Bosnjak et al.[22] studied the general morphology of cat stellate ganglion cells in relation to the synaptic input that each neuron received. Electrical stimulation of pre- and postganglionic nerves followed by intracellular recording and HRP injection. In a special area (caudal part) close to the preganglionic nerve, some ganglion neurons had no morphologically identifiable axons leaving the ganglion. Therefore, these cells can not be excited by antidromic stimulation. The authors indicated that these cells may be interneurons which may contribute to the ganglionic modulation of sympathetic efferent nerve activity. Similar observations were also reported from inferior mesenteric ganglion of the cat [94]. Whether synaptic contact

is present between these cells and the other ganglion neurons and whether these cells are monoaminergic neurons are not known. Evidently, more essential details are needed to establish a full understanding of these neurons with only intraganglionic processes.

d. Ganglionic capsule and blood vessels

Sympathetic ganglion cells are enclosed by a capsule of connective tissue. A thin epineurium, a thick perineurium and a delicate endoneurium make up the layers of the capsule [156]. From the capsule, connective tissue septa segregate groups of ganglion cells [156]. It is well to note that the perineurium of autonomic ganglia acts as a diffusion barrier [81]. Sixty minutes after applying to the surface of SCG, the HRP was still excluded from the endoneurial spaces by the overlapping layers of the perineurium [8]. This capsule usually prevents the penetration of microelectrodes in electrophysiological studies unless the capsule is opened or younger animal with thinner capsule is chosen [37,130].

Sympathetic ganglia were believed to receive a rich blood supply to maintain an active metabolism [37]. From the surface capsule, blood vessels travel down into the ganglion via the septa and divide into capillary plexus. Another important role of the blood vessels in SCG is to transport catecholamines released from SIF cells to other neurons within a single ganglion [79]. The capillary beds around the principal neurons were found to be downstream from that of SIF cells [79], suggesting a vascular path for the SIF cells' transmitter transportation. The permeability of the blood vessels was studied by vascular injected HRP [41,86]. Low concentrations of HRP barely diffused across the capillary endothelium [41] while higher concentrations of HRP are able to pass the

endothelium [86], suggesting that a higher concentration of HRP may provide an increase in vascular permeability [37].

2. Parasympathetic Ganglia

The parasympathetic ganglia have been less well studied than the sympathetic ganglia. To date the parasympathetic ganglia that have been studied include: the cat pelvic ganglia [68,150], the mammalian and amphibian intracardiac ganglia [56,100,131,139], the chick ciliary ganglia [128], the cat ciliary ganglia [134], submandibular ganglia of rat [134], ganglionated plexus of guinea pig gallbladder [33], and the cat pancreatic ganglia [126]. Some of these parasympathetic ganglia are very simple system, such as the frog intracardiac ganglion, the rat and the cat ciliary ganglia and the rat submandibular ganglion. These ganglia do not appear to possess interneurons or SIF cells and had no slow potentials. Hence, these ganglia may have less integration capabilities. Other parasympathetic ganglia have some complex features similar to the sympathetic ganglia.

The morphology of intracardiac parasympathetic ganglion neurons have been reported from different species [56,100,139], especially from the frog and mudpuppy [131,132]. In the frog heart, principal ganglion neurons are unipolar cells. In mudpuppy intracardiac ganglia, 10 of 40 examined principal cells are bipolar, and the rest are unipolar [131]. The principal neurons in mammalian intracardiac ganglia are multipolar cholinergic cells [139,148]. With the exception of frog cardiac ganglion, SIF cells have been found in various populations of different intracardiac ganglia [131,139]. A relative high ratio of SIF vs principal neuron per ganglion (106/250) has been reported in mudpuppy intracardiac ganglia [131]. Preganglionic nerve terminals in frog intracardiac ganglia are

exclusively cholinergic [132] while the intracardiac neurons in the mudpuppy heart receive innervation from three sources: vagal preganglionic cholinergic fibers, adrenergic processes arising from intraganglionic SIF cells and vagal postganglionic fibers or axon collaterals from the fellow intraganglionic principal cells [131,176,190]. In the mudpuppy intracardiac ganglia, gap junctions are found between the somata, the soma and processes or between the processes of adjacent ganglion cells [131], which have not been demonstrated in mammalian intracardiac ganglia. Electrical coupling is also demonstrated in cat and chick ciliary ganglia. However, electrical coupling in the chick occurs across the chemical synapse that courses from preganglionic to postganglionic neurons, whereas in the mudpuppy, electrical junctions are present between adjacent principal neurons [128,131]. The presence of both electrical and chemical transmission make these ganglia differ from most of the autonomic ganglion, but similar to certain neuronal systems of the brain [10,64,81].

C.   SYNAPTIC TRANSMISSION IN AUTONOMIC GANGLIA

1. Nicotinic Cholinergic Transmission

The fast excitatory postsynaptic potential (f-EPSP) is the main synaptic ganglionic potential primarily responsible for synaptic transmission. Generally, the f-EPSP can be evoked by a single, brief pulse of preganglionic, neural stimulation. The f-EPSP rises to a peak within a few milliseconds and decays exponentially with a time constant longer than the cell membrane time constant [105]. As confirmed by many studies, the f-EPSP is unequivocally induced by the nicotinic action of ACh in both sympathetic and

parasympathetic ganglia [40,69,106,154,176].

Acetylcholine when released by preganglionic stimulation, activates nicotinic receptors on the postsynaptic neurons, which then activate the ion channel mechanisms leading to the postsynaptic membrane depolarization. The molecular structure of the nicotinic receptor has been studied in the electric organ and is an oligomeric glycoprotein molecule 6-10 nm in diameter. This protein is comprised of five subunits: two α-subunits and one each of β-, γ-, and δ-subunits. The subunits are assembled in a transmembrane pentamer and arranged in a circle about a central pit (possibly the channel) [123,136]. Each neuron in a mammalian sympathetic ganglion contains about 9.2 x 10^5 nicotinic receptors that spread over the dendrites and the perikaryon [62]. They are concentrated under the synaptic boutons, thus making the subsynaptic membrane more sensitive to ACh than the extrasynaptic membrane [75]. On the basis of comparison of the single channel current flowing through a nicotinic receptor ionic channel with the whole cell currents induced by a quantum of ACh, each quantum activates about 150 nicotinic receptors in a mammalian sympathetic ganglion neuron [97].

The nicotinic receptor channel is similar to other ligand-gated channels. When the particular molecules at both α-subunits are occupied, a conformational change is induced, followed by an increased channel conductance to a mean value of 30 pS [179]. The ionic currents permeated via nicotinic receptor channel have been well investigated [106,179]. The reversal potentials for the excitatory postsynaptic currents (EPSCs) or EPSPs on neurons in autonomic ganglia range from -5 to -10 mV [105,142]. This is similar to the reversal potential resultant from the application of ACh on the

ganglion cell [40]. The reversal potential of the f-EPSP obtained by an extrapolation, becomes more negative when the sodium or potassium concentration of the extracellular solution is reduced, while it shifts to a less negative value with increasing potassium concentration. The removal of extracellular chloride has no effect [105]. Therefore, sodium and potassium are the ions which are permeable via the ganglionic nicotinic receptor channel and are responsible for the nicotinic transmission. In addition, some studies have suggested the involvement of an increased calcium conductance via nicotinic receptor [151]. Acetylcholine induces a higher membrane conductance (g) for sodium than that for potassium ($g_{Na}/g_K = 1.8$) [52] and generates a net inward current which contributes to f-EPSP.

The EPSC underlying the f-EPSP was first recorded by Kuba and Nishi [107] by voltage-clamping a bullfrog sympathetic ganglion cell with two intracellular electrodes. Similar experiments were done on parasympathetic ganglion cells [173]. The EPSC has a peak time of 2 ms and a half-decay of 4.3 ms (recorded at -70 mV) [108] which reflects the rate of closing of the ion channel [106]. From the analysis of the kinetics of channel gating, two different subgroups of nicotinic receptor ion channels are suggested, which are distinguished by their different closing rates [173]. The physiological significance of the subtypes of nicotinic receptor channel is not presently clear.

2. Muscarinic Cholinergic Transmission

Since the finding of the effects of ACh on the atropine sensitive receptors in adrenal medulla near sixty years ago [60], many studies have been performed on muscarinic transmission in autonomic ganglia. Based on early observations that preganglionic nerve

stimulation can evoked a series of potential changes [53,113], Eccles and Libet [54,118] provided evidence to demonstrate the presence of two types of cholinergic receptors on ganglion cells from the isolated rabbit SCG. Following the preganglionic nerve stimulation, their extracellular recordings showed a complex response which consisted of an initial negative (N) potential followed by a positive (P) potential and by a prolonged late negative (LN) potential. A low concentration of atropine depressed both the P and LN components without having any effect on the N potential. They suggested that the P potential might be produced by the action of catecholamine released from chromaffin cells when the muscarinic receptors of these cells are activated by ACh liberated from preganglionic nerve terminals [4,54]. The P potential was subsequently recorded intracellularly as a hyperpolarizing response and referred to as the slow postsynaptic potential (s-IPSP) [184]. The LN potential was first recorded intracellularly by Tosaka et al.[184] and then by Nishi and Koketsu [143] from paravertebral ganglion cells of frog and bullfrog, respectively, and later by Kabayashi and Libet from rabbit SCG [101]. The intracellular counterpart of the LN potential is the slow excitatory postsynaptic potential (s-EPSP). Eccle and Libet suggested that LN potential was mediated by ACh via muscarinic receptors [54,118].

a. Muscarinic action of ACh in s-EPSP and s-IPSP

Muscarinic action of ACh fulfills all the criteria for mediator of s-EPSP in autonomic ganglia [4]: i). Muscarinic receptors have been found on autonomic ganglion cells [74,77,188] ii). The LN potential, s-EPSP and the slow depolarization produced by ACh or muscarinic agonists were completely blocked by atropine but not by nicotinic antagonists [54,118,143,185]; iii). Iontophoresis of ACh to a curarized single ganglion cell

produced a slow depolarization (slow ACh potential) that had a time-course and latency similar to those of the s-EPSP and was blocked by atropine [103]; iv). The s-EPSP and slow ACh potential were augmented and prolonged by anticholinesterase agents [103,119]; v). The slow ACh potential could be recorded in Ca^{2+} - free high Mg^{2+} solution, in which the release of transmitter was inhibited [119]. These observations suggest a direct generation of the slow ACh potential vi). The ionic mechanisms of slow ACh potentials and the s-EPSP are the same [4], which are different from that of nicotinic response (f-EPSP). The existence of muscarinic excitatory transmission (s-EPSP) is now well documented in sympathetic ganglia even though species differences do exist [4]. The s-EPSPs or slow ACh depolarizations are also found, to a lesser extent, in parasympathetic ganglia [7,68].

On the other hand, there are inconsistencies among different laboratories and different ganglia regarding the neurotransmitter and receptor directly responsible for the s-IPSP [102]. It is generally proposed that in sympathetic ganglia, the s-IPSP is elicited by a direct action of either ACh or a catecholamine. Acetylcholine is undoubtedly released from preganglionic nerve terminals, but the catecholamine could be released from SIF cells or ganglion cells [102].

Eccles and Libet proposed a bisynaptic mediation of the s-IPSP. When ACh is applied directly to the ganglion in the presence of nicotinic antagonist, a slow ACh hyperpolarization and a slow ACh depolarization, corresponding to the s-IPSP and s-EPSP, respectively, were evoked. If these responses are generated by a direct action of ACh, they can be expected to be present after the preparations are exposed to a

low Ca^{2+}/ high Mg^{2+} solution that arrests the release of all transmitters [102]. However, Eccles and Libet found that only the slow ACh depolarization was persistent in a low Ca^{2+}/ high Mg^{2+} solution. This suggested that the s-EPSP but not the s-IPSP is generated by a direct action of ACh, the s-IPSP being then produced by a bisynaptic pathway [54]. Additionally, the s-IPSP could be blocked by adrenergic blocking agents [54]; iontophoresis of dopamine onto noncurarized ganglion cells evoked a similar slow hyperpolarization [47]; prolonged treatment with a muscarinic agent resulted in depletion of catecholamine stores in chromaffin cells and a depression of the s-IPSP [121]; and afferent and efferent synapses were found on SIF cells [105]. Therefore, Libet's group provided a bisynaptic model in sympathetic ganglia, that involves both muscarinic and adrenergic mechanisms.

However, there are some weaknesses in Libet's model. For instance, the action of the adrenergic blocking agents on the s-IPSP was not clear-cut [31,189]; the depression of s-IPSP by bethanechol may not be related to catecholamine depletion [45]. Some more recent studies supported the monosynaptic model which involves a direct muscarinic action of ACh on the s-IPSP. In another words, muscarinic mechanisms mediate both s-IPSP and s-EPSP directly. Cole and Shinnick-Gallagher [32] reported clear evidence indicating a monosynaptic activation of muscarinic receptors located on the ganglion neurons. They found that the slow ACh hyperpolarization of rabbit SCG persisted in a Ca^{2+} free solution when the synaptic s-IPSP was blocked. The s-IPSP of the same ganglion was not blocked by catecholamine antagonists that blocked the catecholamine-induced hyperpolarization [31]. They concluded a direct muscarinic mechanism for the

sympathetic s-IPSP. Presently, the nature of the transmitter and the receptor which are directly responsible for the s-IPSP has not been completely elucidated.

In parasympathetic ganglia muscarinic mechanisms have been described to mediate both the s-IPSP and s-EPSP. From the studies of cat vesical pelvic ganglia [68,69], Griffith et al. reported that a f-EPSP followed by a s-IPSP and a s-EPSP could be induced by preganglionic nerve stimulation. The s-IPSP and s-EPSP could be blocked by atropine and be mimicked by exogenous muscarinic agonists in the presence of low Ca^{2+}/ high Mg^{2+} solution. In mudpuppy cardiac ganglia, an early study found only a s-IPSP mediated via muscarinic receptor [76]. A more recent study reported that both slow hyperpolarizing and slow depolarizing responses could be evoked by the muscarinic agonist bethanechol [104]. Muscarinic transmission has also been reported from mammalian intracardiac ganglia [7,135]. Although catecholamine caused hyperpolarization in parasympathetic ganglion neurons [69,177], it seems unlikely to be the direct neurotransmitter for either s-IPSP or s-EPSP.

b. Mechanism for ganglionic s-EPSP: muscarinic suppression of M current (I_M)

The conductance or resistance changes during the s-EPSP or slow excitatory postsynaptic current (s-EPSC) or the muscarinic action of ACh were variable and depended on the cell. In neurons of the bullfrog sympathetic ganglia, at least three types of conductance change were found during s-EPSC [3]. In most of the cells, membrane resistance was increased. In the rest of the cells, membrane resistance was decreased or was decreased at hyperpolarizing membrane potential while increased at depolarizing membrane potential. In the case of mammalian autonomic ganglion neurons, the

resistance varied in cells and preparations [7,48,135].

One of the hypotheses to explain the decreased conductance during s-EPSP is that it results from a fall in membrane potassium conductance. Weight and Votava [191] obtained a reversal of the s-EPSP at the potassium equilibrium potential and found an increase in membrane resistance during its generation. Hence, they suggested that the inactivation of the potassium conductance underlies the generation of the s-EPSP in bullfrog sympathetic ganglion cells.

This was further confirmed by Adams and Brown [2]. In their voltage-clamp experiments, a time- and voltage-dependent potassium current (I_M) was first recorded in veterbrate neurons, which was directly under the synaptic control by muscarinic action of ACh and luteinizing hormone-releasing hormone (LH-RH) [24]. This I_M is partly activated at the rest potential, but is more strongly activated as the cell is depolarized. It activates over the membrane potential range -70 to -30 or -40 mV in which it forms the dominant outward component of membrane current [26]. I_M apparently differs from the delayed rectifier current I_K in several aspects of channel kinetics [26], e.g. more negative activation range, much lower maximum conductance and total absence of time-dependent inactivation. The latter also serves to distinguish I_M from the transient potassium current I_A, while, unlike the calcium dependent potassium current I_C, I_M is not dependent upon external calcium and is not modified by intracellular calcium injection [26]. The most unique property of I_M is that it is selectively blocked by muscarinic cholinergic receptor agonists [25,26] and by external Ba^{2+} ions [26,34]. Furthermore, I_M is suppressed by synaptically-released ACh [1], which produces a net inward (depolarizing) current and

contributes to the orthodromically-generated s-EPSP [1]. The transduction between activation of the ganglionic muscarinic receptor and closure of M-channels is rather indirect. Some biochemical elements, e.g. G protein or membrane phospholipids, have been suggested as the candidate second messenger [24].

Although the muscarinic suppression of I_M has not been universally accepted as the sole cause of the s-EPSP [4,25], I_M-inhibition appears to be the predominant cause of the s-EPSP and increased excitability at resting membrane potential and above [24]. In addition to sympathetic ganglia and central nervous system [24,72,73], I_M-inhibition has also been suggested as the mechanism for the muscarinic depolarization in parasympathetic ganglia [7].

c. Subtypes of the muscarinic receptor

The first indication that muscarinic receptors were not homogeneous came from the observation that gallamine, a neuromuscular blocking agent usually regarded as a nicotinic drug, blocked the action of ACh on the heart [174], but did not affect the action of ACh elsewhere. Recently, more interest in exploring subtypes of the muscarinic receptor came from the introduction of pirenzepine. Pharmacological analysis suggested that pirenzepine differentiated between at least 2 receptor subtypes: M_1, which were located in gastrointestinal system and were sensitive to pirenzepine, and M_2, which were not sensitive to pirenzepine and were mainly located in the heart and exocrine glands [19]. An analog of pirenzepine, AF-DX 116, has a higher affinity for receptors in the heart than that in the exocrine glands. Therefore, the M_2 receptor could be further classified as a cardiac type of M_2 and a glandular type of M_2. Genetic experiments have shown

five distinct gene sequences that appear to code for muscarinic receptors [20,21,109,110,153]. Two of them have the properties of the M_1 and M_2 receptors, respectively [20,153]. The others can only be made by cells injected with the appropriate mRNA; there has been no demonstration that these receptors are expressed naturally [196].

The muscarinic receptors in autonomic ganglia also constitute a heterogeneous population. Some experiments dealing with the binding characteristics indicated that the muscarinic receptor in ganglionic tissue belongs to the M_1 category [74,188]. Mutschler and Lamrecht [140] have shown that muscarinic receptors in rat sympathetic ganglia that control release of norepinephrine in vasculature are of the M_1 subtype. There is evidence that the I_M in mammalian sympathetic ganglia is inhibited by M_1 receptor activation [147]. On the other hand, both M_1 and M_2 receptors have been found in presynaptic terminals [165]. Some investigators have indicated that the s-EPSP and the s-IPSP may be related to different subtypes of muscarinic receptors [7]. It is apparent that more conclusive experiments are needed to elucidate the distribution and functional significance of subtypes of the muscarinic receptor in autonomic ganglia.

3. Peptidergic Transmission

A long lasting excitatory transmission was first observed by Nishi and Koketsu [143] in 1968. They found that a neurally evoked slow depolarization was resistant to both nicotinic and muscarinic antagonists in bullfrog sympathetic ganglia. Tetanic preganglionic stimulation in the presence of nicotine and atropine induced a slow onset (1 - 5 sec after stimulation) and long-lasting (5 - 10 min in duration) depolarization. This depolarization was diminished by a low Ca^{2+}/ high Mg^{2+} solution and was called the late

s-EPSP in the lumbar sympathetic ganglion of the bullfrog [143] or the noncholinergic s-EPSP in the inferior mesenteric ganglion of the guinea pig [46,49,141]. Similar observations were made on other mammalian sympathetic ganglia, including the SCG of the dog [28], cat [5] and rabbit [9], and the coeliac ganglion [50,51] of the guinea pig. However, peptidergic transmission has received little attention in parasympathetic ganglia.

Utilizing the immunohistochemical techniques, a number of peptides have been localized in the autonomic ganglia [90,96]. Among these peptides, LH-RH and substance P appear to be the most probable candidates for a transmitter responsible for the late s-EPSP in sympathetic ganglia [96]. These peptides were found in preganglionic nerve fibers or synaptic boutons and released from the preganglionic nerve terminals [82,91]. Electrophysiological and pharmacological experiments demonstrated that the response to these peptides mimicked the late s-EPSP [49]. The electrophysiological characteristics and ionic mechanisms of late s-EPSP and peptide-induced depolarization were identical [96]. Therefore, it has been suggested that the LH-RH is a transmitter candidate for the late s-EPSP and the substance P is a transmitter candidate for the noncholinergic s-EPSP. The ionic mechanisms underlying the LH-RH depolarization and the late s-EPSP was suggested to be the suppression of I_M [24,93].

Although these studies reveal a new mechanism for ganglion transmission in addition to classic cholinergic transmission, the functional significance of the peptidergic transmission is not clear. In the case of substance P, since the substance P-containing fiber in the inferior mesenteric ganglia may be the collateral branches of primary sensory neurons of the dorsal root ganglia [38], the noncholinergic s-EPSP may represent the

transmission of sensory signals from the gastrointestinal tract to these ganglia. This provides a mechanism for a peripheral reflex regulation of gastrointestinal activity [46,99].

D. REFERENCES

1 Adams, P.R. and Brown, D.A., Ionic basis of the slow excitatory post-synaptic current studied in voltage-clamped bullfrog sympathetic neurons, *J. Physiol. (Lond.)*, 303 (1980) 66p.

2 Adams, P.R. and Brown, D.A., Synaptic inhibition of the M-current: Slow excitatory postsynaptic potential mechanism in bullfrog sympathetic neurons, *J. Physiol. (Lond.)*, 332 (1982) 263-272.

3 Akasu, T., Gallagher, J.P., Koketsu, K. and Shinnick-Gallagher, P., Slow excitatory postsynaptic currents in bull-frog sympathetic neurons, *J. Physiol. (Lond.)*, 351 (1984) 583-593.

4 Akasu, T. and Koketsu, K., Muscarinic transmission. In A.G. Karczmar, K. Koketsu and S. Nishi (Eds.), *Autonomic and Enteric Ganglia*, Plenum Press, New York and London, 1986, pp. 161-179.

5 Alkadhi, K.A. and McIsaac, R.J., Non-nicotinic ganglionic transmission during partial ganglionic blockade with chlorisondamine, *Fed. Proc. Fed. Am. Soc. Exp. Biol.*, 30 (1971) 655.

6 Allen, T.G.J. and Burnstock, G., Intracellular studies of the electrophysiological properties of cultured intracardiac neurons of the guinea-pig, *J. Physiol. (Lond.)*, 388 (1987) 349-366.

7 Allen, T.G.J. and Burnstock, G., M_1 and M_2 muscarinic receptors mediate excitation and inhibition of guinea-pig intracardiac neurons in culture, *J. Physiol. (Lond.)*, 422 (1990) 463-480.

8 Arvidson, B., A study of the peripheral diffusion barrier of a peripheral ganglion, *Acta Neuropathol.*, 46 (1979) 139-144.

9 Ashe, J.H. and Libet, B., Orthodromic production of non-cholinergic slow depolarizing response in the superior cervical ganglion of the rabbit, *J. Physiol. (Lond.)*, 320 (1981) 333-346.

10 Baker, R. and Llinas, R., Electrical coupling between neurons in the rat mesencephalic nucleus, *J. Physiol. (Lond.)*, 203 (1971) 550-570.

11 Belardinelli, L. and Isenberg, G., Isolated atrial myocytes: adenosine and acetylcholine increase potassium conductance, *Am. J. Physiol.*, 224 (1983) H734.

12   Belardinelli, L., Klockner, U. and Isenberg, G., Modulation of potassium and calcium currents in atrial and nodal cells. In H.M. Piper and G. Isenberg (Eds.), *Isolated Adult Cardiomyocytes. Volume II: Electrophysiology and Contractile Function*, CRC Press, Boca Raton, Florida, 1989, pp. 155-180.

13   Bjorklund, A., Cegrell, L., Falck, B., Ritzen, M. and Rosengren, E., Dopamine-containing cells in sympathetic ganglia, *Acta. Physiol. Scand.*, 78 (1970) 334-338.

14   Blelecki, K. and Lewartowski, B., The influence of hemicholinium No. 3 and vagus stimulation on acetylcholine distribution in the cat's heart, *Pflugers Arch. Ges. Physiol.*, 279 (1964) 149-155.

15   Bluemel, K.M., Wurster, R.D., Randall, W.C., Duff, M.J. and O'Tool, M.F., Parasympathetic postganglionic pathways to the sinoatrial node, *Am. J. Physiol.*, 259 (1990) H1504-H1510.

16   Bohm, M., Schmitz, W., Scholz, H. and Wilken, A., Pertussis toxin prevents adenosine receptor- and M-cholinergic-mediated sinus rate slowing and AV conduction block in the guinea-pig heart, *Naunyn. Schmiedebergs. Arch. Pharmacol.*, 339 (1989) 152-158.

17   Bojsen-Moller, F. and Tranum-Jensen, J., Whole-mount demonstration of cholinesterase-containing nerves in the right atrial wall, nodal tissue, and atrioventricular bundle of the pig heart, *J. Anat.*, 108 (1971) 375-386.

18   Bojsen-Moller, F. and Tranum-Jensen, J., Rabbit heart nodal tissue, sinuatrial ring bundle and atrioventricular connexions identified as a neuromuscular system, *J. Anat.*, 112 (1972) 367-382.

19   Bonner, T.I., The molecular basis of muscarinic receptor diversity, *TINS*, 12 (1989) 148-151.

20   Bonner, T.I., Buckley, N.J., Young, A.C. and Brann, M.R., Identification of a family of muscarinic acetylcholine receptor genes, *Science*, 237 (1987) 527-532.

21   Bonner, T.I., Young, A.C., Brann, M.R. and Buckley, N.J., Cloning and expression of the human and rat m5 muscarinic acetylcholine receptor genes, *Neuron*, 1 (1988) 403-410.

22   Bosnjak, Z.J. and Kampine, J.P., Electrophysiological and morphological characterization of neurons in stellate ganglion of cats, *Am. J. Physiol.*, 248 (1985) 288-292.

23 Bouman, L.N., Gerlings, E.D., Biersteker, P.A. and Bonke, F.I.M., Pacemaker shift in the sino-atrial node during vagal stimulation, *Pflugers. Arch.*, 302 (1968) 255-267.

24 Brown, D.A., M-currents: an update, *TINS*, 11 (1988) 294-299.

25 Brown, D.A. and Adams, P.R., Muscarinic suppression of a novel voltage-sensitive K current in a vertebrate neurone, *Nature*, 283 (1980) 673-676.

26 Brown, D.A., Adams, P.R. and Constanti, A., Voltage-sensitive K-currents in sympathetic neurons and their modulation by neurotransmitters, *J. Auton. Nerv. Syst.*, 6 (1982) 23-35.

27 Brown, O.M., Cat heart acetylcholine: structural proof and distribution, *Am. J. Physiol.*, 231 (1976) 781-785.

28 Chen, S.S., Transmission in superior cervical ganglion of the dog after cholinergic suppression, *J. Physiol. (Lond.)*, 221 (1971) 209-213.

29 Chiba, T., Black, A.C. and Williams, T.H., Evidence for dopamine-storing interneurons and paraneurons in rhesus monkey sympathetic ganglia, *J. Neurocytol.*, 6 (1977) 441-453.

30 Codina, J., Yatani, A., Grenet, D., Brown, A.M. and Birnbaumer, L., The alpha subunit of the GTP binding protein G_k opens atrial potassium channels, *Science*, 236 (1987) 442.

31 Cole, A.E. and Shinnick-Gallagher, P., Alpha-adrenoceptor and dopamine receptor antagonists do not block the slow inhibitory postsynaptic potential in sympathetic ganglia, *Brain Res.*, 187 (1980) 226-230.

32 Cole, A.E. and Shinnick-Gallagher, P., Muscarinic inhibitory transmission in mammalian sympathetic ganglia mediated by increased potassium conductance, *Nature*, 307 (1984) 270-271.

33 Combrooks, E.B., Pouliot, W.A. and Mawe, G.M., Ultrastructure of HRP labeled neurons in the ganglionated plexus of the guinea pig gallbladder, *Soc. Neurosci. Abs.*, 16 (1990) 861-861.(Abstract)

34 Constanti, A., Adams, P.R. and Brown, D.A., Why do barium ions imitate acetylcholine?, *Brain Res.*, 206 (1981) 244-250.

35 Cooper, T., Terminal innervation of the heart. In W.C. Randall (Ed.), *Nervous Control of the Heart*, Williams & Williams, Baltimore, 1965, pp. 130-153.

36 Coupland, R.E., Pyper, A.S. and Hopwood, D., A method for differentiating between adrenaline and noradrenaline-storing cells in the light and electron microscope, *Nature*, 201 (1964) 1240-1242.

37 Dail, W.G. and Barton, S., Structure and organization of mammalian sympathetic ganglia. In L-G. Elfvin (Ed.), *Autonomic Ganglia*, John Wiley & Sons, Chichester, 1983, pp. 3-25.

38 Dalsgaard, C.J., Hokfelt, T., Elfvin, L.-G., Skirboll, L. and Emson, P., Substance P-containing primary sensory neurons projecting to the inferior mesenteric ganglion: Evidence from combined retrograde tracing and immunohistochemistry, *Neuroscience*, 7 (1982) 647-654.

39 De Castro, F., Sympathetic ganglia, normal and pathological. In W. Penfiels (Ed.), *Cytology and Cellular Pathology of the Nervous System*, Hoeber, New York, 1932, pp. 319-379.

40 Dennis, M.J., Harris, A.J. and Kuffler, S.W., Synaptic transmission and its duplication by focally applied acetylcholine in parasympathetic neurons of the frog, *Proc. Roy. Soc. Lond.*, 177 (1971) 509-539.

41 DePace, D., A study of the permeability of the blood vessels of the rat superior cervical ganglion, *Anat. Rec.*, 199 (1981) 66A.

42 DiFrancesco, D. and Tromba, C., Acetylcholine inhibits activation of the cardiac hyperpolarizing-activated current,if, *Eur. J. Physiol.*, 410 (1987) 139-142.

43 DiFrancesco, D. and Tromba, C., Muscarinic control of the hyperpolarization-activated current (I_f) in rabbit sino-atrial node myocytes, *J. Physiol. (Lond.)*, 405 (1988) 493-510.

44 DiFrancesco, D. and Tromba, C., Inhibition of the hyperpolarization-activated current (if) induced by acetylcholine in rabbit sino-atrial node myocytes, *J. Physiol. (Lond.)*, 405 (1988) 477-491.

45 Dun, N.J., Ganglionic transmission: Electrophysiology and pharmacology, *Fed. Proc. Fed. Am. Soc. Exp. Biol.*, 39 (1980) 2982-2989.

46 Dun, N.J. and Jiang, Z, G., Non-cholinergic excitatory transmission in inferior mesenteric ganglia of the guinea-pig: Possible mediation by substance P, *J. Physiol. (Lond.)*, 325 (1982) 145-159.

47   Dun, N.J., Kaibara, K. and Karczmar, A.G., Dopamine and adenosine 3',5'-monophosphate responses of single mammalian sympathetic neurons, *Science*, 197 (1977) 778-780.

48   Dun, N.J., Kaibara, K. and Karczmar, A.G., Muscarinic and cGMP induced membrane potential changes: Differences in electrogenic mechanisms, *Brain Res.*, 150 (1978) 658-661.

49   Dun, N.J. and Karczmar, A.G., Actions of substance P on sympathetic neurons, *Neuropharmacology*, 18 (1979) 215-218.

50   Dun, N.J., Kiraly, M. and Ma, R.C., Evidence for a serotonin-mediated slow excitatory potential in the guinea pig coeliac ganglia, *J. Physiol. (Lond.)*, 351 (1984) 61-76.

51   Dun, N.J. and Ma, R.C., Slow non-cholinergic excitatory potentials in neurones of the guinea-pig coeliac ganglia, *J. Physiol. (Lond.)*, 351 (1984) 47-60.

52   Dun, N.J., Nishi, S. and Karczmar, A.G., Alteration in nicotinic and muscarinic responses of rabbit superior cervical ganglion cells after chronic preganglionic denervation, *Neuropharmacology*, 15 (1976) 211-218.

53   Eccles, R.M., Action potentials of isolated mammalian sympathetic ganglia, *J. Physiol. (Lond.)*, 117 (1952) 181-195.

54   Eccles, R.M. and Libet, B., Origin and blockade of the synaptic responses of curarized sympathetic ganglia, *J. Physiol. (Lond.)*, 157 (1961) 484-503.

55   Edvinsson, L., Fredholm, B.B., Hamel, E., Jansen, I. and Verrecchia, C., Perivascular peptides relax cerebral arteries concomitant with stimulation of cyclic adenosine monophosphate accumulation or release of an endothelium-derived relaxing factor in the cat, *Neurosci. Lett.*, 58 (1985) 213-217.

56   Ehinger, B., Falck, B., Persson, H. and Sporrong, B., Adrenergic and cholinesterase-containing neurons of the heart, *Histochemistry*, 16 (1968) 197-205.

57   Endoh, M., Maruyama, M. and Iijima, T., Attenuation of muscarinic cholinergic inhibition by islet-activating protein in the heart, *Am. J. Physiol.*, 249 (1985) H309-H320.

58   Eranko, O. and Harkonen, M., Histochemical demonstration of fluorogenic amines in the cytoplasm of sympathetic ganglion cells of the rat, *Acta. Physiol. Scand.*, 58 (1963) 285-286.

59 Fee, J.D., Randall, W.C., Wurster, R.D. and Ardell, J.L., Selective ganglionic blockade of vagal inputs to sinoatrial and /or atrioventricular regions, *J. Pharmacol. Exp. Ther.*, 242 (1987) 1006-1012.

60   Feldberg, W. and Gaddum, J.H., The chemical transmitter at synapses in sympathetic ganglion, *J. Physiol. (Lond.)*, 81 (1934) 305-319.

61 Fujita, T., The gastro-enteric endocrine cell and its paraneuronic nature. In R.E. Coupland and T. Fujita (Eds.), *Enterochromaffin and Related Cells*, Elsevier, Amsterdam, 1976, pp. 191-208.

62 Fumagalli, L., DeRenzis, G. and Miani, N., Acetylcholine receptors: number and distribution in intact and deafferented superior cervical ganglion of the rat, *J. Neurochem.*, 27 (1976) 47-52.

63   Furukawa, Y. and Levy, M.N., Temporal changes in the sympathetic - parasympathetic interactions that occur in the perfused canine atrium, *Circ. Res.*, 55 (1984) 835-841.

64   Gallagher, J.P. and Shinnick-Gallagher, P., Excitatory transmission in parasympathetic ganglia. In A.G. Karczmar, K. Koketsu and S. Nishi (Eds.), *Autonomic and Enteric Ganglia*, Plenum Press, New York and London, 1986, pp. 341-351.

65 Gaskell, W.H., On the structure, distribution and function of nerves which innervate the visceral and vascular systems, *J. Physiol. (Lond.)*, 7 (1886) 1-80.

66 Geis, W.P., Kaye, M.P. and Randall, W.C., Major autonomic pathway to the atria and SA and AV nodes of the canine heart, *Am. J. Physiol.*, 224 (1973) 202-208.

67   Giles, W. and Noble, S.J., Changes in membrane currents in bullfrog atrium produced by acetylcholine, *J. Physiol. (Lond.)*, 261 (1976) 103-123.

68   Griffith, W.H.III, The physiology and pharmacology of a mammalian parasympathetic ganglion. Dissertation. University of Texas Graduate School of Biomedical Science at Galveston, (1980) (UnPub)

69   Griffith, W.H.III, Gallagher, J.P. and Shinnick-Gallagher, P., An intracellular investigation of cat vesicle pelvic ganglia, *J. Neurophysiol.*, 143 (1980) 343-354.

70 Grillo, M.A., Electron microscopy of sympathetic tissues, *Pharmacol. Rev.*, 18 (1966) 387-399.

71 Gunn, C.G., Sevelius, G., Puiggari, M.J. and Myers, F.K., Vagal cardiomotor mechanisms in the hindbrain of the dog and cat, *Am. J. Physiol.*, 214 (1968) 258-262.

72 Halliwell, J.V., M-current in human neocortical neurones, *Neurosci. Lett.*, 67 (1986) 1-6.

73 Halliwell, J.V. and Adams, P.R., Voltage-clamp analysis of muscarinic excitation in hippocampal neurons, *Brain Res.*, 250 (1982) 71-92.

74 Hammer, R., Berrie, C.P., birdsall, N.J.M., Burgen, A.S.V. and Hulme, E.C., Pirenzepine distinguishes between different subclasses of muscarinic receptors, *Nature*, 283 (1980) 90-92.

75 Harris, A.J., Kuffler, S.W. and Dennis, M.J., Defferential chemosensitivity of synaptic and extrasynaptic area of the neuronal surface membrane in parasympathetic neurons of the frog, tested by microapplication of acetylcholine, *Proc. Roy. Soc. Lond.*, Ser B 177 (1971) 541-553.

76 Hartzell, H.C., Kuffler, S.W., Stickgold, R. and Yoshikami, D., Synaptic excitation and inhibition resulting from direct action of acetylcholine on two type of chemoreceptors on individual parasympathetic neurons, *J. Physiol. (Lond.)*, 271 (1977) 817-846.

77 Hassall, C.J.S., Buckley, N.J. and Burnstock, G., Autoradiographic localization of muscarinic receptors on guinea-pig intracardiac neurons and atrial myocytes in culture, *Neurosci. Lett.*, 74 (1987) 145-150.

78 Hescheler, J., Kameyama, M. and Trautwein, W., On the mechanism of muscarinic inhibition of the cardiac Ca current, *Pflugers. Arch.*, 407 (1986) 182-189.

79 Heym, Ch. and Williams, T.H., Evidence for autonomic paraneurons in sympathetic ganglia of a shrew (tupaia glis), *J. Anat.*, 129 (1979) 151-164.

80 Hoff, H.E., Vagal stimulation before the Webers, *Ann. Med. Hist.*, 8 (1936) 138-144.

81 Hokfelt, T., In vitro studies on central and peripheral monoamine neurons at the ultrastructural level, *Z. Zellforsch. Mikrosk. Anat.*, 91 (1968) 1-74.

82 Hokfelt, T., Elvin, L.-G., Schulzberg, M., Goldstein, M. and Nilsson, G., On the occurrence of substance P-containing fibers in sympathetic ganglia: Immunohistochemical evidence, *Brain Res.*, 132 (1977) 29-41.

83 Iijima, T., Irisawa, H. and Kameyama, M., Membrane currents and their modification by acetylcholine in isolated single atrial cells of the guinea-pig, *J. Physiol. (Lond.)*, 359 (1985) 485.

84 Jacobowitz, D., Catecholamine fluorescent studies of adrenergic neurons and chromaffin cells in sympathetic ganglia, *Fed. Proc.*, 29 (1970) 1929-1944.

85 Jacobowitz, D. and Woodward, J.K., Adrenergic neurons in the cat superior cervical ganglion and cervical sympathetic nerve trunk. A histochemical study, *J. Pharmacol. Exp. Ther.*, 162 (1968) 213-226.

86 Jacobs, J.M., Penetration of systemically injected horseradish peroxidase into ganglia and nerves of the autonomic vervous system, *J. Neurocytol.*, 6 (1977) 607-618.

87 Jalife, J., Hamilton, A.J., Lamanna, V.R. and Moe, G.K., Effects of current flow on pacemaker activity of the isolated kitten sinoatrial node, *Am. J. Physiol.*, 238 (1980) H307-H316.

88 Jalife, J. and Moe, G.K., Phasic effects of vagal stimulaiton on pacemaker activity of the isolated sinus node of the young cat, *Circ. Res.*, 45 (1979) 595-607.

89 James, T.N., Cardiac innervation: anatomic and pharmacologic relations, *Bull. NY Acad. Med.*, 43 (1967) 1041-1086.

90 Jan, L.Y. and Jan, Y.N., Peptidergic transmission in sympathetic ganglia of the frog, *J. Physiol. (Lond.)*, 327 (1982) 219-246.

91 Jan, L.Y., Jan, Y.N. and Brownfield, M.S., Peptidergic transmission in synaptic boutons of sympathetic ganglia, *Nature*, 288 (1980) 380-382.

92 Jew, J.Y., Connections of local circuit neurons in guinea pig and rabbit superior cervical ganglia. In O. Eranko, S. Soinila and H. Paivarinta (Eds.), *Histochemistry and Cell Biology of Autonomic Neurons, SIF cells, and Paraneurons*, Raven Press, New York, 1980, pp. 119-125.

93 Jones, S.W., A muscarinic-resistant M-current in C cells of bullfrog sympathetic ganglia, *Neurosci. Lett.*, 74 (1987) 309-314.

94 Julé, Y., Krier, J. and Szurszewski, J.H., Patterns of innervation of neurones in the inferior mesenteric ganglion of the cat, *J. Physiol. (Lond.)*, 344 (1983) 293-304.

95 Karczmar, A.G., Historical development of concepts of ganglionic transmission. In A.G. Karczmar, K. Koketsu and S. Nishi (Eds.), *Autonomic and Enteric Ganglia*, Plenum Press, New York and London, 1986, pp. 3-25.

96 Katayama, Y. and Nishi, S., Peptidergic transmission. In A.G. Karczmar, K. Koketsu and S. Nishi (Eds.), *Autonomic and Enteric Ganglia*, Plenum Press, New York and London, 1986, pp. 181-199.

97 Kato, E. and Kuba, K., Inhibition of transmitter release in bullfrog sympathetic ganglia induced by r-aminobutyric acid, *J. Physiol. (Lond.)*, 298 (1980) 271-283.

98 keely, S., lincoln, T. and Corbin, J., Interaction of acetylcholine and epinephrine on heart cyclic AMP-dependent protein kinase, *Am. J. Physiol.*, 234 (1978) H432-H438.

99 King, B.F. and Szurszewski, J.H., An electrophysiological study of inferior mesenteric ganglion of the dog, *J. Neurophysiol.*, 51 (1984) 607-615.

100 king, T.S. and Coakley, J.B., The intrinsic nerve cells of the cardiac atria of mammals and man, *J. Anat.*, 92 (1958) 353-376.

101 Kobayashi, H. and Libet, B., Generation of slow postsynaptic potentials without increases in ionic conductance, *Proc. Natl. Acad. Sci. USA*, 60 (1968) 1304-1311.

102 Koketsu, K., Inhibitory transmission: Slow inhibitory postsynaptic potential. In A.G. Karczmar, K. Koketsu and S. Nishi (Eds.), *Autonomic and Enteric Ganglia*, Plenum Press, New York and London, 1986, pp. 201-223.

103 Koketsu, K., Nishi, S. and Noda, Y., Effects of physostigmine on the after discharge and slow postsynaptic potentials of bullfrog sympathetic ganglia, *Br. J. Pharmacol.*, 34 (1968) 177-188.

104 Konopka, L.M. and Parsons, R.L., The muscarinic agonist bethanechol initiates hyperpolarization and depolarization of mudpuppy intracardiac neurons, *Soc. Neurosci. Abs.*, 16 (1990) 1055-1055.(Abstract)

105 Kuba, K. and Koketsu, K., Synaptic events in sympathetic ganglia, *Prog. Neurobiol.*, 11 (1978) 77-169.

106 Kuba, K. and Minota, S., General characteristics and mechanisms of nicotinic transmission in sympathetic ganglia. In A.G. Karczmar, K. Koketsu and S. Nishi (Eds.), *Autonomic and Enteric Ganglia*, Plenum Press, New York and London, 1986, pp. 107-135.

107 Kuba, K. and Nishi, S., Membrane current associated with the fast EPSP of sympathetic neurons, *Physiologist*, 14 (1971) 176.

108 Kuba, K. and Nishi, S., Characteristics of fast excitatory postsynaptic current in bullfrog sympathetic ganglion cells, *Pflugers. Arch.*, 378 (1979) 205-212.

109 Kubo, T., Fukuda, K., Mikami, A., Maeda, A., Takahashi, H., Mishina, M., Haga, T., Haga, K., Ichiyama, A., Kangawa, K., Kojima, M., Matsuo, H., Hirose, T.

and Numa, S., Cloning, sequencing and expression of complementary DNA encoding the muscarinic acetylcholine receptor, *Nature*, 323 (1986) 411-416.

110 Kubo, T., Meada, A., Sugimoto, K., Akiba, I., Mikami, A., Takahashi, H., Haga, T., Haga, K., Ichiyama, A., Kangawa, M., Matsuo, H., Hirose, T. and Numa, S., Primary structure of porcine cardiac muscarinic acetylcholine receptor deduced from the cDNA sequence, *FEBS*, 209 (1986) 367-372.

111 Langley, J.N., On the physiology of the salivary secretion: The influence of the chorda tympani and sympathetic nerves upon the secretion of the maxillary gland of the cat, *J. Physiol. (Lond.)*, 1 (1878) 96-103.

112 Langley, J.N., *The Autonomic Nervous System. Part 1*, W.Heffer, Cambridge, 1921.

113 Laporte, Y. and Lorente de No, R., Potential changes evoked in a curarized sympathetic ganglion by presynaptic volleys of impulses, *J. Cell. Comp. Physiol.*, 35 (Suppl.2) (1950) 61-106.

114 Lazzara, R., Scherlag, B.J., Robinson, M.J. and Samet, P., Selective in situ parasympathetic control of the canine sinoatrial and atrioventricular nodes, *Circ. Res.*, 32 (1973) 393-401.

115 Lees, G.M., Anatomy, histology, and electron microscopy of sympathetic, parasympathetic, and enteric neurons. In A.G. Karczmar, K. Koketsu and S. Nishi (Eds.), *Autonomic and Enteric Ganglia - Transmission and its Pharmacology*, Plenum Press, New York, 1986, pp. 27-60.

116 Levy, M.N., Sympathetic-parasympathetic interaction in the heart, *Circ. Res.*, 29 (1971) 437.

117 Levy, M.N. and Martin, P.J., Neural control of the heart. In R.M. Berne (Ed.), *Handbook of Physiology. Section 2: The Cardiovascular System*, Bethesda, Maryland, 1979, pp. 581-620.

118 Libet, B., Slow synaptic responses and excitatory changes in sympathetic ganglia, *J. Physiol. (Lond.)*, 174 (1964) 1-25.

119 Libet, B., Long latent periods and further analysis of slow synaptic responses in sympathetic ganglia, *J. Neurophysiol.*, 30 (1967) 494-514.

120 Libet, B., Functional roles of SIF cells in slow synaptic actions. In O. Eranko, S. Soinila and H. Paivarinta (Eds.), *Histochemistry and Cell Biology of Autonomic Neurons, SIF Cells and Paraneurons*, Raven Press, New York, 1980, pp. 111-118.

121 Libet, B. and Tosaka, T., Dopamine as a synaptic transmitter and modulator in sympathetic ganglia: A different mode of synaptic action, *Proc. Natl. Acad. Sci. USA*, 67 (1970) 667-673.

122 Lichtman, J.W., Purves, D. and Yip, J.W., On the purpose of selective innervation of guinea-pig superior cervical ganglion cells, *J. Physiol. (Lond.)*, 292 (1979) 69-84.

123 Lindstrom, J., Antibodies as probes of acetylcholine receptor structure and function. In H. Yamamura, W. Olsen and E. Usdin (Eds.), *Psychopharmacology and Biochemistry of Neurotransmitter Receptors*, Elsevier/North-Holland, Amsterdam, 1980, pp. 63-84.

124 Lipsius, S.L. and Vassalle, M., Effects of acetylcholine on potassium movements in the guinea-pig sinus node, *J. Pharmacol. Exp. Ther.*, 201 (1977) 669-677.

125 Logothetis, D.E., Kurachi, Y., Galper, J., Neer, E.J. and Clapham, D.E., The beta-gamma subunits of GTP-binding protein activate the muscarinic K channel in heart, *Nature*, 325 (1987) 321.

126 Ma, R.C. and Szurszewski, J.H., Effects of cholecystokinin on neurons of cat pancreatic ganglia, *Soc. Neurosci. Abs.*, 15 (1989) 212-212.(Abstract)

127 Malor, R., Taylor, S., Chesher, G.B. and Griffin, C.J., The intramural ganglia and chromaffin cells in guinea pig atria: an ultrastructural study, *Cardiovasc. Res.*, 8 (1974) 731-744.

128 Martin, A.R. and Pilar, G., Dual mode of synaptic transmission in the avian ciliary ganglion, *J. Physiol. (Lond.)*, 168 (1963) 443-463.

129 Matthews, M.R. and Raisman, G., The ultrastructure and somatic efferent synapse of small granule-containing cells in the superior cervical ganglion, *J. Anat.*, 105 (1969) 255-282.

130 McLachlan, E.M., The formation of synapses in mammalian sympathetic ganglia reinnervated with preganglionic or somatic nerves, *J. Physiol. (Lond.)*, 237 (1974) 217-242.

131 McMahan, M.N. and Purves, D., Visual identification of two kinds of nerve cells and their synaptic contacts in a living autonomic ganglion of the mudpuppy (necturus maculosus), *J. Physiol. (Lond.)*, 254 (1976) 405-425.

132 McMahan, U.J. and Kuffler, S.W., Visual identification of synaptic boutons on living ganglion cells and of varicosities in postganglionic axons in the heart of the frog, *Proc. Roy. Soc. Lond.*, Ser B 177 (1971) 485-508.

133 Meckel, J.F., Observation anatomique avec l'examen physiologique du veritable usage des noeuds, ou ganglions des nerfs, *Mem. Acad. Roy. Sci.*, 5 (1751) 84-178.

134 Melnichenko, L.V. and Skok, V.I., Natural electrical activity in mammlian parasympathetic ganglion neurons, *Brain Res.*, 23 (1970) 277-279.

135 Mihara, S., Ikeda, K. and Nishi, S., Muscarinic M_2 receptors on cardiac ganglion neurons of the guinea-pig heart, *Kurume Med. J.*, 35 (1988) 183-192.

136 Mishina, M., Kurosaki, T., Tobimatsu, T., Morimoto, Y., Noda, M., Yamamoto, T., Terao, M., Lindstrom, J., Takahashi, T., Kuno, M. and Numa, S., Expression of functional acetylcholine receptor from cloned cDNAs, *Nature*, 307 (1984) 604-608.

137 Mizeres, N.J., Isolation of the cardioinhibitory branches of the right vagus nerve in the dog, *Anat. Rec.*, 123 (1955) 437-446.

138 Mizeres, N.J., The course of the left cardioinhibitory fibers in the dog, *Anat. Rec.*, 127 (1957) 109-116.

139 Moravec, J. and Moravec, M., Intrinsic nerve plexus of mammalian heart: morphological basis of cardiac rhythmical activity?, *Int. Rev. Cytol.*, 106 (1987) 89-149.

140 Mutschler, E. and Lamrecht, G., Selective muscarinic agonists and antagonists in functional tests. In R.R. Levine and J.M. Birdsall (Eds.), *Subtypes of Muscarinic Receptors. Trends Pharmacol.Sci.Supplement*, Elsevier, 1984, pp. 39-44.

141 Neild, T.O., Slowly-developing depolarization of neurones in the guinea pig inferior mesenteric ganglion following repetitive stimulation of the preganglionic nerves, *Brain Res.*, 140 (1978) 231-239.

142 Nishi, S. and Koketsu, K., Electrical properties and activities of single sympathetic neurons in frogs, *J. Cell. Comp. Physiol.*, 55 (1960) 15-30.

143 Nishi, S. and Koketsu, K., Early and late after-discharges of amphibian sympathetic ganglion cells, *J. Neurophysiol.*, 31 (1968) 109-121.

144 Noma, A. and Trautwein, W., Relaxation of the ACh-induced potassium current in the rabbit sinoatrial node cell, *Pflugers. Arch.*, 377 (1978) 193-200.

145 Norberg, K.A., Ritzen, M. and Ungerstedt, U., Histochemical studies on a special catecholamine-containing cell type in sympathetic ganglia, *Acta. Physiol. Scand.*, 67 (1966) 260-270.

146 Norberg, K.A. and Sjoqvist, F., New possibilities for adrenergic modulation of ganglionic transmission, *Pharmacol. Rev.*, 18 (1966) 743-751.

147 North, R.A., Muscarinic cholinergic receptor regulation of ion channels. In J.H. Brown (Ed.), *The Muscarinic Receptors*, The Hunama Press, Clifton, Neu Jersey, 1990, pp. 341-373.

148 Osborne, L.W. and Silva, D.G., Histological, acetylcholinesterase, and fluorescence histochemical studies on the atrial ganglia of the monkey heart, *Exp. Neurol.*, 27 (1970) 497-511.

149 Osterrieder, W., Noma, A. and Trautwein, W., On the kinetics of the potassium channel activated by acetylcholine in the S-A node of the rabbit heart, *Pflugers. Arch.*, 386 (1980) 101-109.

150 Owman, C., Alm, P. and Sjoberg, N-O., Pelvic autonomic ganglia: structure, transmitters, function and steroid influence. In L-G. Elfvin (Ed.), *Autonomic ganglia*, John Wiley & Sons, Chichester, 1983, pp. 125-143.

151 Pappano, A.J. and Volle, R.L., Observation on the role of calcium ions in ganglionic responses to acetylcholine, *J. Pharmacol. Exp. Ther.*, 152 (1966) 171-180.

152 Pardini, B.J., Patel, K.P., Schmid, P.G. and Lund, D.D., Location, distribution and projections of intracardiac ganglion cells in rat, *J. Auton. Nerv. Syst.*, 20 (1987) 91-101.

153 Peralta, E.G., Winslow, J.W., Peterson, G.L., Smith, D.H., Ashkenazi, A., Ramachandran, J., Schimerlik, M.I. and Capon, D.J., Primary structure and biochemical properties of an M2 muscarinic receptor, *Science*, 236 (1987) 600-605.

154 Perry, W.L.M. and Talesnik, J., The role of acetylcholine in synaptic transmission at parasympathetic ganglia, *J. Physiol. (Lond.)*, 119 (1953) 445-469.

155 Pfaffinger, P.J., Martin, J.M., Hunter, D.D., Nathanson, N.M. and Hille, B., GTP-binding proteins couple cardiac muscarinic receptor to a K channel, *Nature*, 317 (1985) 536-538.

156 Pick, J., *The Autonomic Nervous System*, J.B.Lippincott, Philadelphia, 1970.

157 Plecha, D.M., Randall, W.C., Geis, G.S. and Wurster, R.D., Localization of vagal preganglionic somata controlling sinoatrial and atrioventricular nodes, *Am. J. Physiol.*, 255 (1988) R703-R708.

158 Prigioni, I. and Russo, G., Intracellular recordings from "recurrent neurons" in the rat superior cervical ganglion, *J. Auton. Nerv. Syst.*, 31 (1990) 85-90.

159 Priola, D.V., Intrinsic innervation of the canine heart, *Circ. Res.*, 47 (1980) 74-79.

160 Priola, D.V., O'Brien, W.J., Dail, W.J. and Simpson, W.W., Cardiac catecholamine stores after cardiac sympathectomy, 6-OHDA and cardiac denervation, *Am. J. Physiol.*, 240 (1981) H889-H895.

161 Priola, D.V. and Spurgeon, H.A., Cholinergic sensitivity of the denervated canine heart, *Circ. Res.*, 41 (1977) 600-606.

162 Priola, D.V., Spurgeon, H.A. and Geis, W.P., The intrinsic innervation of the canine heart: A functional study, *Circ. Res.*, 40 (1977) 50-56.

163 Purves, D., Functional and structural changes in mammalian sympathetic neurones following interruption of their axons, *J. Physiol. (Lond.)*, 252 (1975) 429-463.

164 Purves, D. and Hume, R.I., The relation of postsynaptic geometry to the number of presynaptic axons that innervate autonomic ganglion cells, *J. Neurosci.*, 1 (1981) 441-452.

165 Raiteri, M., Leardi, R. and Marchi, M., Heterogenerty of presynaptic muscarinic receptors regulating neurotransmitter release in rat brain, *J. Pharmacol. Exp. Ther.*, 228 (1984) 209-214.

166 Randall, W.C., Selective autonomic innervation of the heart. In W.C. Randall (Ed.), *Nervous Control of Cardiovascular Function*, Oxford University Press, New York, 1984, pp. 46-67.

167 Randall, W.C. and Ardell, J.L., Selective parasympathectomy of autonomic and conductile tissue of the canine heart, *Am. J. Physiol.*, 248 (1985) H61-H68.

168 Randall, W.C., Ardell, J.L. and Becker, D.M., Differential responses accompanying sequential stimulation and ablation of vagal branches to dog heart, *Am. J. Physiol.*, 249 (1985) H133-H140.

169 Randall, W.C., Ardell, J.L., Calderwood, D., Milosavljevic, M. and Goyal, S.C., Parasympathetic ganglia innervating the canine atrioventricular nodal region, *J. Auton. Nerv. Syst.*, 16 (1986) 311-323.

170 Randall, W.C., Ardell, J.L., O'Toole, M.F. and Wurster, R.D., Differential autonomic control of SAN and AVN regions of the canine heart: structure and function. In T. Mazgalev, L.S. Dreifus and E.L. Michelson (Eds.), *Electrophysiology of the Sinoatrial and Atrioventricular Nodes*, Alan R. Liss, Inc., New York, 1988, pp. 15-31.

171 Randall, W.C., Ardell, J.L., Wurster, R.D. and Milosavljevic, M., Vagal postganglionic innervation of the canine sinoatrial node, *J. Auton. Nerv. Syst.*, 20 (1987) 13-23.

172 Randall, W.C., Milosavljevic, M., Wurster, R.D., Geis, G.S. and Ardell, J.L., Selective vagal innervation of the heart, *Ann. Clin. Lab. Sci.*, 16 (1986) 198-208.

173 Rang, H.P., The characteristics of synaptic currents and responses to acetylcholine of rat submandibular ganglion cells, *J. Physiol. (Lond.)*, 311 (1981) 23-55.

174 Riker, W.F. and Wescoe, W.C., The pharmacology of flaxedil with observations on certain analogs, *Ann. N. Y. Acad. Sci.*, 54 (1951) 373-394.

175 Roberts, L.A., Slocum, G.R. and Riley, D.A., Morphological study of the innervation pattern of the rabbit sinoatrial node, *Am. J. Anat.*, 185 (1989) 74-88.

176 Roper, S., An electrophysiological study of chemical and electrical synapses on neurons in the parasympathetic cardiac ganglion of the mudpuppy ,necturus maculosus: evidence for intrinsic ganglionic innervation, *J. Physiol. (Lond.)*, 254 (1976) 427-454.

177 Shinnick-Gallagher, P., Gallagher, J.P. and Griffith, W.H.III, Inhibition in parasympathetic ganglia. In A.G. Karczmar, K. Koketsu and S. Nishi (Eds.), *Autonomic and Enteric Ganglia*, Plenum press, New York and London, 1986, pp. 353-367.

178 Siegrist, G., Ribaupierre, F.de., Dolivo, M. and Rouiller, C., Les cellules chromaffines des ganglions cervicaus superieurs du rat, *J. Microse.*, 5 (1966) 791-794.

179 Skok, V.I., Nicotinic receptors: Activation and block. In A.G. Karczmar, K. Koketsu and S. Nishi (Eds.), *Autonomic and Enteric Ganglia*, Plenum Press, New York and London, 1986, pp. 137-159.

180 Soejima, M. and Noma, A., Mode of regulation of the ACh-sensitive K channel by the muscarinic receptor in the rabbit atrial cells, *Pflugers. Arch.*, 400 (1984) 424-431.

181 Sorota, S., Tsuji, Y., Tajima, T. and Pappano, A.J., Pertussis toxin treatment blocks hyperpolarization by muscarinic agonist in chick atrium, *Circ. Res.*, 57 (1985) 748-758.

182 Taxi, J., Derer, M. and Domich, A., Morphology and histophysiology of SIF cells in the autonomic ganglia. In L-G. Elfvin (Ed.), *Autonomic Ganglia*, John Wiley & Sons, Chichester, 1983, pp. 67-95.

183 Ten Eick, R., Nawrath, H., McDonald, T.F. and Trautwein, W., On the mechanism of the negative inotropic effect of acetylcholine, *Pflugers. Arch.*, 361 (1976) 207-213.

184 Tosaka, T., Chichibu, S. and Libet, B., Intracellular analysis of slow inhibitory and excitatory postsynaptic potentials in sympathetic ganglia of the frog, *J. Neurophysiol.*, 31 (1968) 396-409.

185 Tosaka, T. and Libet, B., Additional (adrenergic) synaptic step in sympathetic ganglia, *Fed. Proc. Fed. Am. Soc. Exp. Biol.*, 29 (1970) 716.

186 Urthaler, F., Neely, B.H. and Hageman, G.R., Differential sympathetic-parasympathetic interactions in sinus node and AV junction, *Am. J. Physiol.*, 250 (1986) H43-H51.

187 Verhofstad, A.A.J., Steinbusch, H.W.M., Penke, B., Verga, J. and Joosten, H.W.J., Serotonin-immunoreactive cells in the superior cervical ganglion of the rat, *Brain Res.*, 212 (1981) 39-49.

188 Vickroy, T.W., Watson, M., Yamamura, H.I. and Roeske, W.R., Agonist binding to multiple muscarinic receptors, *Fed. Proc. Fed. Am. Soc. Exp. Biol.*, 43 (1984) 2785-2798.

189 Volle, R.L. and Hancock, J.C., Transmission in sympathetic ganglia, *Fed. Proc. Fed. Am. Soc. Exp. Biol.*, 29 (1970) 1913-1918.

190 Watanabe, H., The organization and fine structure of autonomic ganglia of amphibia. In L-G. Elfvin (Ed.), *Autonomic Ganglia*, John Wiley & Sons, Chichester, 1983, pp. 183-201.

191 Weight, F.F. and Votava, J., Slow synaptic excitation in sympathetic ganglion cells: Evidence for synaptic inactivation of potassium conductance, *Science*, 170 (1970) 755-758.

192 Weiss, G.K. and Priola, D.V., Brainstem sites for activation of vagal cardioaccelerator fibers in the dog, *Am. J. Physiol.*, 223 (1972) 300-304.

193 Williams, T. and Jew, J., Monoamine connections in sympathetic ganglia. In L-G. Elfvin (Ed.), *Autonomic Ganglia*, John Wiley & Sons, Chichester, 1983, pp. 235-265.

194 Williams, T.H., Black, A.C.Jr., Chiba, T. and Bhalla, R.C., Morphology and biochemistry of small, intensely fluorescent cells of sympathetic ganglia, *Nature*, 256 (1975) 315-317.

195 Williams, T.H., Chiba, T., Black, A.C., Jr., Bhalla, R.C. and Jew, J., Species variation in SIF cells of superior cervical ganglia: are there two functional types?, *Fogarty. Int. Cent. Proc.*, 30 (1976) 143-162.

196 Wolfe, B.B., Subtypes of muscarinic cholinergic receptors: Ligand binding, functional studies, and cloning. In J.H. Brown (Ed.), *The Muscarinic Receptors*, The Humana Press, Clifton, New Jersey,1989, pp. 125-150.

197 Yatani, A., Codina, J., Brown, A.M. and Birnbaumer, L., Direct activation of mammalian atrial muscarinic potassium channels by GTP regulatory protein G_k, *Science*, 235 (1987) 207.

198 Yokota, R., The granule-containing cell somata in the superior cervical ganglion of the rat, as studied by a serial sampling method for eletron misroscopy, *Z. Zellforsch. Mikrosk. Anat.*, 141 (1973) 331-345.

CHAPTER III

GENERAL METHODS

A.   ISOLATION OF INTRACARDIAC GANGLIA FROM PULMONARY VEIN FAT PAD (PVFP) OF CANINE RIGHT ATRIUM

In order to investigate the physiology and morphology of intracardiac ganglion cells, a new tissue preparation was developed consisting of dissected ganglia from the adult canine heart.

Mongrel dogs of either sex were preanesthetized with morphine (2.0 mg/kg, sc.) approximately 15-20 minutes before being anesthetized with α-chloralose (Sigma, 80-100 mg/kg, iv., in solution with sodium borate, ratio of 1:1.23, chloralose: borate). Alpha-chloralose was used as the general anesthetic, since it does not suppress autonomic reflexes [6,8,21,40]. The trachea was cannulated with a glass Y-tube which was connected to a Harvard respirator. Each dog was ventilated with room air at a positive end-expiratory pressure of 5 cm of water.

Right thoracotomies were performed in the 4th intercostal space to expose the pulmonary veins, superior and inferior venae cavae and the heart. After the opening of pericardium, right atrium and right ventricle were then observed. As described by Randall and coworkers [15,17,33-36], the PVFP is located subepicardially in right atrium, at an area adjacent to right pulmonary vein - left atrial junction and superior venae cavae - right atrial junction (Fig. 3-1). The PVFP was medial to the reflection of the

FIGURE 3-1

LOCATION OF THE PULMONARY VEIN FAT PAD (PVFP)
IN CANINE HEART
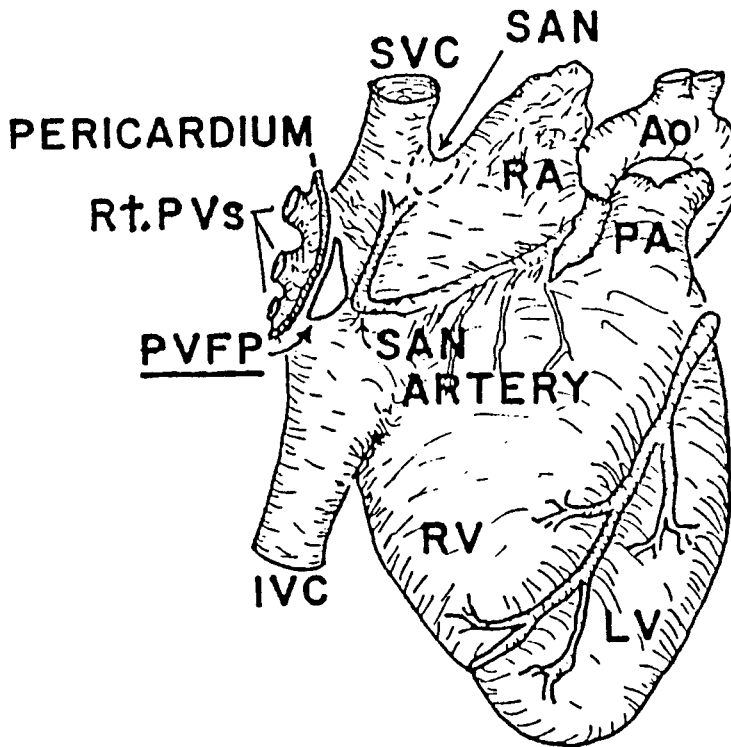
Schematic right lateral view of canine heart and great vessels.
SVC = superior vena cava, SAN = sinoatrial node, RA = right atrium,
Ao = aorta, PA = pulmonary artery, Rt.PVs = right pulmonary veins,
IVC = inferior vena cava, RV = right ventricle, LV = left ventricle

pericardium, originating from the right atrial surface overlying the right pulmonary veins. The PVFP is usually triangular in shape with roughly equilateral dimensions of approximately 1 cm, its base extending from superior to inferior veins along the reflection of the pericardium, and its apex extending nearly to the sinus nodal artery as it courses rostrally in the sulcus terminalis. Underneath the PVFP was the subepicardium of interatrial septum and right atrium.

The entire PVFP, including its surrounding cardiac muscle, was then rapidly removed with scissors, while the heart was pumping or immediately after electrical cardiac fibrillation. To isolate ganglia from the fat pad, the whole mount tissue was pinned to the bottom of a petri dish covered with a translucent silicone resin (Sylgard, Dow Corning), and quickly immersed into cold (0 - 5 °C) Krebs solution (See Section G of Chapter III) continuously aerated with 95% O_2 and 5% CO_2. The PVFP region was then carefully dissected under a dissecting microscope (40 x) using jeweler's forceps and fine scissors, removing much of the superficial fat which was one to several millimeters thick. As the underlying muscle layer was approached, a plexus of 10 to 20 ganglia interconnected by fine interganglionic nerves was readily observed on each piece. The largest percentage of visually identifiable ganglia was located on the ventral half of the PVFP. These ganglia were surrounded by fatty tissue and frequently in close proximity to the subepicardial muscle layer. The remaining fatty tissue above the ganglia was dissected away carefully and thoroughly to expose the top surface of intact ganglionic capsules and connected interganglionic nerves. The interface between the ganglia and the underneath tissue was not disturbed to prevent damage to the ganglia. An

approximate 3 mm x 2 mm x 1 mm (length x width x depth) portion of the tissue

containing one to several surface-cleaned ganglia and connected interganglionic nerves

overlying a thin layer of fatty tissue and cardiac muscle was transferred to the tissue bath

(Fig. 3-2).

Characteristically, this *in vitro* preparation was developed as a ganglionic plexus

composing of *in situ* ganglion cells with intact synaptic connections [30]. The maximum

diameters of identifiable ganglia under dissecting microscopy (40x) varies from 0.2 up

to 3.0 mm [39]. The approximate size of the cells in the ganglion was determined using

hematoxylin-eosin staining of sliced PVFP tissue [39]. Each ganglion contained a few to

over a hundred somata in addition to numerous small satellite cells. The somata had a

mean maximum diameter of 44.6 $\pm$ 7.8 μm with the range of 29.1 - 52.2 μm (n = 40).

These ganglia have been considered parasympathetic in nature even though they may

receive sympathetic innervation [7,38]. These ganglion cells *in vivo* regulate the activities

of the SA node, subsidiary pacemakers and atrial myocytes [2,4,7,35].

In order to acquire a sufficient number of experimental animal, dogs were

sometimes obtained from other laboratories after their primary experiments. The criteria

of selecting experimentally used dogs were 1) the PVFP area and related autonomic

nerves were anatomically intact; and 2) no pharmacological agents have been used other

than the anesthetics. Among the total of 142 dogs used in this dissertation work, 73 dogs

were previously experimented on. Some had acute surgery on the intestines or kidney

for medical students' surgical practice (surgical lab. group, n = 34); these dogs

had intact thoracic cages. Another group of dogs was from the experiments of acute

FIGURE 3-2

ISOLATED INTRACARDIAC GANGLION TISSUE AND ELECTRODES
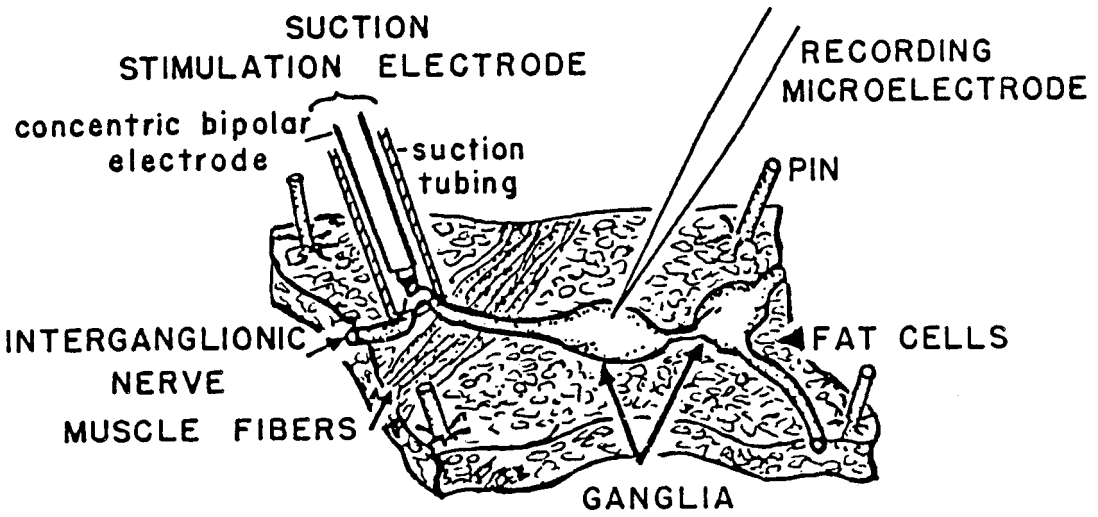
A diagrammatic representation of the isolated intracardiac ganglion tissue viewed by dissecting microscopy. Recording microelectrode is inserted into a ganglion and a suction electrode is placed on an interganglionic nerve.

circumflex coronary artery occlusion and reperfusion (coronary occlusion group, n = 31). Since the blood supply of PVFP region located in the right atrium is provided by right coronary artery, it is assumed that these intracardiac ganglia were not included in the ischemic area (risk zone). The third group of dogs had hemorrhage shock for three hours (hemorrhage shock group, n = 8). The mean blood pressure decrease was usually 30 to 35 mmHg from control.

Since most of the experimentally used dogs were employed in intracellular microelectrode studies, comparisons were made of the passive and active electrical properties (Table 3-1) as well as synaptic transmission of cells from different groups. Fifteen to thirty cells were recorded from 5 to 7 consecutive preparations of each group. As shown in Table 3-1, there were no significant differences in tested passive and active membrane properties among neurons from dogs which were not previously experimented (control group) and dogs from all the other three groups. Spontaneous miniature EPSP-like depolarizations were observed in 9 / 20 (45%) control cells and 26 / 55 (47%) cells of the other three groups. Nerve evoked f-EPSPs were observed in most of the cells from all four groups. In addition, to minimize the effects of the previous procedures, these tissue preparations were always superfused with a Krebs solution for more than one hour before impalement. Therefore, the potential influences of the previous experiments were presumably negligible in these experiments.

TABLE 3-1

PASSIVE AND ACTIVE ELECTRICAL PROPERTIES

OF CELLS FROM DIFFERENT CANINE GROUPS

	RESTING POTENTIAL mV	INPUT RESISTANCE MΩ	TIME CONSTENT ms	ACTION* POTENTIAL AMPLITUDE mV	ACTION* POTENTIAL THRESHOLD -mV
CONTROL GROUP n = 30	59.1 ±1.7 (42.2 - 89.5)	59.1 ±14.3 (8.0 - 205.0)	3.1 ±0.2 (1.4 - 6.9)	77.1 ±2.1 (61.2 - 94.4)	32.4 ±2.6 (22.1 - 44.2)
SURGICAL LABORATORY GROUP n = 30	58.8 ±1.6 (42 - 86)	55.3 ±10.8 (6.9 - 187.5)	2.9 ±0.3 (1.1 - 5.1)	76.4 ±1.5 (56.5 - 88.1)	34.1 ±3.4 (24.8 - 50.0)
CORONARY OCCLUSION GROUP n = 20	60.2 ±2.1 (44 - 90)	58.8 ±7.1 (7.5 - 180.6)	3.1 ±0.6 (1.3 - 8.1)	78.6 ±3.0 (59.1 - 90.3)	31.8 ±3.9 (22.5 - 54.2)
HEMORRHAGE SHOCK GROUP n = 15	59.8 ±1.5 (45 - 87)	54.2 ±11.5 (5.8 - 197.8)	3.3 ±0.7 (1.7 - 9.0)	74.7 ±3.8 (54.3 - 84.4)	32.7 ±1.7 (23.0 - 49.2)
P	NS	NS	NS	NS	NS

Values represent mean ±standard error of the mean. Statistical analysis was done using one way ANOVA. NS =no statistical difference (P >0.05). * intrasomal stimulation evoked action potential

B. INTRACELLULAR RECORDING SYSTEM

A custom designed tissue bath (Fig. 3-3) for intracellular recording was constructed from acrylic plastic. The bottom of the bath was covered with a transparent silicone resin (Sylgard, Dow Corning). The temperature of the bath was controlled by a rubber-coated nichrome heating element placed in the hollow base, a DC proportional temperature control circuit (Fine Science Inc.) and a thermistor placed in the bath adjacent to the tissue. To conduct and maintain the heat, the hollow base was filled with ethylene glycol. In addition, superfusion solutions were preheated before entering the tissue bath by passing these fluids first through stainless steel tubes coiled in the hollow base. In this manner, the tissue and the superfusion fluids were maintained at 34.0 ± 0.5 °C throughout the experiment as recommended by others [27-29].

Unless otherwise mentioned, the bath and tissue were superfused at a rate of approximately 4 ml / min, using a gravity system controlled by a roller clamp. With a volume of 0.6 ml, the turnover time of the tissue chamber was approximately 9 seconds. A double three way valve system was connected to stainless steel tubes (Fig. 3-3) as they exited from the hollow base and in close proximity to the tissue bath. This system allowed for two solutions to have a maintained temperature by their continuous flow through the base. By switching this valve system, rapid changes in the superfusion solutions were possible without affecting the temperature of the bath or the tissue. The fluid removal was accomplished by a cotton wick connected to a small drain sink close to the chamber. Using a dissecting microscopy (Zeiss), the tissue of ganglia isolated from PVFP was carefully pinned to the silicone rubber floor of the tissue bath with fine

FIGURE 3-3

TISSUE BATH AND ACCESSARIES
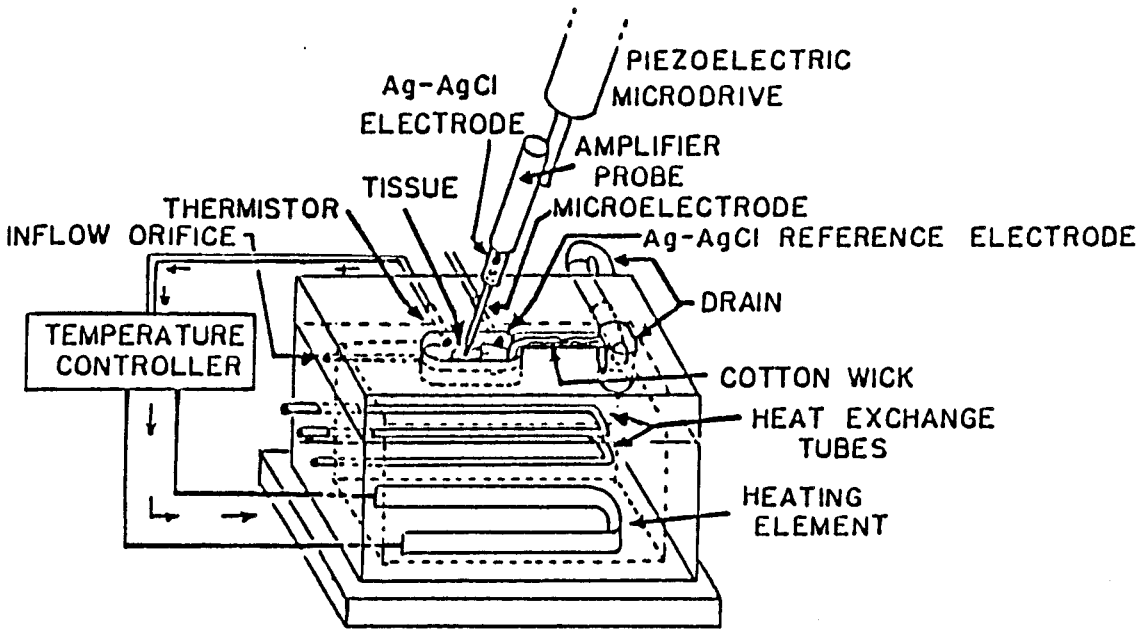
Schematic diagram of the tissue bath, temperature control system, solution superfusion system and microelectrode system.

stainless steel pins. Special care was taken not to damage either the ganglia or the interganglionic nerves.

The tissue bath, associated equipment and electrode holder were mounted on approximate 1 cm thick steel plate which rested on a marble table. To minimize vibrations, the table was mechanically isolated from the floor using rubber shock mounts and sand around the table legs.

Transmembrane potentials were recorded using high resistant, fine electrodes and a high impedance amplifier system as shown in Fig. 3-4. Megohm microelectrodes were made from glass pipettes (FHC, Borosic 1.5 mm OD x 0.75 mm ID) drawn by a horizontal pipette puller (Industrial Science Associates Inc. MI) and filled with 3 M KCl. The microelectrode was placed into a microelectrode holder (FHC) filled also with 3 M KCl and containing a Ag-Ag/Cl half cell. The microelectrode holder was then attached to an amplifier probe mounted to a piezoelectric microdrive attached to a micromanipulator (ENCO, Model 360). This microdrive and its remote controller (Burleigh,PZ 550) allowed for very rapid movements of 2 μm or greater into or out of the tissue. The amplifier probe consisted of a high impedance preamplifier (WP Instruments, Model 701) connected to an amplifier system providing capacitance neutralization, current injection and a virtual bridge circuit. The two unity gain outputs from the amplifier (membrane potentials and voltages proportional to applied currents) were then continuously displayed on a dual beam digital oscilloscope (Nicolet, Model 4094). These signals could be stored on a floppy disk recorder (Nicolet, XF-44) and later plotted on a digital plotter (HP,7475A). Slow membrane potential and current

changes were also simultaneously recorded on a two channel chart recorder (Grass, Model 79C). The transmembrane potentials could be also differentiated to determine the rate of potential changes.

The tissue bath was grounded by a silver-silver chloride (Ag-Ag/Cl) reference electrode immersed in the perfusion solution of the chamber. Thus, the voltage signal recorded was a direct current (DC) recording of the potential change between the recording microelectrode and the reference electrode.

The microelectrode resistance was measured by placing the tip of a microelectrode in the tissue bath containing Krebs solution and passing a 0.2 - 0.3 nA pulse across the tip. The resultant voltage drop across the microelectrode was displayed on the oscilloscope. This voltage drop could be counter balanced by the virtual bridge circuit of the amplifier system, allowing for a direct reading of the electrode resistance. Only electrodes with tip resistances of 40-70 MΩ were used.

C.   RECORDING OF TRANSMEMBRANE POTENTIALS

Standard intracellular recording techniques were used to record transmembrane potentials. The preparations were allowed to be superfused by a Krebs solution aerated with 95% O_2 / 5% CO_2 for more than 1 hour before impalement. Direct intrasomal stimulation was performed during impalement. Pulses of hyperpolarizing or depolarizing current (0.2 nA, 20-30 ms, 1.0 Hz) were injected via recording microelectrode using the virtual bridge circuit which was previously balanced outside of the cell. A stimulator (Grass, model S44) with a stimulus isolation unit was employed for direct intrasomal

stimulation (Fig. 3-4) in all experiments. Penetration of the cells resulted in a sudden negative shift in the observed potential and initiated electrical responses to intrasomal current injection.

Conventional extracellular stimulation techniques were applied. Orthodromic or antidromic responses were elicited using suction electrodes placed on the interganglionic nerves containing preganglionic or postganglionic fibers. The suction electrode method involves the application of a negative pressure which draws the nerve into the end of a polyethylene tube (PE-10) containing a concentric bipolar electrode (Fig.3-2). The tip of the suction electrode was immersed into the perfusion solution so that the nerve was continuously superfused. A Grass S48 stimulator with a stimulus isolation unit was used for extracellular stimulation in all experiments. This experimental system is shown in Fig. 3-4.

The extrinsic parasympathetic and sympathetic efferent innervation to the heart is via the cardiopulmonary nerves [1]. These nerves branch into numerous fine nerve fibers when they enter the heart. It was impossible, under our experimental conditions, to follow the fine nerve fibers through the cardiac tissue to the PVFP. Furthermore, ganglia in the PVFP were usually located in a plexus or in series with each other, so that cardiopulmonary nerve fibers may possibly pass through several ganglia along interganglionic nerves before they innervate a particular ganglion. The interganglionic nerves, hence, could be composed of both preganglionic cardiopulmonary fibers and postganglionic axons which originated from a related ganglion in the PVFP. Thus, stimulation of an interganglionic nerve often activated both pre- or postganglionic fibers

FIGURE 3-4

INTRACELLULAR ELECTRICAL RECORDING SYSTEM
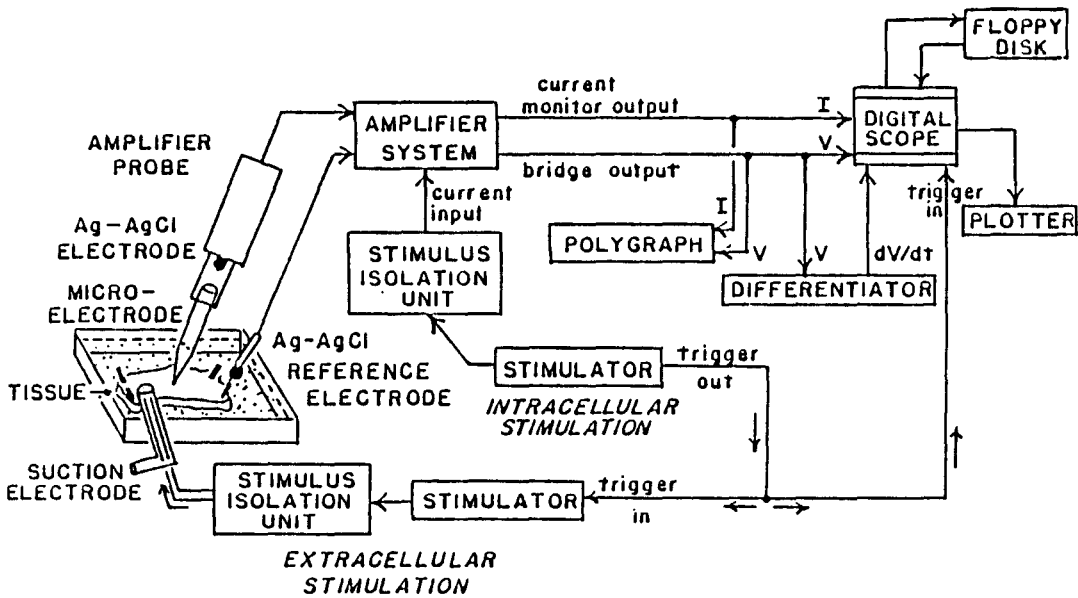
Schematic diagram of the tissue bath and intracellular recording system.

of the ganglion from which the recordings were made (for details, see Chapter VI).

Necessarily, antidromic and orthodromic responses to interganglionic nerve stimulation

were distinguished by the following established criteria[9,22,31]: 1) Orthodromic fast

excitatory postsynaptic potentials (f-EPSPs) possess longer delay times. Orthodromic

action potentials are preceded by f-EPSPs and have a apparently graded or gradual rising

phase. Antidromic action potentials have shorter delay time and a steep rising phase.

Sometimes an inflection is observed at the rising phase of the antidromic action potential.

2) Antidromic action potentials can be separated into two components, initial segment

(IS) spike and soma-dendrite (SD) spike [31,32], by either a hyperpolarizing current pulse

(usually 20-30 mV hyperpolarization) or a repetitive stimulation (up to 30 Hz). Using

the above procedures, the SD spike is blocked and the full action potential is converted

to a short, fast-rising IS spike (Fig. 3-5). 3) Identified antidromic action potentials are

completely unaffected by hexamethonium (10^{-4} M), while orthodromic f-EPSPs and

spikes are consistently abolished.

D.   HORSERADISH PEROXIDASE (HRP) IONTOPHORESIS

Intracellular HRP iontophoresis was employed to characterize the morphological

features of individual canine intracardiac ganglion cells. The isolated whole mount tissue

(See Section A of Chapter III) was pinned down to a strip of silicon rubber (Sylgard,

Dow Corning) adhered to a thin brass plate (4 mm x 5 mm x 0.5 mm). This allowed

the tissue to be removed and histologically prepared without disturbing the tissue. A

Krebs solution was used to superfuse the tissue.

FIGURE 3-5

ANTIDROMIC ACTIVATION OF CANINE INTRACARDIAC NEURON
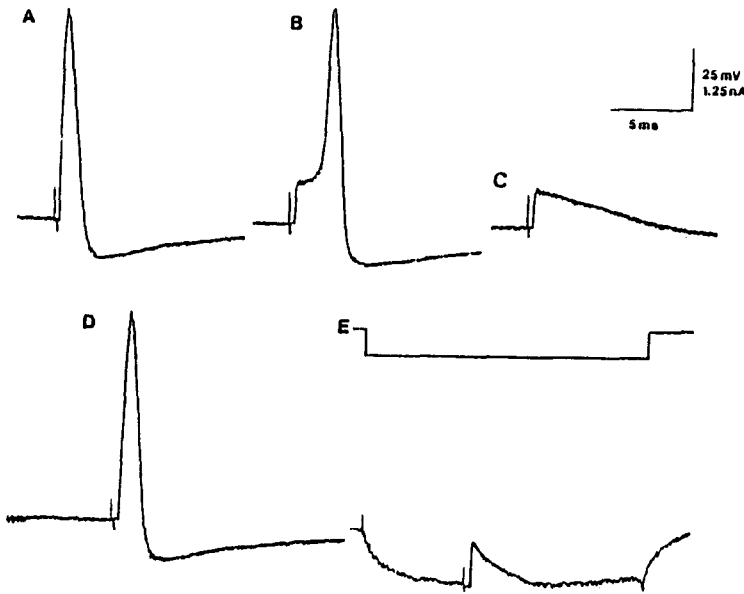
Responses of a ganglionic cell to stimulation of the interganglionic nerve in the presence of hexamethonium (10^{-4} M). A. Antidromic action potential with a steep rising phase. B and C. When the stimulation frequency was increased to 30 Hz, the soma-dendritic (SD) spike is delayed in B and then, fully blocked in C which shows an isolated initial segment (IS) spike. D and E are recorded before and during intrasomal injection of hyperpolarizing current pulse (upper trace in E) while antidromic stimulating at a frequency of 1.0 Hz. Note the hyperpolarizing pulse converts the antidromic action potential (D) to a short, fast-rising IS spike (lower trace in E).

Intracellular injection procedure was performed according to the method of Bosnjak and Kampine [5]. Similar procedures are also used in different laboratories [12,16]. The glass microelectrodes (40-70 MΩ, when filled with 3 M KCl) used for iontophoretic injection were filled with 5% (w/v) HRP (Sigma type IV) in 0.5 M KCl buffered to Ph 7.6 with 0.05 M Tris HCl. Resistance of the microelectrodes filled with HRP solution was higher than 80 MΩ. Ganglion cells were identified by stable resting membrane potentials and the responses to intracellular current injection. After impalement of a ganglion cell, depolarizing current pulses (7.5 nA, 3 Hz, 100 ms duration for 2-10 minutes) were applied to drive iontophoretically the HRP out of the microelectrode into the cytoplasm. Comparable amounts of current have been verified not to damage the cells [27]. Electrophysiological response of the cell could be evaluated when HRP-iontophoresis was stopped momentarily, which permitted one to ascertain whether the microelectrode tip remained within the same neuron for the entire iontophoretic period. Only a few cells were injected in any given ganglion so that injected cell and its processes could be clearly recognized.

Following injection of the cells with HRP, the preparation was superfused for 4 to 5 hours to allow the enzyme to diffuse throughout the processes of the injected neurons [5]. The tissue was then processed by a modification of procedures previously described by Hanker et al. [19,20,5]. After removing from the tissue bath, the undisturbed pinned tissue with the brass plate was incubated for 20 minutes at room temperature into a fresh solution of 10 ml Tris buffer (Ph 7.6) to which was added 100 μl 3% H_2O_2, 10 mg p-phenylenediamine dihydrochloride and 20 mg pyrocatechol. After a saline rinse,

the tissue was then fixed overnight using a phosphate buffered (pH 7.4) solution of 4% paraformaldehyde and 5% glutaraldehyde recommended by Karnowsky [23]. Then the tissue was progressively dehydrated by a series of 10 ml immersions of 50% (10 minutes), 70% (10 minutes), 95% (10 minutes) and 100% (20 minutes) ethanol. A solution of 8% methyl-benzoate in ethanol was utilized for clearing and storage of the tissue before microscopic analysis. These HRP-labeled cells could be preserved in 8% methyl-benzoate solution for months.

To examine microscopically the HRP-labeled cells, the whole tissue was placed in a well formed by gluing a neoprene O-ring (1 cm diameter) to a glass slide and filled with glycerine. The tissue was then examined using a light microscope (Leitz-orthoplan 2) with magnification of 10x, 25x and 40x. Tracing of the cells filled with HRP-reaction products were made using a camera lucida drawing attachment. A Nikon 35 mm camera and film (Kodax T-Max 100) were used for photomicrography. Lengths and diameters were measured from camera lucida tracings by a computer program (Carl Zeiss Videoplan).

E.   GLYOXYLIC ACID FLUORESCENCE OF MONOAMINERGIC NEURONS AND NERVES

Nearly three decades ago, Falck and Hillarp [13,14] took advantage of the fact that in the presence of formaldehyde, monoamines, e.g. dopamine, noradrenaline, adrenaline and serotonin, condense (cyclize) to form intensely fluorescent products. With a fluorescence microscope, neurons containing monoamines could be visualized in thin

sections obtained from tissue previously exposed to formaldehyde vapor. Numerous investigators have used this technique [37]. However, Falck-Hillarp technique is restricted by its prolonged and complicated procedures [11,13,14]. The sensitivity and consistency of this technique, moreover, are not fully acceptable [11]. A much more sensitive and simpler method was introduced using glyoxylic acid by Axelsson [3] and Lindvall and Bjorklund [25,26]. Glyoxylic acid condensed with catecholamines results in a more enhanced and stable fluorophor than the formaldehyde technique, providing a better visualization of the cell bodies and fine axons [37]. Therefore, glyoxylic acid condensation technique was chosen for this dissertation work.

The modified glyoxylic acid condensation technique used in this experiment is reported by De La Torre and Surgeon [10,11]. Their standardized sucrose-potassium phosphate-glyoxylic acid (SPG) method provides advantages over other techniques, e.g. 1). SPG reaction takes only 3 seconds and the entire procedure is done within 15 minutes; 2). very simple equipment and glassware are required and 3). more important, the tissue section will maintain their fluorescence for several months [10].

The SPG solution was prepared as follows: 1). The sucrose (10.2g / 150 ml, 0.200 M) and KH_2PO_4 (4.8g / 150 ml, 0.236 M) crystals were dissolved in 100 ml distilled water using a magnetic stirrer. 2). The glyoxylic acid crystals (1.5g / 150 ml, 1%) were added and stirred until solution became clear. 3). The solution was adjusted by titrating with 1 N NaOH (about 35 ml) to pH 7.4. And 4). A final volume of 130 ml was obtained by adding distilled water (about 15 ml).

The PVFP was quickly dissected from canine right atrium (See Section A of

Chapter III) and cut into smaller pieces (3-4 mm^3). A few drops of distilled water were placed on the surface of a pre-cooled cryostat chuck and a small piece of tissue was oriented on it. The chuck with the tissue was quickly returned to the -30 °C cryostat for rapid freezing at an average rate of -8 °C /min. After the tissue became frozen in the cryostat (6-9 min.), 16 or 32 μ sections were cut. Each section was picked up with clean but non-treated, room temperature glass slide by gently pressing the slide against the cryostat knife blade. The tissue would adhere to the slide, and several seconds were allowed for the section to melt onto the slide. The section then was quickly dipped 3 times (1 dip/sec) in the room temperature SPG solution . Excess fluid was removed from the slide with absorbent paper by tilting the slide and wiping off the edges and bottom, taking care not to disturb the tissue. The wet tissue section slides were then completely dried by a fan using room air (several minutes). Slides were put in a pre-warmed oven set at 80 °C for exactly 5 minutes. After 5 minutes, slides were removed from oven, a few drops of mineral oil were added near the tissue followed by placing a cover-slip on top of the tissue.

Tissue sections were examined using a epifluorescent microscope (Olympus, Model A041). Photomicrographs were taken by an attached camera and films (Kodax T-Max 100).

F. DATA ANALYSIS

All data were expressed as mean $\pm$ standard error of the mean (Mean $\pm$ SEM). Analysis of data was performed by comparison of two or more groups (paired or

unpaired) and by applying the Student's t-test or appropriate form of analysis of variance, respectively [18]. All statistical tests were run on a software package Primer [18]. The particular tests used and data analysis will be discussed under each specific project. Differences were considered statistically significant at a $P < 0.05$ level.

G.   SOLUTIONS, PHARMACOLOGIC AGENTS AND CHEMICAL REAGENTS

1. Solutions

The physiological Krebs solution used to superfuse the preparation has the following compositions: NaCl 117mM, KCl 4.7mM, $CaCl_2$ 2.5mM, $MgCl_2$ 1.2mM, $NaHCO_3$ 25mM, NaH_2PO_4 1.2mM and glucose 11mM. After aerated with 95% O_2 and 5% CO_2 at room temperature, the pH was 7.36 ± 0.04 (n = 10). Krebs solution was prepared 2 - 4 hours before each experiment and only twice distilled, deionized water was used. Ice cold Krebs solution was made by putting the solution into a freezer till it was frozen.

The low Ca^{2+}, high Mg^{2+} solution was prepared as follows: NaCl 108.45mM, KCl 4.7mM, $CaCl_2$ 0.25mM, $MgCl_2$ 12.0mM, $NaHCO_3$ 25mM, NaH_2PO_4 1.2mM and glucose 11mM. pH was similar to standard Krebs solution.

The high K^+ solution was prepared by substituting KCl for NaCl.

2. Pharmacologic Agents

The drugs were applied to the preparation by dissolving them in the Krebs

solution superfusing the preparation. In some experiments, acetylcholine or bethanechol was introduced by a pressure micro-ejection system. This system consisted of ejecting very small quantities of agents in a microelectrode in close proximity to the recording cell, using high pressure nitrogen (1700 mmHg) and a very fast solenoid valve controlled by a stimulator (Grass, Model S4). By varying the open duration of the valve, the amount of agent ejected was proportionally varied.

Anesthetics

morphine

alpha-chloralose (Sigma)

sodium borate (Sigma)

Cholinomimetics

acetylcholine chloride (Sigma)

bethanechol chloride (Sigma)

physostigmine sulfate (Sigma)

Cholinolytics

hexamethonium bromide (Sigma)

atropine (Sigma)

4-diphenyl-acetoxy-N-methyl piperidine methiodide (4-DAMP, Sigma)

pirenzepine dihydrochloride (Sigma)

Adrenolytic drugs

phentolamine hydrochloride (Regitine, CIBA Pharmaseutical Co.)

l-propranolol (Sigma)

Sodium channel blocker

Tetrodotoxin (TTX, Sankyo or Sigma)

3. Chemical Reagents

horseradish peroxidase (Sigma type IV)

Tris Base (Trizma, Sigma)

p-phenylenediamine dihydrochloride (Sigma)

pyrocatechol (Sigma)

paraformaldehyde (J.T.Baker)

glutaraldehyde (Kodak)

ethanol (USI Chemical Co.)

methyl-benzoate (MCIB)

poly-l-lysine (Sigma)

potassium phosphate KH_2PO_4 (SP)

glyoxylic acid monohydrate (Sigma)

sucrose crystals (SP)

H. REFERENCES

1 Armour, J.A. and Hopkins, D.A., Anatomy of extrinsic efferent autonomic nerves and ganglia innervating the mammalian heart. In W.C. Randall (Ed.), *Nervous Control of Cardiovascular Function*, Oxford University Press, New York, 1984, pp. 20-45.

2 Armour, J.A., Yuan, B. and Butler, C.K., Cardiac responses elicited by peptides administered to canine intrinsic cardiac neurons, *Peptides*, 11 (1990) 753-761.

3 Axelsson, S., Bjorklund, A., Falck, B., Lindvall, O. and Svensson, L.A., Glyoxylic acid condensation: A new fluorescence method for the histochemical demonstration of biogenic monoamines, *Acta. Physiol. Scand.*, 87 (1973) 57-62.

4 Bluemel, K.M., Wurster, R.D., Randall, W.C., Duff, M.J. and O'Tool, M.F., Parasympathetic postganglionic pathways to the sinoatrial node, *Am. J. Physiol.*, 259 (1990) H1504-H1510.

5 Bosnjak, Z.J. and Kampine, J.P., Electrophysiological and morphological characterization of neurons in stellate ganglion of cats, *Am. J. Physiol.*, 248 (1985) 288-292.

6 Brown, R.V. and Hilton, J.G., The effectiveness of the baroreceptor reflexes under different anesthetics, *J. Pharmacol. Exp. Ther.*, 118 (1956) 198-203.

7 Butler, C.K., Smith, F.M., Cardinal, R., Murphy, D.A., Hopkins, D.A. and Armour, J.A., Cardiac responses to electrical stimulation of discrete loci in canine atrial and ventricular ganglionated plexi, *Am. J. Physiol.*, 259 (1990) H1365-H1373.

8 Cox, R.H. and Bagshaw, R.J., Effects of anesthesia on carotid sinus reflex control of arterial hemodynamics in the dog, *Am. J. Physiol.*, 239 (1980) H681-H691.

9 Crowcroft, P.J. and Szurszewski, J.H., A study of the inferior mesenteric and pelvic ganglia of guinea-pigs with intracellular electrodes, *J. Physiol. (Lond.)*, 219 (1971) 421-441.

10 De La Torre, J.C., An improved approach to histofluorescence using the SPG method for tissue monoamines, *J. Neurosci. Methods*, 3 (1980) 1-5.

11 De La Torre, J.C. and Surgeon, J.W., A methodological approach to rapid and sensitive monoamine histofluorescence using a modified glyoxylic acid technique: the SPG method, *Histochemistry*, 49 (1976) 81-93.

12 Dryer, S.E. and Chiappinelli, V.A., An intracellular study of synaptic transmission and dendritic morphology in sympathetic neurons of the chick embryo, *Dev. Brain Res.*, 22 (1985) 99-111.

13 Falck, B., Observation on the possibilities of the cellular localization of monoamines by a fluorescence method, *Acta. Physiol. Scand.*, 56 (1962) suppl. 197-suppl. 203.

14 Falck, B., Hillarp, N.A., Thieme, G. and Torp, A., Fluorescence of catecholamines and related compounds condensed with formaldehyde, *J. Histochem. Cytochem.*, 10 (1962) 348-354.

15 Fee, J.D., Randall, W.C., Wurster, R.D. and Ardell, J.L., Selective ganglionic blockade of vagal inputs to sinoatrial and /or atrioventricular regions, *J. Pharmacol. Exp. Ther.*, 242 (1987) 1006-1012.

16 Forehand, C.J. and Purves, D., Regional innervation of rabbit ciliary ganglion cells by the terminals of preganglionic axons, *J. Neurosci.*, 4 (1984) 1-12.

17 Gagliardi, M., Randall, W.C., Bieger, D., Wurster, R.D., Hopkins, D.A. and Armour, J.A., Activity of in vivo canine cardiac plexus neurons, *Am. J. Physiol.*, 255 (1988) 789-800.

18 Glantz, S.A., *Primer of Biostatistics*, 2nd edn., McGraw-Hill Book Company, New York, 1988, 64 pp.

19 Hanker, J.S., Yates, P.E., Metz, C.B. and Rustioni, A., A new specific, sensitive and non-carcinogenic reagent for the demonstration of horseradish peroxidase, *Histochem. J.*, 9 (1977) 789-792.

20 Hanker, J.S., Yates, P.E., Metz, C.B. and Rustoni, A., A new specific, sensitive and non-carcinogenic reagent for the demonstration of horseradish peroxidase, *Histochem. J.*, 9 (1977) 789-792.

21 Harvey, S.C., Hypnotics and sedatives. In A.G. Gilman, L.S. Goodman, T.W. Rall and F. Murad (Eds.), *The Pharmacological Basis of Therapeutics*, Macmillan Publishing Company, New York, 1985, pp. 339-371.

22 Julé, Y., Krier, J. and Szurszewski, J.H., Patterns of innervation of neurones in the inferior mesenteric ganglion of the cat, *J. Physiol. (Lond.)*, 344 (1983) 293-304.

23 Karnowsky, M.J.A., Formaldehyde-glutaraldehyde fixative of high osmolarity for uses in electron microscopy (Abstract), *J. Cell Biol.*, 27 (1965) 137A-138A.

24 Kondo, H., Dun, N.J. and Pappas, G.D., A light and electron microscopic study of the rat superior cervical ganglion cells by intracellular HRP-labeling, *Brain Res.*, 197 (1980) 193-199.

25 Lindvall, O. and Bjorklund, A., The glyoxylic acid fluorescence histochemical method: A detailed account of the methodology for the central catecholamine neurons, *Histochemistry*, 39 (1974) 97-127.

26 Lindvall, O., Bjorklund, A., Hokfelt, T. and Ljungdahl, A., Application of the glyoxylic acid method to vibratome sections for improved visualization of central catecholamine neurons, *Histochemistry*, 35 (1973) 31-38.

27 Ma, R.C. and Dun, N.J., Vasopressin depolarizes lateral horn cells of the neonatal rat spinal cord in vitro, *Brain Res.*, 348 (1985) 36-43.

28 Ma, R.C. and Dun, N.J., Excitation of lateral horn neurons of the neonatal rat spinal cord by 5-hydroxytryptamine, *Dev. Brain Res.*, 24 (1986) 89-98.

29 Mo, N. and Dun, N.J., Is glycine an inhibitory transmitter in rat lateral horn cells?, *Brain Res.*, 400 (1987) 139-144.

30 Mostafa, M.H., Xi, X., Wurster, R.D., LaVelle, F. and Neafsey, E.J., Light and electron microscopic study of neurons in cardiac ganglia of the rat and dog, *Soc. Neurosci. Abs.*, 16 (1990) 860-860.(Abstract)

31 Perri, V., Sacchi, O. and Casella, C., Synaptically mediated potentials elicited by the stimulation of post-ganglionic trunks in the guinea-pig superior cervical ganglion, *Pflugers. Arch.*, 314 (1970) 55-67.

32 Prigioni, I. and Russo, G., Intracellular recordings from "recurrent neurons" in the rat superior cervical ganglion, *J. Auton. Nerv. Syst.*, 31 (1990) 85-90.

33 Randall, W.C. and Ardell, J.L., Selective parasympathectomy of autonomic and conductile tissue of the canine heart, *Am. J. Physiol.*, 248 (1985) H61-H68.

34 Randall, W.C. and Ardell, J.L., Differential innervation of the heart. In D. Zipes and J. Jalife (Eds.), *Cardiac Electrophysiology and Arrhythmias*, Grune & Stratton, New York, 1985, pp. 137-144.

35 Randall, W.C., Ardell, J.L., Wurster, R.D. and Milosavljevic, M., Vagal postganglionic innervation of the canine sinoatrial node, *J. Auton. Nerv. Syst.*, 20 (1987) 13-23.

36 Randall, W.C., Milosavljevic, M., Wurster, R.D., Geis, G.S. and Ardell, J.L., Selective vagal innervation of the heart, *Ann. Clin. Lab. Sci.*, 16 (1986) 198-208.

37 Weiner, N. and Molinoff, P.B., Catecholamines. In G.J. Siegel, B.W. Agranoff, R.W. Albers and P.B. Molinoff (Eds.), *Basic Neurochemistry*, Reven Press, New York, 1989, pp. 233-269.

38 Wurster, R.D., Xi, X., Webber, M. and Randall, W.C., Morphological organization of ganglion cells and small intensely fluorescent (SIF) cells of the canine intracardiac ganglia, *Soc. Neurosci. Abs.*, 16 (1990) 860-860.(Abstract)

39 Xi, X., Thomas, J.X., Randall, W.C. and Wurster, R.D., Intracellular recordings from canine intracardiac ganglion cells, *J. Auton. Nerv. Syst.*, 32 (1991) 177-182.

40 Zimfer, M., Sit, S.P. and Vatner, S.F., Effects of anesthesia on the canine carotid chemoreceptor reflex, *Cardiovasc. Res.*, 48 (1981) 400-406.

CHAPTER IV

MORPHOLOGY OF CANINE INTRACARDIAC GANGLION CELLS ---

INTRACELLULARLY LABELED GANGLION NEURONS AND

HISTOCHEMICALLY STAINED SIF CELLS

A. INTRODUCTION

Understanding of the structure and function of intracardiac ganglion cells has been

derived primarily from studies of amphibians [45], where these cells are located in a nearly

transparent interatrial septum [48,49]. One can directly see the cellular details (e.g. cell

bodies, axons and boutons) in living tissue with differential interference contrast optics.

There are two types of neurons in the mudpuppy intracardiac ganglia [48]: unipolar

principal cells (30-50 μm) that send post-ganglionic parasympathetic axons to cardiac

muscle, and SIF cells or catecholamine-containing interneurons (10-30 μm), with short

processes synapsing upon principal neurons. Principal cell bodies receive synapses from

preganglionic neurons, interneurons and other principal cells. The small intensely

fluorescent (SIF) cells are innervated by vagal terminals that make contact on their

processes. Moreover, gap junctions are formed between the SIF cells and principal

neurons. One vagal preganglionic fiber diverges to innervate more than one ganglion

cells. However, each ganglion cell receives inputs from only one vagal preganglionic

fiber. Recently, the distribution of some novel peptides has been reported in principal

neurons and interneurons [52,59,60]. In addition, exogenous adrenergic fibers, most likely

73

sympathetic postganglionic axons, have also been demonstrated in these ganglia [51,52]. On the other hand, the intracardiac ganglia of frog are relatively simple with no observed SIF cells or interneurons [24,45,48,49,76].

Compared to amphibian ganglia, far less is known about the morphological features and organization of mammalian intracardiac ganglia [19,21,37,41,46,57,58]. This is due mainly to inaccessibility of these ganglia [45]. Histological studies revealed oval shaped cell bodies (30-50 μm in diameter) with one or more nucleoli, surrounded by small satellite cells [41,57] in the wall of the atrium.

Most autonomic ganglia have a variable number of small cells which have a high content of catecholamines. The nomenclature for these cells, e.g. SIF cells, small granule-containing cells or catecholamine-containing interneurons, reflects the methodology by which they were studied. The functional role of the SIF cells is not well understood. In earlier studies, SIF cells were not found in mammalian intracardiac ganglia [12,19,20,68]. After pretreatment with both a monoamine oxidase inhibitor and a precursor of catecholamines, Jacobowitz [37] obtained monoamine fluorescence in intracardiac ganglia of rats, cats, guinea pigs and mice. Varicose adrenergic fibers were seen in close apposition to some cholinergic ganglion cells. Most SIF cells are innervated by cholinesterase-staining nerve fibers. Some of them also receive a postganglionic parasympathetic innervation from cholinergic intracardiac ganglion cells.

The characteristics of synaptic structures and neurochemistry of mammalian intracardiac ganglion cells have been studied primarily on embedded or frozen sectioned tissue. Malor and coworkers [46] described the ultrastructure of guinea pig intracardiac

ganglia, identifying three types of synapses: axo-dendritic, axo-somatic and axo-axonal synapses. All presynaptic nerves were cholinergic. No nerve terminals synapsed on chromaffin cells. Based upon histochemical and silver staining of atrial ganglia of monkey, Osborne et al.[57] noted that most neurons were acetylcholinesterase-positive. Neurons were classified by their intensity of silver staining as large multipolar neurons with a deeply impregnated cytoplasm, lightly stained bipolar or tripolar neurons and intermediate neurons.

Morphological features of primary cultured intracardiac ganglion cells of guinea-pig have been recently published by Hassall and Burnstock [33]. Somata were 25-35 μm in diameter with relative large nuclei (5 x 10 μm in diameter). Groups of neurons were often associated with bundles of neurites extending for hundreds of μm. All cells were shown to contain acetylcholinesterase. Occasionally, SIF cells were observed after glyoxylic acid fluorescence histochemistry. No catecholamine-containing ganglion neurons were found.

Although histochemical and immunocytochemical experiments usually reveal a great number of neurons, reconstruction of individual neurons and their fine processes is frequently difficult [64]. Relatively few details are available on the morphology and organization of intact mammalian intracardiac overall ganglion cells. As an obligatory first step to a better understanding of how the parasympathetic nervous system directly contributes to the control of cardiac function of mammals, it is important to establish the morphological characteristics of neurons in the ganglia. Consequently, the present experiments were designed to assess their morphology and organization in the canine

heart. Specifically, the following hypotheses were tested:

1. Canine intracardiac ganglion neurons are morphologically heterogenous.

2. Both postganglionic projection cell and cell which has only *intra*ganglionic activity are present.

3. SIF cells exist in dog intracardiac ganglia.

4. Morphological distinctions are present between previously identified functional cell types, i.e. R-, S- and N-cells [77,78] (See Chapter V).

The dog model was chosen because our laboratory had localized canine intracardiac ganglia in a right atrial fat pad or pulmonary vein fat pad (PVFP) [62,63,78]. Vagal regulation of heart rate in canine is mediated by clusters of ganglion cells located in PVFP [62,63]. Those studies enabled me to isolate the ganglion and generate a new ganglionic preparation of canine intracardiac ganglia [78] (see Chapter V).

As discussed in Chapter V, canine intracardiac ganglion cells could be categorized electrophysiologically into three groups, based upon their responses to outward, depolarizing current injection for 200 ms [77,78]: R-cells responded with multiple spikes, S-cells responded with only one or two spikes at the onset of the pulse and N-cells exhibited no action potential. These cell types have significantly different passive membrane properties. R-cells have the smallest resting membrane potential, the longest time constant and highest input resistance. N-cells have the largest resting membrane potential, the shortest time constant and the lowest input resistance. S-cells have properties between R- and N-cells.

Intracellular HRP staining on whole mount tissue is one of the only means to

acquire information on the orientation of neurons in relation to other neurons and the extent of processes of individual cells [13]. The advantages of using HRP intracellular iontophoresis technique to elucidate cellular morphology are that: a). HRP could be readily transported anterogradely into fine terminals, hence a high resolution is provided; b). combined with the intracellular recording technique, one may easily correlate structure with function of any single neuron; and c). a three dimensional view of the intact neurons could be possibly seen using whole mount tissue and a light microscopy. In addition, a separate group of experiments was performed using glyoxylic acid fluorescent technique to verify the presence of SIF cells in canine intracardiac ganglia [33,37,48].

B.   METHODS

1. HRP Iontophoresis

Right thoracotomies were performed on mongrel dogs (15-20 kg) of either sex, which were anesthetized with morphine (2 mg/kg, sc) followed by α-chloralose (80-100 mg/kg, iv). The PVFP was rapidly removed and placed in cold Krebs solution (see Chapter III) continuously aerated with 95% O_2 and 5% CO_2. The fat pad region was then dissected under a dissecting microscope. The portion of the fat pad (3 mm x 2 mm x 1 mm) containing some of the ganglia was transferred to the tissue bath and pinned down to a strip of silicon rubber adhered to a thin brass plate. This was placed in the bottom of the tissue bath and allowed removal and histological preparation without disturbing the tissue.

The tissue bath was maintained at 34.0 $\pm$ 0.5 °C and was superfused with Krebs solution aerated with 95% O_2 and 5% CO_2. Transmembrane potentials were recorded with glass microelectrodes and a high impedance amplifier (WP Instruments, model M701). These microelectrodes (40-70 MΩ, when filled with 3 M KCl) were filled with 5% HRP (Sigma type VI) and 0.5 M KCl buffered to pH 7.6 with 0.05 M Tris. During impalement by the microelectrode, a 1.0 Hz, 0.2 nA current injections were applied for 20-30 ms using a virtual bridge circuit which was previously balanced outside the cell. Membrane potentials and voltages proportional to applied currents were monitored and stored on a digital oscilloscope (Nicolet, model 4094).

After recording stable resting membrane potential and responses to intracellular stimulations (200 ms), depolarizing current pulses (7.5 nA, 3 Hz, 100 ms duration for

2-10 minutes) were applied to drive iontophoretically the HRP out of the microelectrode into the cytoplasm. Electrophysiological responses of the cell could be evaluated when HRP-iontophoresis was stopped momentarily, which permitted us to ascertain whether the microelectrode tip remained within the same neuron for the entire iontophoretic period. Only a few cells were injected in any one ganglion so that we could clearly recognize each injected cell and its processes. Following labeling of cells, the preparation was superfused for 3 to 5 hours to allow the HRP to diffuse throughout the processes of the injected neurons. Following removal from the tissue bath, the undisturbed, pinned tissue was incubated for 20 minutes at room temperature in a fresh solution of 10 ml Tris buffer (pH 7.6) to which was added 100 μl 3% H_2O_2, 10 mg p-phenylenediamine dihydrochloride (Sigma) and 20 mg pyrocatechol (Sigma). After a saline rinse, the tissue was fixed overnight using phosphate buffered (pH 7.4) solution of 4% paraformaldehyde and 5% glutaraldehyde. Then the tissue was progressively dehydrated by a series of immersions in 50%, 70%, 95% and 100% ethanol. The tissue was cleared and stored in 8% methyl-benzoate in ethanol.

To examine microscopically the tissue, the whole tissue was placed on a glass slide in a well formed by gluing a neoprene O-ring (1 cm diameter) to a glass slide and filled with glycerine. The tissue was examined using a light microscope (Leitz-orthoplan 2) with magnifications of 10x, 25x and 40x. All cells filled with HRP-reaction products were traced using a camera lucida drawing attachment. While tracing the entire course of processes, neurons were viewed in different focal planes so as to achieve an accurately focused trace of all segments of any fine process. These tracings were reconstructions

of two dimensional projections of three dimensional microscopic images. Photomicrographs of some neurons and their processes were taken at different planes of focus using a Kodak T-Max 100 (black and white) negative film. Sometimes those photomicrographs were superimposed to form a photomontage to reconstruct the cell's morphology.

Measurements: Lengths of neuronal processes and diameters of cell bodies were measured using cell tracings and Carl Zeiss Videoplan which provides the digital length of a curve or area of a profile. Short and long axes of a soma represented the smallest and largest dimensions of the oval cell body. Soma area was the area within the confines of two dimensional soma trace. Primary dendrites were the processes protruding directly from soma. Secondary and tertiary dendrites were the processes coming off of primary and secondary dendrites, respectively. Total dendrite length was obtained by adding up the lengths of all dendrites. Attention has been paid to observe the entire three dimensional structure of each cell by adjusting the focus of the microscopy.

Tissue shrinkage may occur from the fixation strategy. It has been reported from some other studies that tissue shrinkage was insignificant (<1%) [42,69]. However, shrinkage may affect various components of the tissue unequally, and the processes of injected and filled cells may corrugate rather than reducing in length if shrinkage occur [42]. Considering these complexities, no correction for shrinkage has been made in the present study. As well, since all lengths were measured from two dimensional camera lucida tracings, no correction for three-dimensional projection errors has been applied. Therefore, it is important to know that the length values reported in the present

study may be somehow underestimated.

Criteria for Identification of Structures: Axons were distinguished by their small diameter, paucity of spinous processes and extended length [1,64]. Axon collaterals were the branches arising from a point along an axon, which could be followed more than 20 μm and distinguished from nearby or crossing dendritic processes [47,66]. Process swellings were defined as discrete outbulgings having at least twice the diameter of the adjacent parts of the parent process [11]. Spines were short protuberances with the length less than 15-20 μm [47].

Classification of Neurons: Morphologically, *intra*ganglionic neurons refer to the cells whose all processes were restricted in the confines of the ganglion; principal neurons are the postganglionic parasympathetic projection neurons with their axon protruding into the cardiac tissue via interganglionic nerve; *inter*ganglionic neurons are an assumed cell type which sent their axons to the neurons of another ganglion via interganglionic nerve. A three dimensional observation of the interaction of processes from different neurons was particularly confirmed by adjusting the focus of the microscopy.

2. Glyoxylic Acid Fluorescent Staining [14]

The PVFP was quickly dissected from canine heart and cut into smaller pieces (3-4 mm^3). One of the small pieces was oriented on a pre-cooled cryostat chuck. When the tissue has frozen in the cryostat (6-9 minutes), 16 or 32 μM sections were made. The section was picked up with a glass slide and then dipped three times into the sucrose - potassium phosphate - glyoxylic acid solution. The wet tissue section slides were then

completely dried by a fan using room air (several minutes). Slides were put in a pre-warmed oven at 80 °C for 5 minutes. Then slides were removed from the oven, a few drops of mineral oil were added; and then a cover-slip was ultimately placed on top of the tissue. Tissue sections were examined in a fluorescent microscope (Olympus, Model A041) with a 560 nM wavelength filter, from which photomicrographs were made. (See Chapter II for details)

3. Statistical Analysis

All quantitative data were expressed as mean $\pm$ standard error of the mean (Mean $\pm$ SEM). The comparison between two groups in Table 1 was achieved using Student's t test (unpaired). The comparison among three groups in Table 2 was performed by applying the One Way Analysis of Variance. Statistical differences between groups were identified by Student-Newman-Keuls test. All statistical tests were run on the software of Primer [27]. Differences were considered statistically significant at a $P < 0.05$ level.

C. RESULTS

1. HRP-Labeled Neurons

Forty-six injections were made in 32 ganglia from 19 dogs, yielding 40 successfully labeled neurons whose distal processes were completely and intensely labeled. The ganglionic neurons impaled with HRP-filled microelectrodes had resting membrane potentials of -45 mV to -90 mV (mean, -60 $\pm$ 2 mV). Intracellular injection of HRP did not cause appreciable changes in the transmembrane potential.

a. Somata

In whole tissue mounts using light microscopy, all labeled somata appeared dark brown and oval or elongated with a mean long axis of 62 $\pm$ 3 μm and a short axis of 40 $\pm$ 2 μm (Fig. 4-1). Spine-like protuberances arose from the soma of most of the cells and achieved lengths of a few μm. Soma were equally distributed throughout the confines of ganglia.

b. Dendrites

Each ganglion neuron contained 2 to 12 primary dendrites (5.4 $\pm$ 0.4) which ranged in length between 16 and 276 μm (mean, 77 $\pm$ 6 μm), tapering gradually and branching frequently (Fig. 4-2). Many primary dendrites had multiple secondary and tertiary branches which were shorter in length. The sum of the length of all dendrites of individual neurons varied from 26 to 2153 μm (653 $\pm$ 61 μm). All dendritic trees remained within the ganglion usually extending over 20% - 43% of the area of the ganglion (Figs. 4-2 and 4-3). Close interactions between processes of two adjacent neurons were observed in cases when more than one neurons were labeled in the same

FIGURE 4-1

A HRP-LABELED NEURON IN CANINE INTRACARDIAC GANGLION IN PULMONARY VEIN FAT PAD (PVFP)
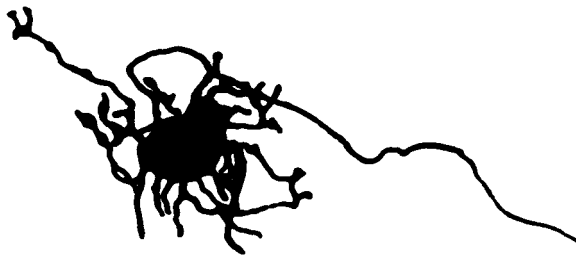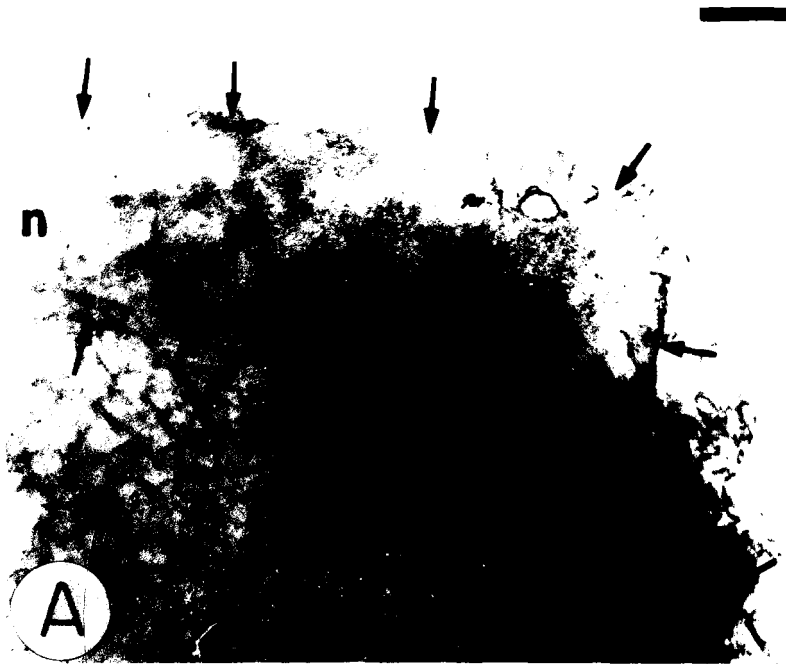
A HRP-labeled neuron in canine intracardiac ganglion in pulmonary vein fat pad. A. Photomicrograph of a ganglion with a labeled neuron. The outline of the ganglion is indicated by arrows. N - interganglionic nerve. Calibration bar = 0.1 mm.; B. Camera lucida drawing of the same neuron as in A. Soma was oval with axes of 40 and 68 μm. Note varicosities and terminal swellings on dendrites. Axon terminates within the confines of the ganglion indicating *intra*ganglionic neuron. Calibration bar = 0.1 mm.

FIGURE 4-2

R-, S- AND N-CELL
FUNCTIONAL CLASSIFICATION AND CELL MORPHOLOGY
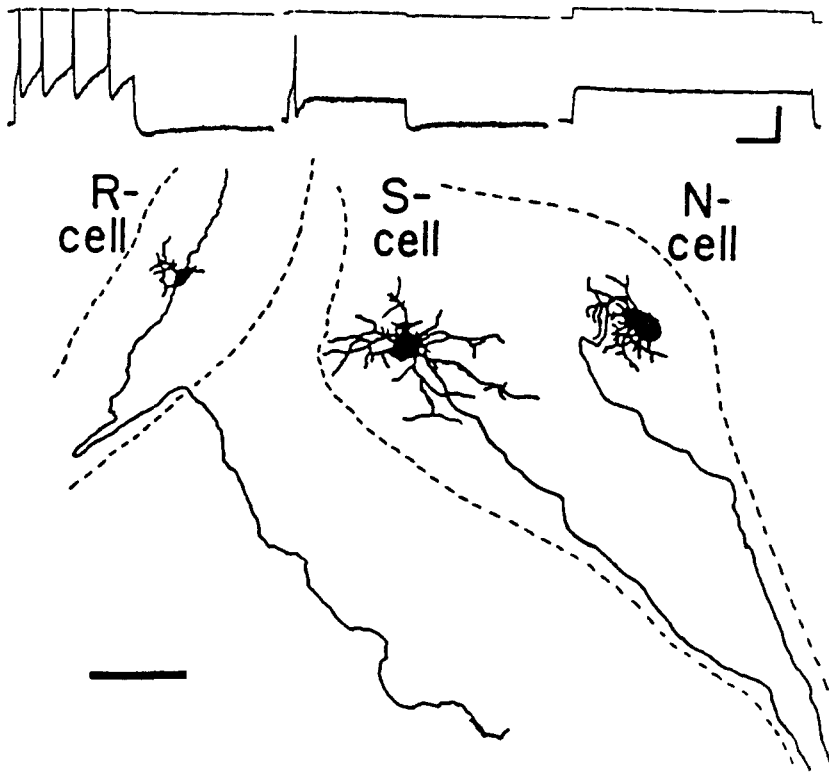
Above: Upper tracings indicate depolarizing current application. Lower tracing is transmembrane potential. In response to depolarizing current, R-cell responds with repetitive action potentials, S-cell responds with one or two action potentials and N-cell does not respond with an action potential no matter how large or long the depolarization. Vertical calibration bar = 50 mV or 1.5 nA. Horizontal calibration bar = 100 ms.

Below: Camera lucida drawings of the above functionally identified cells. The R-cell had soma axes of 34 x 60 μm and axon length of 1,969 μm, the S-cell had soma axes of 51 x 68 μm and axon length of 1,487 μm and the N-cell had soma axes of 46 x 86 μm and axon length of 1,350 μm. The S- and R-cells were from the same ganglion while the R-cell was labeled in another ganglion. Notice the frequently branching of dendrites and the looping and terminal swelling of axon of the R-cell. Dendritic trees remained within the ganglia extending over 20-43% of the area of the ganglia. All three neurons were principal neurons or *inter*ganglionic neurons. Calibration bar = 0.2 mm.

FIGURE 4-3

CAMERA LUCIDA DRAWING OF A PRINCIPAL NEURON
AND AN *INTRA*GANGLIONIC NEURON
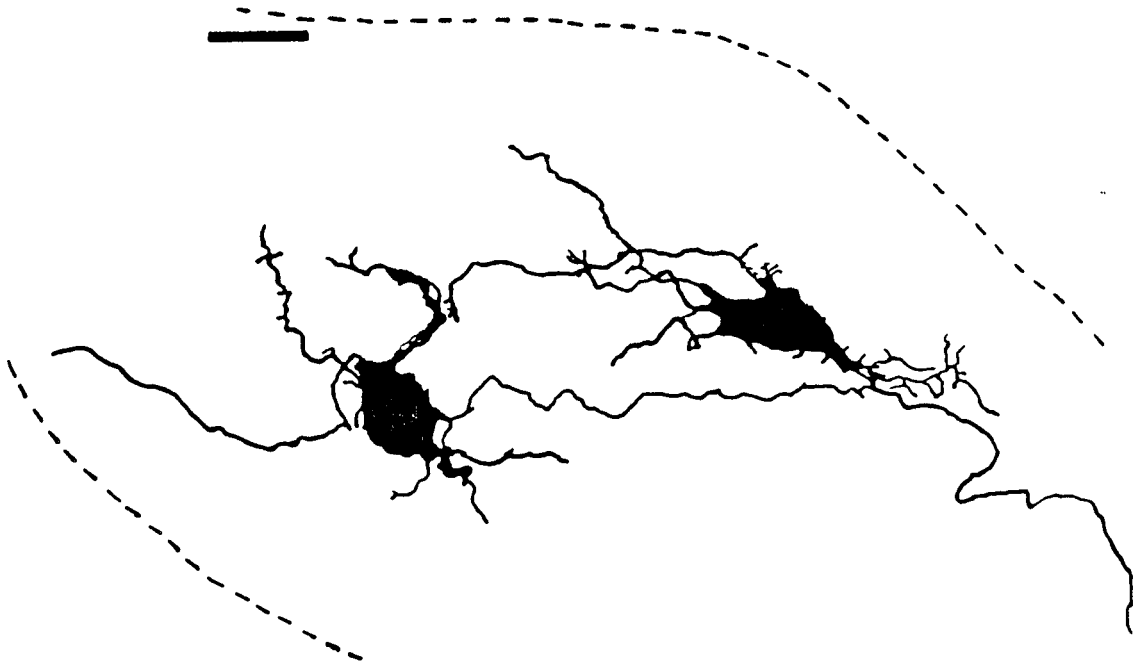
The principal cell (right cell) has a long axon which courses to the interganglionic nerve. The *intra*ganglionic neuron (left neuron) has no long axonal process but rather has an axonal-like process terminating in close proximity to the dendrites of the principal cell. Calibration bar = 0.05 mm.

ganglion (Fig. 4-3). Care has been taken to confirm the close interactions three dimensionally by adjusting the focus of the microscope. One characteristic of dendrites was their numerous spiny processes which varied widely in length, thickness and ended in filamentous and grape-like dilatations (Fig. 4-4). Almost all dendrites had occasion varicosities which occurred at various length along the dendrite (Fig. 4-4). Ending swellings could be readily observed on dendritic terminals of most cells (Fig. 4-4). Spine-like processes were observed mainly on somata and dendritic processes. Spines may represent major sites of synaptic interaction [36,44]; however, actual synaptic structures were not seen without the aid of electron microscopy.

c. Axons

Axons were distinguished morphologically on 34 of 40 HRP-labeled neurons by their extended length, small diameter and paucity of spines. The other 6 HRP-labeled neurons were not included in this axon analysis because they had no distinguishable axon. It is not known whether these neurons had no axon or their axon was meshed amongst dendritic trees. All 34 cells contained only one axon which arose from either the soma (n = 28) or the primary dendrite (n = 6). In the population sampled, no axon collaterals could be found at any distance followed. Traced axon lengths varied from 110 to 2,389 μm. Varicosities and spines were not detected on most axons. However, some axons possessed varicosities (Fig.4-6). Large rounded swelling was observed along the length of axon (Fig. 4-5) or at axon terminals (Fig. 4-2).

FIGURE 4-4

SOMADENDRITIC COMPLEX, SPINES
AND TERMINAL SWELLINGS
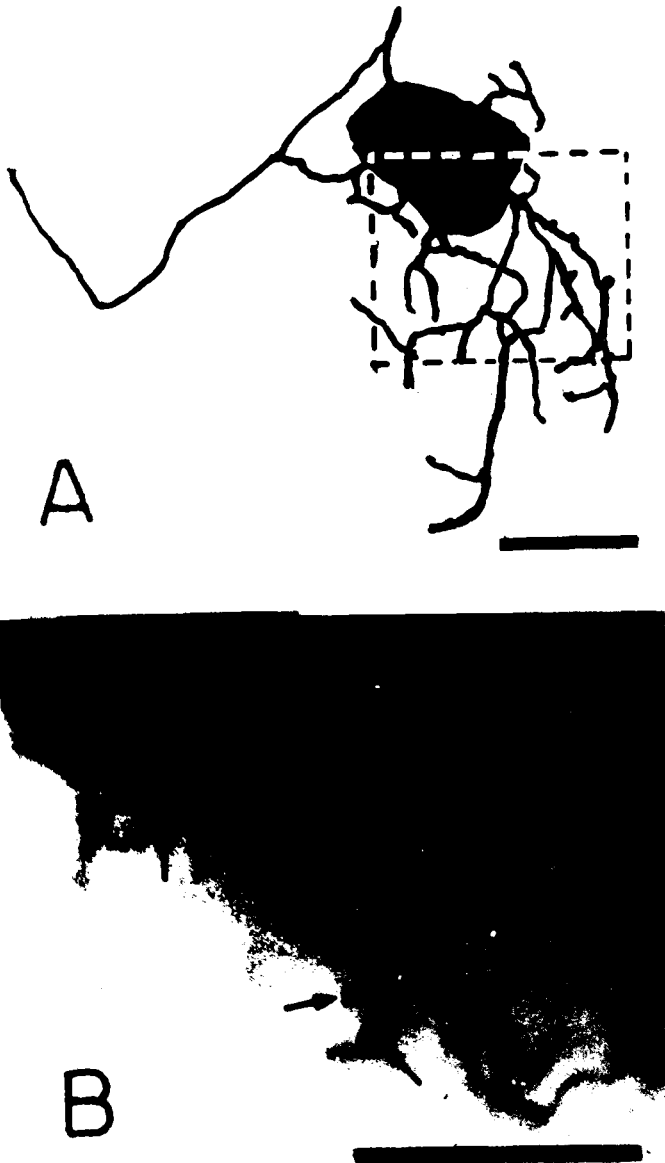
A. A camera lucida drawing of an *intra*ganglionic neuron showing the axon looping and then running to the left. The dashed box indicates the approximate area of the photomicrograph from the same cell shown in B. Arrows indicate some of the varicosities and terminal swellings. Calibration bar = 0.05 mm.

FIGURE 4-5

TERMINAL SWELLINGS AND VARICOSITIES
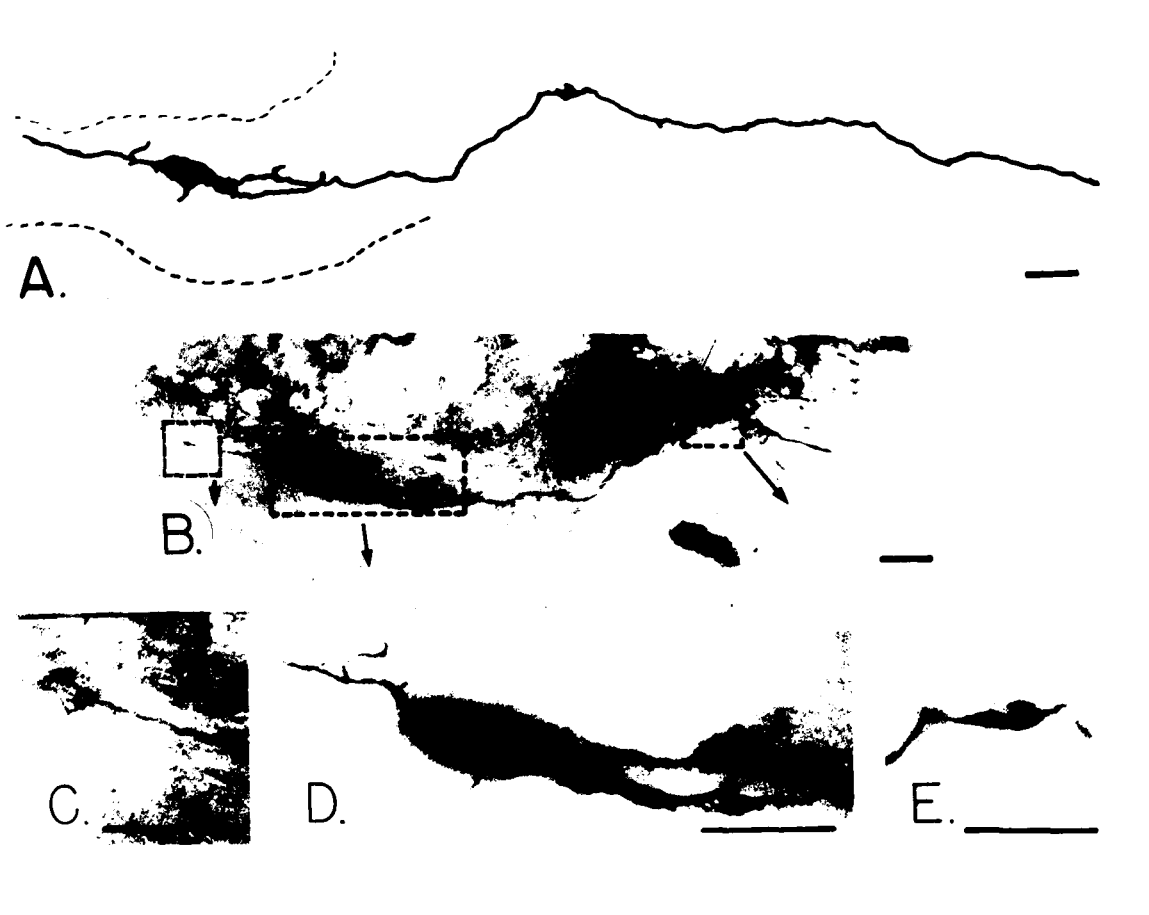
Terminal swellings and varicosities of dendrites and axon of a HRP-labeled principal neuron or *inter*ganglionic neuron. A. Camera lucida drawing of a HRP-labeled cell with varicosities in the long axon. B. Low magnification photomicrographic montage of the same cell as in A. Dashed boxes indicates the approximate areas which are enlarged in C., D. and E.. C. Terminal swelling on dendritic process. D. Somadendritic spines. E. Axonal swelling. All calibration bar = 0.05 mm.

FIGURE 4-6

CAMERA LUCIDA DRAWING OF TWO NEURONS
WITH LONG AXONS IN THE SAME GANGLION
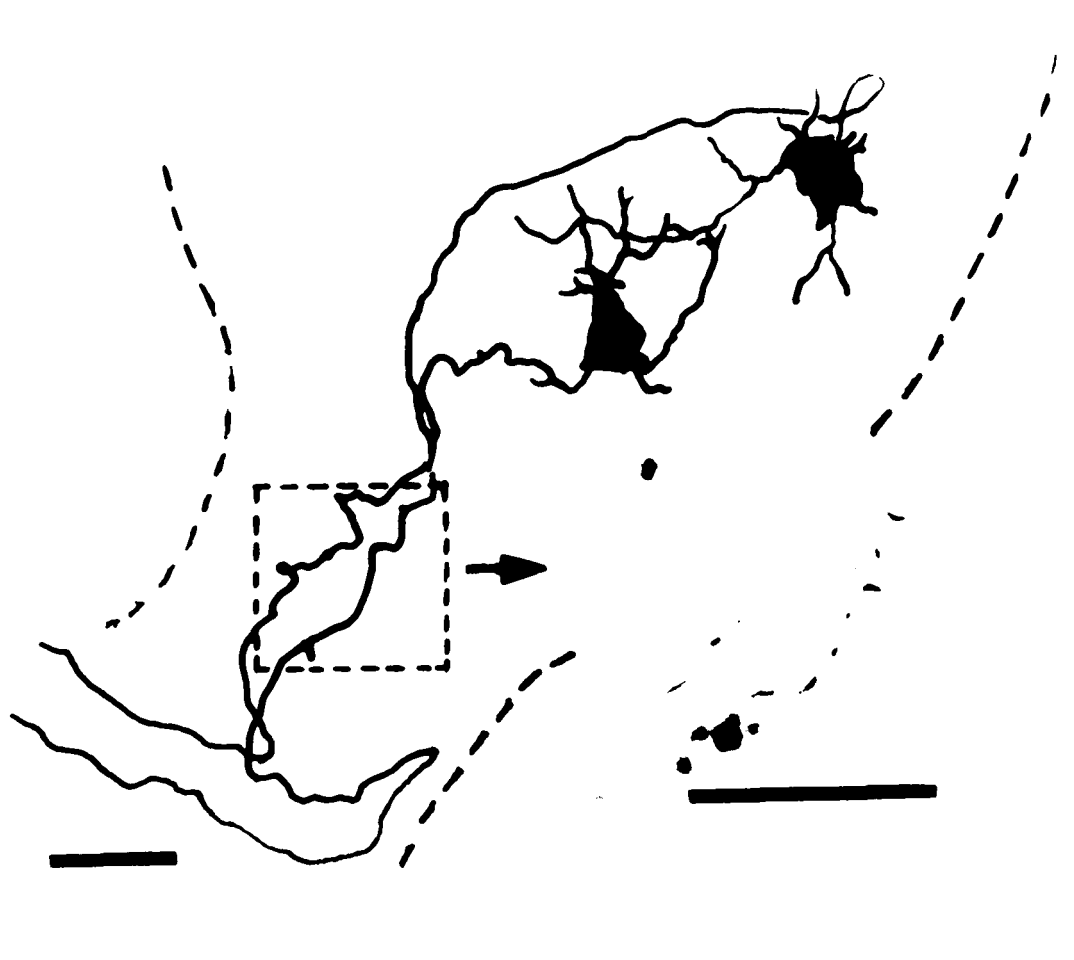
Camera lucida drawing of two principal cells or *inter*ganglionic neurons in the same ganglion. Both axons course parallel to the long axis of the ganglion before abruptly looping and turning perpendicularly. Insert: a photomicrograph of axon varicosities as indicated in dashed area of drawing. Calibration bar = 0.05 mm.

d. Intraganglionic Neuron and Principal or Interganglionic Neuron

Approximately half of the neurons (n = 19) possessed either a short axon (214 $\pm$ 33 μm in length, n = 13) which terminated within the confines of the ganglion (Figs. 4-1,4-3 and 4-4) or indistinguishable axon (n = 6, see section c.). In some multiple labeled ganglia, these short axons could be found to terminate in close proximity to the adjacent neuron (Fig. 4-3). The morphological interaction of two neurons in Fig. 4-3 has been carefully confirmed three dimensionally under the microscopy. Because all their processes terminated within the ganglion of origin, these neurons with short or indistinguishable axons could possibly be *intra*ganglionic neurons. The remaining 21 neurons had much longer axons (1,043 $\pm$ 131 μm, P < 0.05) which coursed out of the confines of the ganglion, towards nearby cardiac muscle or fat tissue or the interganglionic nerves (Figs. 4-2, 4-3, 4-5 and 4-6). The majority of long axons coursed parallel to the long axis of the ganglion; however, sometimes a loop or bend was observed. In some neurons, the axons turned almost perpendicular to the long axis of the ganglion before they enter the surrounding tissue (Figs. 4-2 and 4-6). Although the significance of axonal loops or bends is not clear, they may be due to uneven tissue shrinkage [42] or may allow for mechanical changes accompanying changes in atrial volume. The neurons with long axons running toward cardiac tissue are presumed to be postganglionic projection neurons (principal cells). However, if their long axons entered the interganglionic nerve, these neurons might be either principal neurons or *inter*ganglionic neurons that synapsed on neurons in another ganglion. Cells similar to the *inter*ganglionic neurons have been reported in enteric ganglion of guinea pig [28].

There was no distinguishable localization of different neurons found in a ganglion.

The morphological features of *intra*ganglionic neurons and principal neurons or *inter*ganglionic neurons are shown in Table 4-1. In comparison with principal neurons or *inter*ganglionic neurons, *intra*ganglionic neurons had significantly smaller soma, and fewer dendrites as well as, of course, a shorter axon.

e. Morphological Distinctions of R-, S- and N- Cells

As previously described [77], R-, S- and N-cells (Fig. 4-2) were functionally identified by their responding to a depolarizing current injection with either repetitive firing, a single firing or no firing, respectively. A typical example of each of these cell types is shown on Figure 4-2. There were 20 R-cells, 15 S-cells and 5 N-cells sampled in present experiment. The morphological features of these electrophysiologically different cell types are presented in Table 4-2. Generally, R-cells had the smallest soma size ($P < 0.05$). S-cell's somata were larger than R-cell's ($P < 0.05$) but tended to be smaller than N-cell's. N-cells had the largest cell body and the longest axon and dendrites; but with the relatively small number of cells, no statistically significant differences were found. Fifty-three percent of R-cells, 57% of S-cells and 25% of N-cells were *intra*ganglionic neurons, i.e. axons did not leave the ganglion. The remaining cells were principal neurons or *inter*ganglionic neurons.

2. SIF Cells and Monoamine-Containing Nerve Fibers

Six different pieces of ganglionic tissues from 4 dogs were examined.

a. SIF Cells

The ganglionic neurons generally exhibited an orange-brown autofluorescence

TABLE 4-1

MORPHOLOGICAL DIFFERENCES BETWEEN *INTRA*GANGLIONIC NEURONS

AND PRINCIPAL NEURONS OR *INTER*GANGLIONIC NEURONS

	SOMA AXIS SHORT μm	SOMA AXIS LONG μm	SOMA AREA μm^2	AXON LENGTH μm	DENDRITES NUMBER	TOTAL DENDRITE LENGTH μm	MEAN PRIMARY DENDRITE LENGTH μm
*INTRA*GANGLIONIC NEURON *	37 ±2	58 ±3	1519 ±165	214 ±33	4.5 ±0.5	533 ±102	79 ±7
PRINCIPAL NEURONS OR *INTER*GANGLIONIC NEURON **	43 ±3	67 ±3	2191 ±248	1043 ±131	6.4 ±0.6	712 ±95	80 ±11
P	NS	<0.05	<0.05	<0.05	<0.05	NS	NS

Values represent mean ±standard error of the mean. Statistical analysis was done using Student t test. NS =no statistical difference (P >0.05). * n =19 (n =13 for axon length, the neurons with undistinguishable axon were not included). ** n =21.

TABLE 4-2

MORPHOLOGICAL DIFFERENCE BETWEEN R-, S- AND N-CELLS

	SOMA AXIS SHORT μm	SOMA AXIS LONG μm	SOMA AREA μm^2	AXON LENGTH # μm	DENDRITE NUMBER	TOTAL DENDRITE LENGTH μm	MEAN PRIMARY DENDRITE LENGTH μm
R-CELL n = 20	35 ±2	61 ±3	1475 ±171	589 ±161	5.3 ±0.6	560 ±68	80 ±9
S-CELL n = 15	44 ±3	62 ±4	2157 ±264	703 ±149	5.7 ±0.7	613 ±121	75 ±8
N-CELL n = 5	48 ±2	76 ±6	2951 ±309	876 ±263	5.6 ±1.1	958 ±130	97 ±24
P	<0.05 *	NS	<0.05 *	NS	NS	NS	NS

Values represent mean ±standard error of the mean. Statistical analysis was done using one way ANOVA. NS =no statistical difference (P >0.05). * statistical difference between R- and S- or N-cells. # R-cell n =17, S-cell n =12, neurons with undistinguishable axon were not included.

from cytoplasm inclusions. In contrast, bright, bluish-white fluorescence indicative of monoamines was observed in small somata and fine fibers coursing through the tissue. These SIF cells appeared as single cells or clusters of 2 to 10 cells interspersed between principal cells or intraganglionic neurons (Fig. 4-7). These clusters of SIF cells were often associated with ganglionic neurons but not necessarily with blood vessels. The number of SIF cells varied widely from none to several clusters per ganglion, and was not related to the ganglion size or the number of cells in the ganglion. Somata of SIF cells were much smaller (short and long axes 10 $\pm$ 1.5 x 14 $\pm$ 1.8 μm, n = 26) than the principal cells or *intra*ganglionic neurons labeled by HRP (short and long axes 40 $\pm$ 2 x 62 $\pm$ 3 μm, n = 40, P < 0.05). Much variation in shape and size of these SIF cells was observed. In the same cluster, some SIF cells had no processes while others had short (10 - 20 μm), fine processes. Some of the processes came into close proximity to adjacent ganglionic soma.

b. Monoamine-Containing Nerve Fibers

In addition to the short processes of SIF cells, many long, brightly fluorescent fibers formed a network over ganglion cells and strands of cardiac muscle. Some of these long monoamine-containing fibers appeared to come into close association with ganglion neurons (Fig. 4-8). The long fibers arising from extraganglionic sources sometimes can be traced as they enter the ganglion from interganglionic nerves. Long fluorescent fibers, coursing around neurons or through the ganglion, were also found in some ganglia which had no SIF cells.

FIGURE 4-7

SIF CELLS IN CANINE INTRACARDIAC GANGLION

Photomicrograph of monoamine histofluorescence of a cluster of SIF cells in an intracardiac ganglion. The SIF cells are indicated (arrows). Calibration bar = 0.01 mm.

FIGURE 4-8

MONOAMINE FLUORESCENT FIBERS
IN CANINE INTRACARDIAC GANGLION
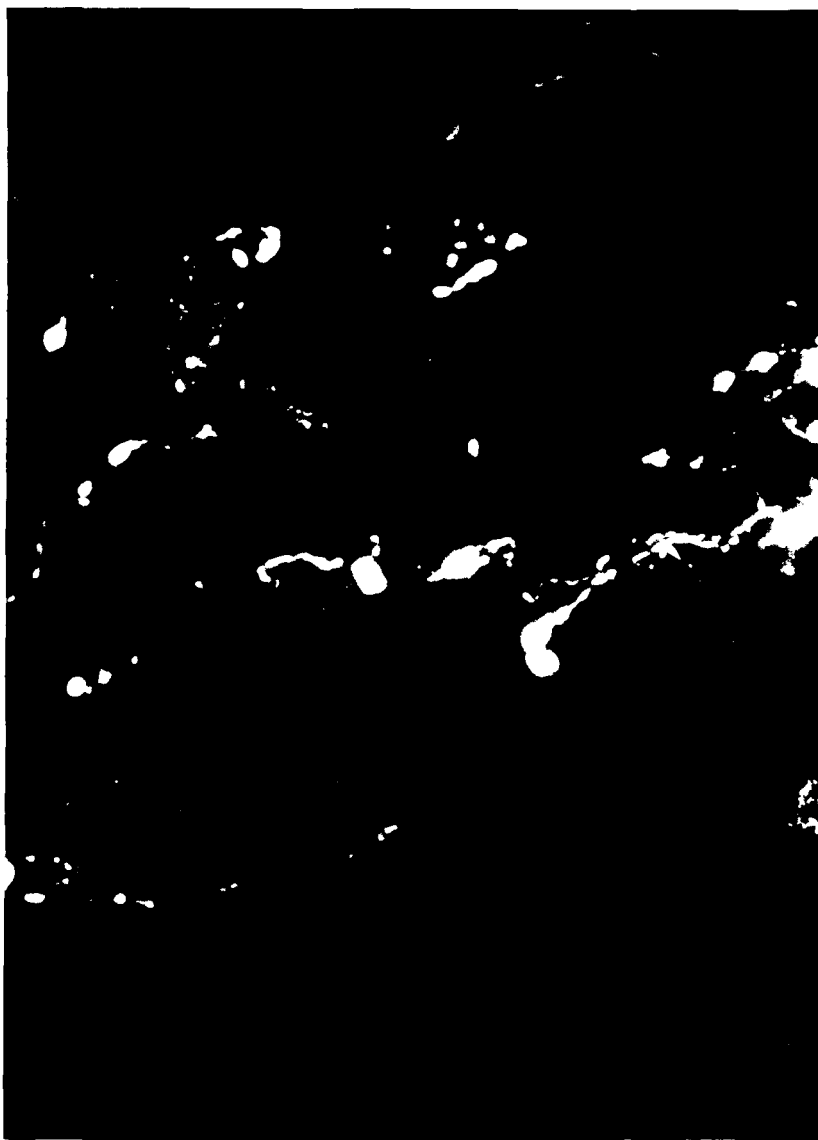
Photomicrograph of long, thin monoamine fluorescent fibers coursing through an intracardiac ganglion. Brightly fluorescencing fibers (F) stand out from the low intensity, nonspecific, autofluorescence of a ganglion soma (S). Calibration bar = 0.05 mm.

D. DISCUSSION

The morphological characteristics of canine intracardiac ganglion cells in whole mount tissue were investigated using the intracellular HRP labelling technique and light microscopy. To stain monoamine-containing cells and nerve fibers, glyoxylic acid fluorescence technique was also applied to sectioned ganglionic tissue. The major findings of present studies were that 1) the presence of *intra*ganglionic neurons was demonstrated morphologically in intracardiac ganglia; 2) morphological differences were revealed between R-, S- and N-cells; and 3) SIF cells were found in canine intracardiac ganglia, which were distinguished from larger, HRP-labeled neurons.

In autonomic ganglia, the possibility of interneurons between preganglionic and principal neurons was first proposed by Dogiel [16] and Lawrentjew [43]. Later, electron microscopic studies of the rat superior cervical ganglion demonstrated interneurons which were small, granule containing cells. These cells receive synaptic contacts from preganglionic nerve terminals and in turn make synaptic contact with principal ganglion cells [30,65,70,71,73]. Histochemical studies revealed that these granule-containing interneurons were identical to SIF cells or catecholamine-containing neurons [22,31,54,55,72]. Since SIF cells receive synapses from preganglionic neurons and also synapse with postganglionic neurons, they were suggested to be monoaminergic interneurons [70].

On the other hand, little is known about the ganglionic interneurons not containing catecholamines. In the cat inferior mesenteric ganglion, functional evidence for *intra*ganglionic neurons was reported for some cells had endogenous activity and were not antidromically activated by stimulation of nerves leaving the ganglion [38,39]. These

neurons were suggested to be interneurons. Based upon the low probability of recording from very small SIF cells, these recorded neurons were likely to be interneurons other than the SIF cells. Similarly, using intracellular recording and HRP labeling techniques, interneurons with short processes were also observed in the cat stellate sympathetic ganglia [4]. Based upon methylene blue staining, Dogiel et al.[15-17] divided the enteric neurons into three groups: type I cells had many short dendrites and one long slender axon which could be followed into the internodal strands; type II cells had a short axon which branched within the ganglion of origin and long dendrites which extended beyond the ganglion; type III cells had intermediate length of dendrites which terminated in the same or adjacent ganglia. Intracellular labeled enteric neurons with long process from the origin ganglion to another ganglion were also reported [28].

*Intra*ganglionic neurons in intracardiac ganglia similar to those in present study have not been previously reported in amphibians or mammals. Their restricted processes suggest an endogenous activity of these neurons. The *intra*ganglionic neurons resembled the interneurons of the inferior mesenteric and stellate ganglia [4]. Morphologically, in addition to short or indistinguishable axons, *intra*ganglionic neurons had slightly, but significantly smaller somata than those with longer axons leaving the ganglion. The number of dendrites was also smaller although the total dendritic length was not obviously different. These *intra*ganglionic neurons seem unlikely to be SIF cells because the cell body sizes are considerably larger than those of SIF cells. As well, these interneurons appear unlikely to be sensory cells for their processes are short and never course out of the confines of the ganglion.

These *intra*ganglionic neurons are most likely nicotinic cholinergic because the majority cardiac ganglion cells are cholinergic [57] and almost 50% of the labeled cell bodies in the present study were classified as *intra*ganglionic interneurons. These neurons, as other neurons, were indistinctly innervated by cholinergic fibers and generate f-EPSP upon orthodromic stimulation (see Chapter VI). However, more direct evidences are required to document the neurochemical and functional roles of these cells.

The *intra*ganglionic neurons are assumed to be ganglionic interneurons in canine heart because of 1). the morphological features suggesting interactions between processes of *intra*ganglionic neurons and neighboring neurons; 2). the morphological characteristics of *intra*ganglionic terminated processes; and 3). the similarity of *intra*ganglionic neurons of canine intracardiac ganglion and the interneurons of inferior mesenteric ganglion and setellate ganglion. Electron microscopic analysis of efferent and afferent synapses of *intra*ganglionic neurons is required to confirm whether they are interneurons. Perhaps these interneurons receive preganglionic or even cardiac afferent inputs and send their excitatory or inhibitory connections to principal cells or other interneurons. These possibilities are supported by extracellular recordings from cat cardiac ganglia, demonstrating excitation of the second neuron which begins after the termination of the activity of a triggering neuron [56]. Although the actual physiological significance of *intra*ganglionic neurons is uncertain, it is possible that these interneurons may mediate peripheral integration in the intracardiac ganglia and cardio-cardiac reflexes.

The group of neurons with a long axon is presumably composed of postganglionic projection neurons (principal cells) and *inter*ganglionic neurons. Some of the long axons

were observed to innervate directly the surrounding muscle or fat tissue. Other long axons proceeded out of the ganglion through interganglionic nerves, presumably to innervate cardiac tissue and/or neurons in other ganglia.

A statistical correlation of cell types and soma size of intracardiac ganglion neurons was clearly revealed in the present study. On the other hand, there were no clear-cut differences of axon and dendrite lengths among the electrophysiologically defined R-, S- and N-cells. It is possible that a correlation of axon or dendrite lengths and other properties, such as immunohistochemical features, may present as reported in the enteric neurons [6-9,25]. Recent work has suggested that intrinsic enteric neurons can be divided into different types on the basis of the transmitter substances they contain. Serotonin immunoreactivity occurs in myenteric neurons with morphological characteristics of Dogiel type I neurons projected in the anal direction in guinea-pig myenteric plexus [7]. Enkephalin immunoreactivity also occurs in myenteric neurons with Dogiel type I morphology [3]. Substance P-immunoreactive substance appears to occur in Dogiel type II and III neurons projected in both oral and anal directions [8]. Accordingly, a further study using a combination of methodologies of morphology, immunohistochemistry and electrophysiology could be expected to verify the difference among types of neurons.

Similar methodology has been used to investigate the function and structure correlations in different peripheral [23,34,35,50,61,67,74] and central nervous systems [10,40,79]. Vast variations could be seen between tissues. In myenteric plexus of guinea-pig small intestine, investigators [23,34,35] have attempted to associate the electrophysiological behavior

with morphology by intracellular injection of dye from the recording electrode. Their results have not revealed any definitive relations between a particular electrophysiological type of neuron and a particular morphological type. On the other hand, in cat parietal cortex , Yamamoto et al. [79] have found two types of neurons. The first type consisted of neurons with larger somata and sparsely spinous apical dendrites. These cells showed faster conduction velocity. The other type of neurons had smaller somata and numerous apical dendrites which possessed slower conduction velocity. Likewise, in canine intracardiac ganglion, the size and shape of somata and length of processes varied considerably even in the same electrophysiologically defined cell type, although statistical differences existed between groups of neurons. These may suggest that the organization of intracardiac ganglia system is as complex as other nervous tissues and that relationship among morphology, electrical behavior and functional role of intracardiac ganglion cells are not simple.

From studies in other tissues, many investigators have assumed that similar "inexcitable" cells with high resting potential, low input resistance and a slow depolarization upon orthodromic stimulation were glial cells [2,26,29,34,53,75]. Most of the publications assumed that these "inexcitable" cells are glial cell or interneurons [2,26,29,53]. This combined functional and morphological study have demonstrated that these "inexcitable" cells or N-cells in canine intracardiac ganglia are neurons. These N-cells have relatively large somata size and less likely to be *intra*ganglionic interneurons for they may have longer processes projecting out of the ganglion. However, the functional role of N-cells is not known.

Small intensely fluorescent cells in the canine intracardiac ganglia are similar in shape to those described in other species [48,55]. In comparison to mudpuppy intracardiac ganglia with a ratio of SIF cells to principal cells of about 1:2 [48], the canine intracardiac ganglia have a relative smaller number of SIF cells. While some ganglia have no SIF cells, other ganglia may have SIF cells appearing in small clusters of 2-10 cells surrounded by as many as a hundred or more ganglion neurons. Similar to sympathetic ganglia [55], two types of SIF cells are observed: SIF cells with processes (Type I) and SIF cells with out processes (Type II). The cells may function as interneurons and endocrine cells, respectively, as have been proposed for sympathetic ganglia [5,72]. In the present studies, both cell types occur in the same cluster as has been reported in sympathetic ganglia of some mammals. It has also been reported in some other species that type I cells are isolated from type II cells [18,72]. Although fine processes of SIF cells of canine intracardiac ganglia are very close to ganglionic neurons, the observation of direct synapses with principal cells is not possible without electron microscopic confirmation.

Since fluorescence can be produced by glyoxylic acid condensation with norepinephrine, epinephrine, dopamine or serotonin, the identity of the specific monoamine present within canine cardiac SIF cells is currently unknown. Depending on the animal species, some studies on cardiac ganglia suggest that either norepinephrine [37] or dopamine [19] is the monoamine in SIF cells.

In canine intracardiac ganglia, many long, thin fluorescent fibers were observed. Because the present SIF cell processes are usually short and thick, most of the long, thin fluorescent fibers were considered to be sympathetic fibers which were observed to enter

and then exit the ganglion. Additionally, these fibers disappeared after sympathetic denervation [37] and degenerated when isolated in primary tissue culture [33]. Furthermore, chemical sympathectomy with 6-hydroxydopamine removed these fibers in mudpuppy cardiac ganglia [51]. Thus, it is suggested that these long, thin fluorescent fibers were exogenous in origin and are probably postganglionic sympathetic fibers [37].

Other than SIF cells, no evidence of other monoamine-containing neuronal cell bodies, such as sympathetic postganglionic neurons, was demonstrated in the present study. A previous study of mammalian cardiac ganglia [37] has shown that the administration of a monoamine oxidase inhibitor followed by 3,4-dihydroxyphenylalanine resulted in the appearance of monoamine fluorescence in some ganglion cells. This suggested that at least some mammalian intracardiac ganglion cells are capable of taking up 3,4-dihydrophenylalanine and synthesizing catecholamine. Using immunohistochemical techniques, the presence of the catecholamine-converting enzymes tyrosine hydroxylase and dopamine β-hydroxylase, and neuropeptide tyrosine (NPY) which is usually co-localized with catecholamines in adrenergic neurons has been reported in some cardiac ganglion neurons [32]. Thus, it is possible that some adrenergic ganglion cells may coexist with the predominant cholinergic neurons in cardiac ganglia. Hence, in the present study, the absence of monoamine-containing cell bodies of principal cells could be due to either species variations or insensitivity of the present method to reveal low level of monoamines.

In summary, the canine intracardiac ganglion is composed of at least three types of cells: 1) Postganglionic projection neurons or principal neurons with large cells bodies

and long axons; 2) *Intra*ganglionic neurons with smaller cell bodies and shorter processes confined within the ganglion; these cells may be ganglionic interneurons; 3) SIF cells with very small cell bodies and sometimes possessing short processes confined within the ganglion. An additional cell type, namely *inter*ganglionic neuron with axons terminating in other intracardiac ganglia, could not be excluded presently. The somata size of neurons was shown to be correlated to their electrophysiological behavior. The interganglionic nerve fibers, likewise, were at least composed of preganglionic cholinergic axons, postganglionic axons, axons of *inter*ganglionic neurons (if present), and long monoamine-containing fibers. From the immunohistochemical studies (unpublished data), calcitonin gene-related peptide (CGRP)-like immunoreactive fibers, which were believed to be sensory or afferent in origin, were found in the interganglionic nerve as well. Therefore, ganglia with different types of neurons were connected by the interganglionic nerves to form a complicated plexus in the PVFP region. These findings provide for the possibility of ganglionic modulation of vagal efferent activity in mammalian heart and the morphological base of different types of cells.

E. REFERENCES

1 Armstrong, W.E., Warach, S., Hatton, G.I. and McNeill, T.H., Subnuclei in the rat hypothalamic paraventricular nucleus: a cytoarchitectural, HRP and immunocytochemical analysis, *Neuroscience*, 5 (1980) 1931-1958.

2 Blackman, J.G. and Purves, R.D., Intracellular recording from ganglia of the thoracic sympathetic chain of the guinea-pig, *J. Physiol. (Lond.)*, 203 (1969) 173-198.

3 Bornstein, J., Lees, G., Costa, M. and Furness, J.B., Correlation between morphology, electrophysiology and immunohistochemistry of enteric neurons, *Proc. Int. Congr. Physiol. Sci.*, 15 (1983) 451-451.(Abstract)

4 Bosnjak, Z.J. and Kampine, J.P., Electrophysiological and morphological characterization of neurons in stellate ganglion of cats, *Am. J. Physiol.*, 248 (1985) 288-292.

5 Chiba, T., Black, A.C. and Williams, T.H., Evidence for dopamine-storing interneurons and paraneurons in rhesus monkey sympathetic ganglia, *J. Neurocytol.*, 6 (1977) 441-453.

6 Costa, M., Furness, J.B., Buffa, R. and Said, S.I., Distribution of enteric nerve cell bodies and axons showing immunoreactivity for vasoactive intestinal polypeptide (VIP) in the guinea-pig intestine, *Neuroscience*, 5 (1980) 587-596.

7 Costa, M., Furness, J.B., Cuello, A.C., Verhofstad, A.A.J., Steinbusch, H.W.M. and Elde, R.P., Neurons with 5-hydroxytryptamine-like immunoreactivity in the enteric nervous system: their visualization and reaction to drug treatment, *Neuroscience*, 7 (1982) 351-363.

8 Costa, M., Furness, J.B., Llewellyn-smith, I.J. and Cuello, A.C., Projection of substance P neurons within the guinea-pig small intestine, *Neuroscience*, 6 (1981) 411-424.

9 Costa, M., Furness, J.B., Llewillyn-Smith, I.J., Davies, B. and Oliver, J., An immunohistochemical study of the projection of somatostatin containing neurons in the guinea-pig intestine, *Neuroscience*, 5 (1980) 841-852.

10 Crunelli, V., Leresche, N. and Parnavelas, J., X- and Y-cells identified in the cat lateral geniculate nucleus in vitro, *Brain Res.*, 380 (1986) 371-374.

11 Cullheim, S. and Kellerth, J.O., A morphological study of the axons and recurrent axon collaterals of cat sciatic alpha-motoneurons after intracellular staining with horseradish peroxidase, *J. Comp. Neurol.*, 178 (1978) 537-558.

12 Dahlstrom, A., Fuxe, K., Mya-Tu, M. and Zetterstrom, B.E.M., Observations on adrenergic innervation of dog heart, *Am. J. Physiol.*, 209 (1965) 689-692.

13 Dail, W.G. and Barton, S., Structure and organization of mammalian sympathetic ganglia. In L-G. Elfvin (Ed.), *Autonomic Ganglia*, John Wiley & Sons, Chichester, 1983, pp. 3-25.

14 De La Torre, J.C., An improved approach to histofluorescence using the SPG method for tissue monoamines, *J. Neurosci. Methods*, 3 (1980) 1-5.

15 Dogiel, A.S., Zur Frage ueber die Ganglien der Daermgeflechte bei den Saeugetieren, *Anat. Anz.*, 10 (1895) 517-528.

16 Dogiel, A.S., Zwei Arten sympathischer Nervenzellen, *Anat. Anz.*, 11 (1896) 679-687.

17 Dogiel, A.S., Ueber den Bau der Ganglien in den Geflechten des Darmes und der Gallenblase des Menschen un der Saeugethiere, *Arch. Anat. Physiol. Anat. Abt.*, (1899) 130-158.

18 Dunn, P.M. and Marshall, L.M., Innervation of small intensely fluorescent cells in frog sympathetic ganglia, *Brain Res.*, 339 (1985) 371-374.

19 Ehinger, B., Falck, B., Persson, H. and Sporrong, B., Adrenergic and cholinesterase-containing neurons of the heart, *Histochemistry*, 16 (1968) 197-205.

20 Ehinger, B., Falck, B. and Sporrong, B., Adrenergic fibers to the heart and to peripheral vessels, *Bibl. Anat.*, 8 (1966) 35-45.

21 Ellison, J.P. and Hibbs, R.G., An ultrastructural study of mammalian cardiac ganglia, *J. Mol. Cell Cardiol.*, 8 (1976) 89-101.

22 Eranko, O. and Harkonen, M., Histochemical demonstration of fluorogenic amines in the cytoplasm of sympathetic ganglion cells of the rat, *Acta. Physiol. Scand.*, 58 (1963) 285-286.

23 Erde, S.M., Gershon, M.D. and Wood, J.D., Morphologically and eletrophysiologically identified types of myenteric neurons by intracellular recording and injection of lucifer yellow in the guinea-pig small bowel, *Soc. Neurosci. Abs.*, 6 (1980) 274-274.(Abstract)

24   Falck, B., Haggendal, J. and Owman, Ch., The localization of drenaline in adrenergic nerves in the frog, *Q. J. Exp. Physiol.*, 48 (1963) 253-257.

25   Furness, J.B., Costa, M., Llewellyn-smith, I.J., Franco, R. and Wilson, A.J., Polarity and projections of peptide-containing neurons in the guinea-pig small intestine. In M.I. Grossman, M.A.B. Brazier and J. Lechago (Eds.), *Cellular Basis of Chemical Messengers in the Digestive System*, Academic Press, New York, 1981,

26   Gallego, R. and Eyzaguirre, C., Membrane and action potential characteristics of A and C nodose ganglion cells studied in whole ganglia and in tissue slices, *J. Neurophysiol.*, 41 (1978) 1217-1232.

27   Glantz, S.A., *Primer of Biostatistics*, 2nd edn., McGraw-Hill Book Company, New York, 1988, 64 pp.

28   Gray, M.J., Hodgkiss, J.P. and Lees, G.M., Morphological characteristics of enteric neurons revealed with different intracellular staining methods, *Neurosci. Lett.*, suppl 5 (1980) S 193-S 193.(Abstract)

29   Griffith, W.H.III, Gallagher, J.P. and Shinnick-Gallagher, P., An intracellular investigation of cat vesicle pelvic ganglia, *J. Neurophysiol.*, 143 (1980) 343-354.

30   Grillo, M.A., Electron microscopy of sympathetic tissues, *Pharmacol. Rev.*, 18 (1966) 387-399.

31   Grillo, M.A., Jacobs, L. and Comroe, J.M.Jr., A combined fluorescence histochemical and electron microscopic method for studying special monoamine-containing cells (SIF cells), *J. Comp. Neurol.*, 153 (1974) 1-14.

32   Gu, J., Polak, J.M., Allen, J.M., Huang, W.M., Sheppard, M.N., Tatemoto, K. and Bloom, S.R., High concentrations of a noval peptide, Neuropeptide Y, in the innervation of mouse and rat heart, *J. Histochem. Cytochem.*, 32 (1984) 467-472.

33   Hassall, C.J.S. and Burnstock, G., Intrinsic neurones and associated cells of the guinea-pig heart in culture, *Brain Res.*, 364 (1986) 102-113.

34   Hodgkiss, J.P. and Lees, G.M., Correlated electrophysiological and morphological characteristics of myenteric plexus neurones, *J. Physiol. (Lond.)*, 285 (1978) 19 P-20 P.(Abstract)

35   Hodgkiss, J.P. and Lees, G.M., Morphological studies of electrophysiologically-identified myenteric plexus neurons of the guinea-pig ileum, *Neuroscience*, 8 (1983) 593-608.

36   Ifft, J.D. and McCarthy, L., Somatic spines in the supraoptic nucleus of the rat hypothalamus, *Cell Tissue Res.*, 148 (1974) 203-211.

37   Jacobowitz, D., Histochemical studies of the relationship of chromaffin cells and adrenergic nerve fibers to the cardiac ganglia of several species, *J. Pharmacol. Exp. Ther.*, 158 (1967) 227-240.

38   Julé, Y., Krier, J. and Szurszewski, J.H., Patterns of innervation of neurones in the inferior mesenteric ganglion of the cat, *J. Physiol. (Lond.)*, 344 (1983) 293-304.

39   Julé, Y. and Szurszewski, J.H., Electrophysiology of neurones of the inferior mesenteric ganglion of the cat, *J. Physiol. (Lond.)*, 344 (1983) 277-292.

40   Kawaguchi, Y. and Hama, K., Two subtypes of non-pyramidal cells in rat hippocampal formation identified by intracellular recording and HRP injection, *Brain Res.*, 411 (1987) 190-195.

41   king, T.S. and Coakley, J.B., The intrinsic nerve cells of the cardiac atria of mammals and man, *J. Anat.*, 92 (1958) 353-376.

42   Larkman, A. and Mason, A., Correlations between morphology and electrophysiology of pyramidal neurons in slices of rat visual cortex. I. Establishment of cell classes, *J. Neurosci.*, 10 (1990) 1407-1414.

43   Lawrentjew, B.J., Zur Morphologie des Ganglion cervical super, *Anat. Anz.*, 58 (1924) 529-539.

44   Leranth, C., Zaborszky, L., Marton, J. and Palkovits, M., Quantitative studies on the supraoptic nucleus in the rat. I Synaptic organization, *Exp. Brain Res.*, 22 (1975) 509-523.

45   Loffelholz, K. and Pappano, A.J., The parasympathetic neuroeffector junction of the heart, *Pharmacol. Rev.*, 37 (1985) 1-24.

46   Malor, R., Taylor, S., Chesher, G.B. and Griffin, C.J., The intramural ganglia and chromaffin cells in guinea pig atria: an ultrastructural study, *Cardiovasc. Res.*, 8 (1974) 731-744.

47   Mason, W.T., Ho, Y.W. and Hatton, G.I., Axon collaterals of supraoptic neurones: anatomical and electrophysiological evidence for their existence in the lateral hypothalamus, *Neuroscience*, 11 (1984) 169-182.

48 McMahan, M.N. and Purves, D., Visual identification of two kinds of nerve cells and their synaptic contacts in a living autonomic ganglion of the mudpuppy (necturus maculosus), *J. Physiol. (Lond.)*, 254 (1976) 405-425.

49 McMahan, U.J. and Kuffler, S.W., Visual identification of synaptic boutons on living ganglion cells and of varicosities in postganglionic axons in the heart of the frog, *Proc. Roy. Soc. Lond.*, Ser B 177 (1971) 485-508.

50 Nagano, M., Heterogeneity of neurons in the crustacean X-organ as revealed by intracellular recording and injection of horseradish peroxidase, *Brain Res.*, 362 (1986) 379-383.

51 Neel, D.S. and Parsons, R.L., Anatomical evidence for the interaction of sympathetic and parasympathetic neurons in the cardiac ganglion of Necturus, *J. Auton. Nerv. Syst.*, 15 (1986) 297-308.

52 Neel, D.S. and Parsons, R.L., Catecholamine, serotonin, and substance P-like peptide containing intrinsic neurons in the mudpuppy parasympathetic cardiac ganglion, *J. Neurosci.*, 6 (1986) 1970-1975.

53 Nishi, S. and North, R.A., Intracellular recording from the myenteric plexus of the guinea-pig ileum, *J. Physiol. (Lond.)*, 231 (1973) 471-491.

54 Norberg, K.A., Ritzen, M. and Ungerstedt, U., Histochemical studies on a special catecholamine-containing cell type in sympathetic ganglia, *Acta. Physiol. Scand.*, 67 (1966) 260-270.

55 Norberg, K.A. and Sjoqvist, F., New possibilities for adrenergic modulation of ganglionic transmission, *Pharmacol. Rev.*, 18 (1966) 743-751.

56 Nozdrachev, A.D. and Pogorelov, A.G., Extracellular recording of neuronal activity of the cat heart ganglia, *J. Auton. Nerv. Syst.*, 6 (1982) 73-81.

57 Osborne, L.W. and Silva, D.G., Histological, acetylcholinesterase, and fluorescence histochemical studies on the atrial ganglia of the monkey heart, *Exp. Neurol.*, 27 (1970) 497-511.

58 Papka, R.E., Studies of cardiac ganglia in pre- and postnatal rabbits, *Cell Tissue Res.*, 175 (1976) 17-35.

59 Parsons, R.L., Neel, D.S., Konopka, L.M. and McKeon, T.W., The presence and possible role of a galanin-like peptide in the mudpuppy heart, *Neuroscience*, 29 (1989) 749-759.

60 Parsons, R.L., Neel, D.S., McKeon, T.W. and Carraway, R.E., Organization of a vertebrate cardiac ganglion: a correlated biochemical and histochemical study, *J. Neurosci.*, 7 (1987) 837-846.

61 Purves, D. and Hume, R.I., The relation of postsynaptic geometry to the number of presynaptic axons that innervate autonomic ganglion cells, *J. Neurosci.*, 1 (1981) 441-452.

62 Randall, W.C., Ardell, J.L., Calderwood, D., Milosavljevic, M. and Goyal, S.C., Parasympathetic ganglia innervating the canine atrioventricular nodal region, *J. Auton. Nerv. Syst.*, 16 (1986) 311-323.

63 Randall, W.C., Ardell, J.L., Wurster, R.D. and Milosavljevic, M., Vagal postganglionic innervation of the canine sinoatrial node, *J. Auton. Nerv. Syst.*, 20 (1987) 13-23.

64 Randle, J.C.R., Bourque, C.W. and Renaud, L.P., Serial reconstruction of lucifer yellow-labeled supraoptic nucleus neurons in perfused rat hypothalamic explants, *Neuroscience*, 17 (1986) 453-467.

65 Siegrist, G., Ribaupierre, F.de., Dolivo, M. and Rouiller, C., Les cellules chromaffines des ganglions cervicaus superieurs du rat, *J. Microse.*, 5 (1966) 791-794.

66 Sofroniew, M.V. and Glasmann, W., Golgi-like immunoperoxidase staining of hypothalamic magnocellular neurons that contain vasopressin, oxytocin or neurophysin in the rat, *Neuroscience*, 6 (1981) 619-643.

67 Teranishi, T., Negishi, K. and Kato, S., Functional and morphological correlates of amacrine cells in carp retina, *Neuroscience*, 20 (1987) 935-950.

68 Vogel, J.H.K., Jacobowitz, D. and Cuidsey, C.A., Distribution of norepinephrine in the failing bovine heart, *Circ. Res.*, 24 (1969) 71-84.

69 West, M.J., Coleman, P.D. and Flood, D.G., Estimating the number of granule cells in the dentate gyrus with the disector, *Brain Res.*, 448 (1988) 167-172.

70 Williams, T.H., Electron microscopic evidence for an autonomic interneuron, *Nature*, 214 (1967) 309-310.

71 Williams, T.H., Black, A.C., Chiba, T. and Bhalla, R.C., Morphology and biochemistry of small, intensely fluorescent cells of sympathetic ganglia, *Nature*, 256 (1975) 315-317.

72 Williams, T.H., Black, A.C.Jr., Chiba, T. and Bhalla, R.C., Morphology and biochemistry of small, intensely fluorescent cells of sympathetic ganglia, *Nature*, 256 (1975) 315-317.

73 Williams, T.H. and Palay, S.L., Ultrastructure of the small neurons in the superior cervical ganglion, *Brain Res.*, 15 (1969) 17-34.

74 Wood, J.D., Enteric neurophysiology, *Am. J. Physiol.*, 247 (1984) G585-G598.

75 Wood, J.D. and Mayer, C.J., Intracellular study of electrical activity of Auerbach's plexus in guinea-pig small intestine, *Pflugers. Arch.*, 374 (1978) 265-275.

76 Woods, R.I., The innervation of the frog's heart. I. An examination of the autonomic postganglionic nerve fibers and a comparison of autonomic and sensory ganglion cells, *Proc. Roy. Soc. Lond.*, B, 176 (1970) 43-54.

77 Wurster, R.D., Xi, X., Thomas, J.X. and Randall, W.C., Electrical properties of mammalian intracardiac ganglion cells, *FASEB J.*, 4 (1990) A707.(Abstract)

78 Xi, X., Thomas, J.X., Randall, W.C. and Wurster, R.D., Intracellular recordings from canine intracardiac ganglion cells, *J. Auton. Nerv. Syst.*, 32 (1991) 177-182.

79 Yamamoto, T., Samejima, A. and Oka, H., Morphological features of layer V pyramidal neurons in the cat parietal cortex: An intracellular HRP study, *J. Comp. Neurol.*, 265 (1987) 380-390.

CHAPTER V

ELECTROPHYSIOLOGICAL PROPERTIES

OF *IN SITU* CANINE INTRACARDIAC GANGLION CELLS

A. INTRODUCTION

Efferent vagal control of cardiac function is mediated via ganglion cells which are located in the heart - the intracardiac ganglion cells [39,42]. Randall and coworkers well documented both the anatomical locations of canine intracardiac ganglia and their differential functional importance [6,17,40,41], thus extending earlier studies on the histological and ultrastructural features of intracardiac ganglia on different species [14,26,29,36]. Extracellular recordings of neuronal activity from intracardiac ganglia have been performed by Nozdrachev et al.[35], Gagliardi et al.[19] and Armour and Hopkins [2,3]. Their studies suggested interneuronal interactions at the ganglion level and interactions between these ganglia and cardiovascular or pulmonary dynamics. However in those studies, electrical activity was recorded from a group of neurons which may not be homogeneous; and artifact from cardiac mechanical movement during *in vivo* recording may compromise the interpretation of their observations. Thus, one aim of this study was to determine the electrophysiological properties of single intracardiac neurons using intracellular recording from an *in vitro* preparation.

With the exception of amphibian intracardiac ganglia [22,30,43,44], few intracellular recordings have been reported from mammalian intracardiac ganglia. This was mainly

113

due to the inaccessibility of intramural cardiac neurons. In an abstract, Konishi et al.[28] reported that neurons in the dissected guinea pig heart ganglia responded to substance P and somatostatin . Since then, only a few intracellular microelectrode studies have been reported from mammalian intracardiac ganglion cells with intact synaptic connections [45,48,49]. It is not known yet whether these intracardiac neurons are electrophysiologically distinctive. Electrophysiological properties of intracardiac neuron subtypes have only been reported from dissociated cells in culture by Allen and Burnstock [1]. They developed this preparation in order to overcome the problems of inaccessibility and diffuse distribution of intramural cardiac neurons. Since the neuronal processes are digested during the dissociation procedure and neurons are no longer physiologically intact, it is of interest to ascertain whether different cell types exist in the *in situ* mammalian intracardiac ganglia with intact synaptic connections. This consideration is fundamental to an overall understanding of ganglionic physiology and cardiac vagal regulation. Hence, another aim of this studies was to test the hypothesis that canine intracardiac ganglia are composed of heterogeneous neurons with respect to their electrophysiological and pharmacological properties. In other words, are these neurons distinguishable not only morphologically, as mentioned in Chapter IV, but also electrophysiologically and pharmacologically?

B.   METHODS

The methods employed are similar to those described previously [49]. Ganglia were isolated from mongrel dogs of either sex which were either anesthetized with sodium pentobarbital (35 mg/Kg, iv) or α-chloralose (80 mg/Kg, iv) after sedation by morphine (2 mg/kg, sc). Following a right thoracotomy, the pulmonary vein fat pad [41,49] was rapidly removed and placed in 5 °C Krebs solution of the following composition (mM): NaCl 117, KCl 4.7, $CaCl_2$ 2.5, $MgCl_2$ 1.2, $NaHCO_3$ 25, NaH_2PO_4 1.2 and glucose 11; the solution was continuously aerated with 95% O_2 and 5% CO_2.

After careful *in vitro* dissection, a portion of the fat pad containing several ganglia was pinned to the base of a tissue bath; the tissue was superfused with aerated Krebs solution and maintained at 34.0 $\pm$ 0.5 °C. Conventional intracellular recording and stimulation techniques were used. Transmembrane potentials were recorded with 3 M KCl-filled glass microelectrodes (40-70 MΩ) and a high impedance amplifier (WP Instruments, model M701) with a bridge circuit. The bridge circuit was balanced before penetrating the cell membrane. The balance was checked again on withdrawal of the microelectrode. Membrane potentials and voltages proportional to applied currents were displayed, stored on a digital oscilloscope (Nicolet, model 4094) and output to a HP-plotter. In some cases, the voltage signals were also recorded on an oscillograph (Grass Instruments, model 79) to monitor changes in resting membrane potentials over long periods of time. Intrasomal current injections (single pulse or train stimulation) were applied via recording microelectrode using the virtual bridge circuit and a stimulator (Grass, model S44) with a stimulus isolation unit.

Orthodromic or antidromic responses were elicited by using suction electrodes to stimulate interganglionic nerves. Unless otherwise mentioned, the pulse duration was always 0.1 ms; the pulse frequency was 1.0 Hz. During repetitive stimulation, the train duration was less than 1.0 sec with a pulse frequency less than 30 Hz. The stimulus intensity varied between preparations but usually was less than 15-20 volts. The suction electrode method involved the application of a negative pressure which draws the nerve into the end of a polyethylene tube (PE-10) containing a concentric bipolar electrode and connected to a Grass S48 stimulator with a stimulus isolation unit.

Because of the complexity and heterogeneity of interganglionic nerves, it was not always possible in this preparation, to stimulate relatively pre- or postganglionic fibers. Antidromic and orthodromic spikes were distinguished by the following established methods [11,25,37]: 1) An orthodromic action potential has a longer delay time and was preceded by a gradually rising phase of a fast excitatory postsynaptic potential (f-EPSP); an antidromic action potential has a shorter delay time and a steep rising phase, sometimes an inflection is observed at the rising phase of the antidromic action potential; 2) An antidromic action potential could be separated into two components, initial segment (IS) and soma-dendrite (SD) spikes. During a hyperpolarizing current pulse (20-30 mV) or increased stimulation frequency (up to 30 Hz), the SD spike is blocked. Therefore, the full action potential is converted to a short fast-rising IS spike (Fig. 3-5). 3) Identified antidromic action potentials are completely unaffected by hexamethonium (10^{-4} M), while orthodromic f-EPSPs and spikes are consistently blocked.

In some experiments, tetrodotoxin (TTX, 3×10^{-7} or 10^{-6} M), hexamethonium (10^{-6} M), low Ca^{2+} (0.25 mM)/high Mg^{2+} (12.0 mM) solution and high K^+ solution (15 mM) were administered by superfusion.

Measurements (Fig. 5-1, upper panel):

1). Resting membrane potentials were recorded for at least 5 minutes after impalement of a healthy cell which had a stable resting membrane potential and action potential overshoot of 10 - 20 mV. A depolarizing current (0.1 - 0.3 nA, 20 ms) was injected intracellularly to evoked action potentials. If no action potential could be evoked by an intracellular current injection, a stable resting membrane potential was obtained for 20 minutes after impalement.

2). Input resistance (Fig.5-1, lower panel) was determined by measuring the plateau amplitudes of the voltage change produced by hyperpolarizing pulses (0.16, 0.24 and 0.32 nA, 175-200 ms). Input resistance is equal to the voltage change divided by the injected current. In some of the cells, the voltage changes were plotted on a current-voltage plot. The slope of the plot was the estimated input resistance.

3). Time constant was the time for electrotonic potentials, produced by intrasomal injection of hyperpolarizing current pulses (0.16, 0.24 and 0.32 nA, 175-200 ms) to reach 63% of the maximum.

4). Responses to intracellular current injection were classified by the number of action potentials evoked by a 175-200 ms depolarizing pulse (0.1 - 0.3 nA).

FIGURE 5-1

REPRESENTATIVE INTRACELLULAR RECORDINGS
OF CANINE INTRACARDIAC NEURONS
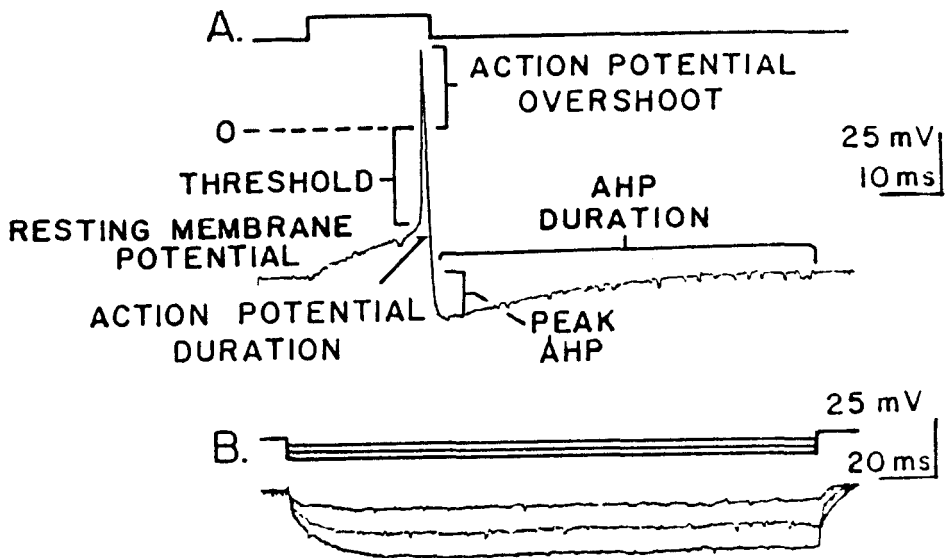
A. A depolarizing current caused the membrane potential to reach threshold initiating an action potential which is followed by an afterhyperpolarization (AHP). The parameters measured were resting membrane potential, threshold, action potential overshoot, action potential duration, the peak afterhyperpolarization (PEAK AHP) and the afterhyperpolarization duration (AHP DURATION).

B. To determine the membrane resistance and time constant, three different inward currents - 0.16, 0.24, and 0.32 nA, were applied resulting in three progressively more hyperpolarized responses. The slope of the relationship between current and membrane potential is equal to the input resistance. The time constant is the time required for a current to cause 63% of a voltage change.

5). Action potential amplitude was the absolute voltage difference between the resting membrane potential and the maximal overshoot of the action potential. Intrasomal action potential was evoked by a minimal depolarizing current pulse with a duration of less than 20 ms.

6). Action potential duration was the time interval between the onset of action potential and the intersection of the descending limb of the action potential and the resting membrane potential. In order to simplify the measurements from different action potentials, some visibly identified markers were arbitrarily selected as the onset point: the onset of intrasomal action potential was the transition point of the fast rising phase from the electrotonic potential; the one for orthodromic action potential was the transition point of the fast rising phase from the preceding EPSP; and the one for antidromic action potential was the transition point between IS and SD.

7). Action potential threshold was the membrane potential at which the action potential was initiated. It was measured from the onset points of different action potentials.

8). Afterhyperpolarization (AHP) duration was the time when the membrane potential was hyperpolarized below the resting potential.

9). The AHP amplitude was the difference between the resting membrane potential and the maximal downward deflection of hyperpolarization after the action potential.

All group data are reported as mean $\pm$ SEM. A paired Student t-test was used for comparison of change in responses from control values. For comparison of properties of the three types of cells, a one way analysis of variance was done followed by a Student-Newman-Keuls test for significance between groups. The level of statistical significance was established for $p < 0.05$.

C. RESULTS

Recordings of this series of experiments were obtained from 151 cells from 34 mongrel dogs.

As a representative recording, Fig. 5-1 (upper panel) shows membrane potential changes recorded from an intracardiac ganglion cell with a resting membrane potential of -60 mV. When a depolarizing current was applied via the microelectrode and the amplifier bridge circuit, the threshold was reached at -39 mV causing an action potential which had a duration of 2.5 ms and an overshoot of 30 mV. This action potential was followed by an AHP of 20 mV lasting for 69 ms. Hyperpolarizing currents (Fig. 5-1, lower panel) were applied to this cell, allowing for an estimation of input resistance of 66.5 MΩ and time constant of 4.2 ms.

1. Passive Membrane Properties:

Stable intracellular recordings were made for 15 minutes to more than one hour from 110 cells which had a mean resting membrane potential of -60.6 ± 1.4 mV. The distribution of these resting membrane potentials is shown in Fig. 5-2. The mean input resistance and mean time constant were 54.8 ± 5.7 MΩ and 3.3 ± 0.6 ms, respectively.

2. Active Membrane Properties:

The active membrane properties of canine intracardiac ganglion neurons were summarized in Table 5-1.

a. Action potential. When action potentials were intrasomally induced by depolarizing current injections, they had a mean amplitude and duration of 78.9 ± 0.8 mV and 2.7 ± 0.05 ms (n = 105), respectively. The action potential

FIGURE 5-2

THE DISTRIBUTION OF RESTING MEMBRANE POTENTIALS
IN CANINE INTRACARDIAC NEURONS
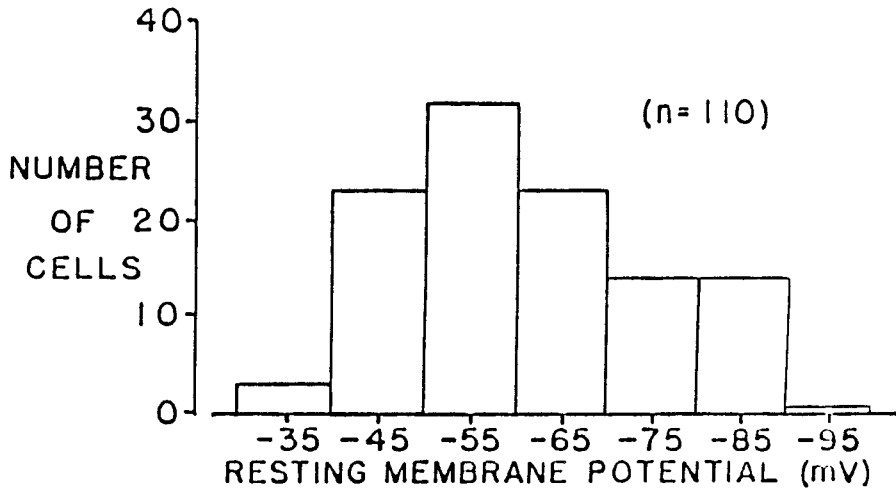
The distribution of stable resting membrane potentials in 110 canine intracardiac ganglion cells. The mode for this plot is -55 mV while the mean is 60.6 $\pm$ 1.4 mV.

TABLE 5-1

ACTIVE PROPERTIES OF CANINE INTRACARDIAC GANGLION NEURONS

	ACTION POTENTIAL				AHP	
	AMPLITUDE mV	OVERSHOOT mV	DURATION ms	THRESHOLD -mV	AMPLITUDE mV	DURATION ms
INTRASOMAL ACTION POTENTIAL	78.9 ±0.8 (54 - 103) n = 105	27.7 ±0.8 (5 - 45) n = 105	2.7 ±0.05 (2 - 4.2) n = 105	31.9 ±0.8 (17 - 53) n = 105	14.2 ±0.3 (9 - 16) n = 132	75.1 ±2.9 (23 - 189) n = 124
ORTHODROMIC ACTION POTENTIAL	76.3 ±1.1 (54 - 94) n = 58	25.0 ±1.2 (5 - 38) n = 58	2.5 ±0.06 (2 - 3.6) n = 56	33.0 ±1.0 (22 - 52) n = 56	13.5 ±0.7 (5 - 19) n = 48	72.5 ±4.9 (18 - 160) n = 44
ANTIDROMIC ACTION POTENTIAL	78.5 ±1.6 (60 - 103) n = 26	24.9 ±2.0 (5 - 39) n = 25	2.7 ±0.1 (2 - 3.5) n = 10	37.9 ±1.0 (32 - 42) n = 10	12.9 ±1.1 (6 - 24) n = 10	68.9 ±10.4 (18 - 124) n = 10

Values represent mean ±standard error of the mean. Statistical analysis was done using one way ANOVA. No statistical difference was found between different groups.

overshoot was 27.7 ± 0.8 mV (n = 105). As a comparison, the characteristics of orthodromic and antidromic action potentials are also listed. There is no significant difference in the active properties among these action potentials evoked separately. The eatures of orthodromic and antidromic action potentials will also be discussed in Chapter VI.

b. Afterhyperpolarization of single spike. All action potentials exhibited post spike AHPs. The AHPs of intrasomally evoked action potentials had a mean amplitude of -14.2 ± 0.3 mV (n = 132) and a mean duration of 75.1 ± 2.9 ms (n = 124). The duration of the AHPs, following action potentials of either R- or S-cells, varied considerably (range 23 - 189 ms). There were no significant difference of the AHPs of intrasomal, orthodromic and antidromic action potentials (Table 5-1).

c. Afterhyperpolarization of multiple spikes. To study the AHP following more than one action potentials in excitable neurons, different periods and rates of firing were induced using trains of intrasomal or antidromic stimulations. In a given stimulation period, the amplitude and the duration of the AHP increased with the stimulation frequency, i.e. the preceding number of action potentials (Fig. 5-3). The input resistance was slightly reduced by 5% - 10% during AHP (e.g. Fig. 5-12) in many of these cells. The maximum AHP response was usually obtained at 20 - 40 Hz with the intrasomal stimulation duration of 0.7 - 0.9 S, which had a mean amplitude and duration of 15.8 ± 0.8 mV and 3.42 ± 0.21 s, respectively (n = 11).

3. Classification of Cell Types:

Among 110 cells tested, three types of cells were categorized based upon their

FIGURE 5-3

EFFECT OF STIMULATION FREQUENCY ON
AFTERHYPERPOLARIZATION
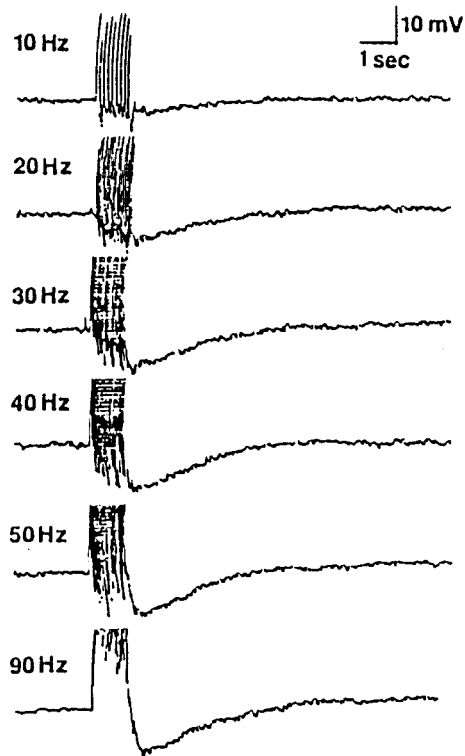
Stimulation frequency dependency of afterhyperpolarization (AHP) followed multiple action potentials in canine intracardiac ganglion neuron. Intracellular recordings were obtained from a R-cell with resting potential of -50 mV. Intrasomal repetitive current injection had a train duration of 0.9 s; a pulse duration of 10 ms and a current intensity of 0.35 nA. Increasing stimulation frequency from 10 (top trace) to 70 Hz (bottom trace) are indicated. The amplitudes of AHP were 3, 8, 10, 12 and 12 mV with duration of 2, 3.4, 4, 4, 4, and 4 s, respectively. Note the action potentials were truncated.

responses to outward, depolarizing current injections for 175-200 ms. As shown in the upper portion of Fig. 5-4, the first group of 23 cells were classified as non-responding (N-cell) because they failed to reach threshold for an action potential during large depolarizations produced by currents exceeding 1 nA. Yet, these cells had stable resting membrane potentials. The second group of 57 cells responded with one action potential at the onset of the current and were categorized as single-responding (S-cells) (middle portion of Fig. 5-4). When the current intensity was increased, these cells reached threshold but failed to discharge more than once or twice despite the maintained depolarization. The third group consisted of 30 cells which responded with repetitive action potentials and were categorized as R-cells (bottom of Fig. 5-4). As depicted in Fig. 5-5, the discharge rate of R-cells depended on the intensity of the current injection, reaching a discharge rate as high as 60 impulses per second or higher. In nearly all R-cells, the discharge frequency decreased somewhat during the maintained outward current injection (Fig. 5-5 A, B and C). Following termination of a hyperpolarizing current injection (Fig. 5-6), many R-cells initiated a single discharge or a brief train of 2 or 3 discharges but rarely did S-cells, which suggested a higher excitability of R-cells. The frequency of these afterdischarges in a train is related to the amount of preceding hyperpolarization.

The passive membrane properties of these three types of cells are represented in Figs. 5-7 and 5-8 and Table 5-2. The mean resting membrane potentials were significantly different, being about 9 mV higher for N-cells (n = 30) than S-cells (n = 57) which were about 6 mV greater than R-cells (n = 23) ($P < 0.05$, Fig. 5-7).

FIGURE 5-4

CLASSIFICATION OF CANINE INTRACARDIAC NEURONS
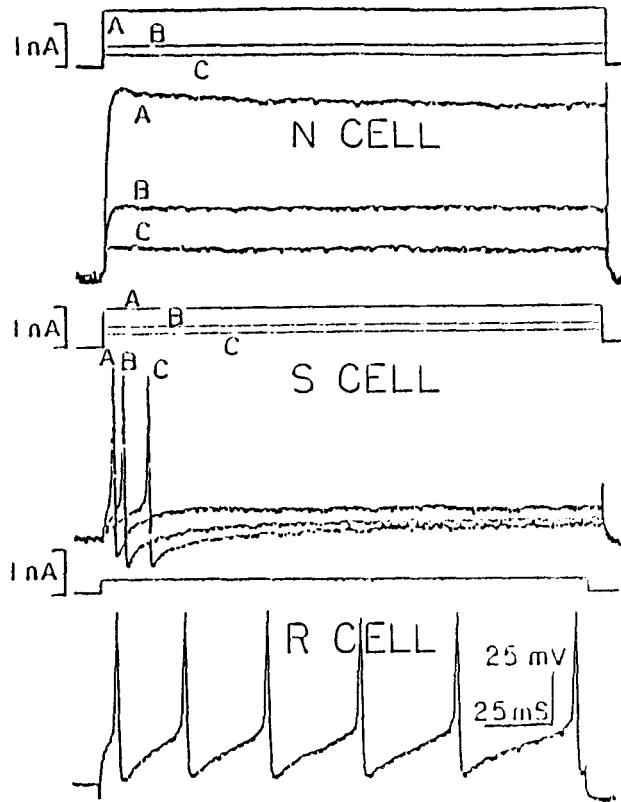
Classification of intracardiac ganglion cells by the responses to 175 ms depolarizing current pulses. N-cell (top section) failed to produce an action potential response even with large depolarizations. S-cell (middle section) responded with only a single action potential despite increasing depolarizing currents. R-cell (bottom section) responded with multiple discharges to a prolonged depolarizing current. In each section depolarizing currents (I) are above and the resultant membrane potential responses are below.

FIGURE 5-5

EFFECT OF STIMULATION INTENSITY
ON R-CELL DISCHARGE RATE
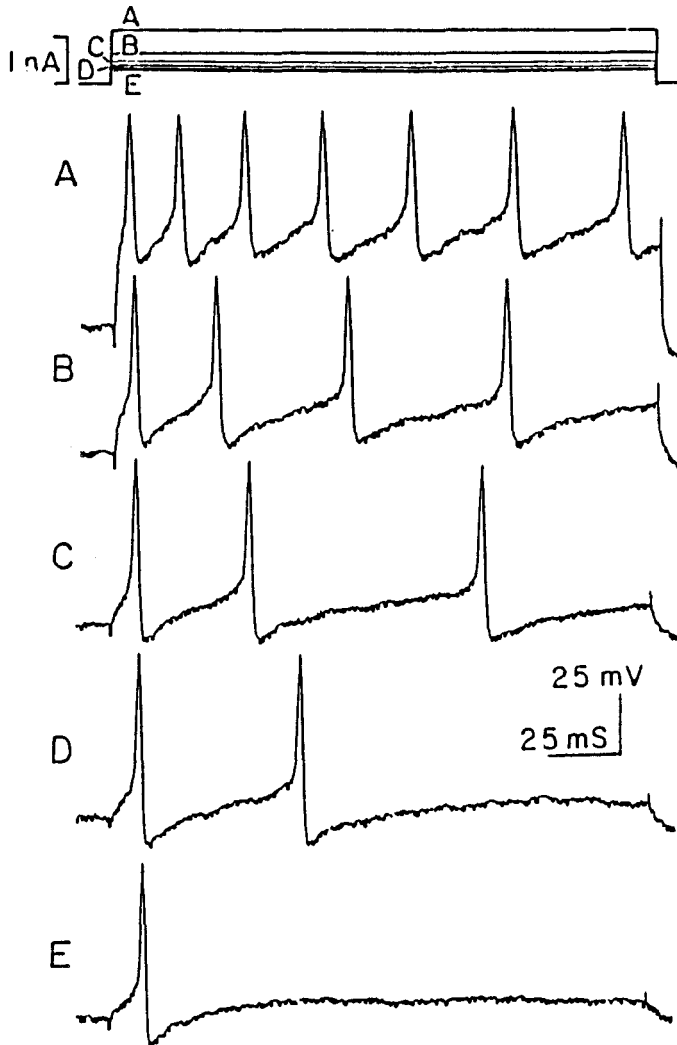
Membrane potential responses (below) of an R-cell to variations in depolarizing currents (above, I). Increasing currents increased the discharge rate. Note, some adaptation of the firing rate occurred.

FIGURE 5-6

AFTERDISCHARGES OBSERVED FROM R-CELLS
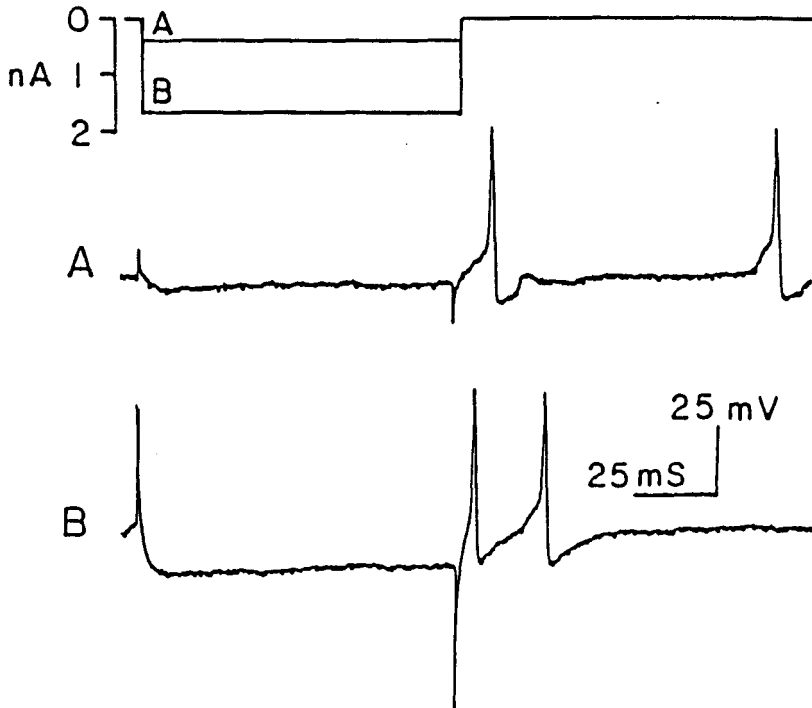
"Off responses" or afterdischarges following termination of hyperpolarizing currents. Different hyperpolarizing current intensities were utilized in A and B, showing that the number of impulses in the "off response" is related to the amplitude of the previous hyperpolarization.

FIGURE 5-7

MEAN RESTING MEMBRANE POTENTIALS OF R-,S-,AND N-CELLS
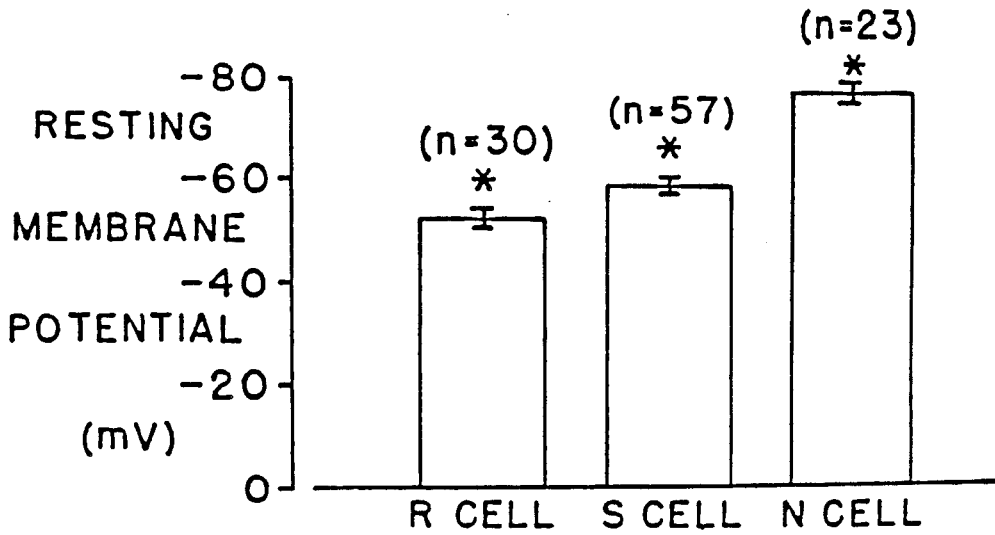
Mean resting membrane potentials: R-cell -52.5 $\pm$ 1.8 mV (n = 30), S-cell -58.8 $\pm$ 1.5 mV (n = 57) and N-cell -77.3 $\pm$ 2.2 mV (n = 30). * indicates statistically significant difference from the other two groups of cells (P < 0.05).

FIGURE 5-8

PASSIVE PROPERTIES OF R-,S- AND N-CELLS
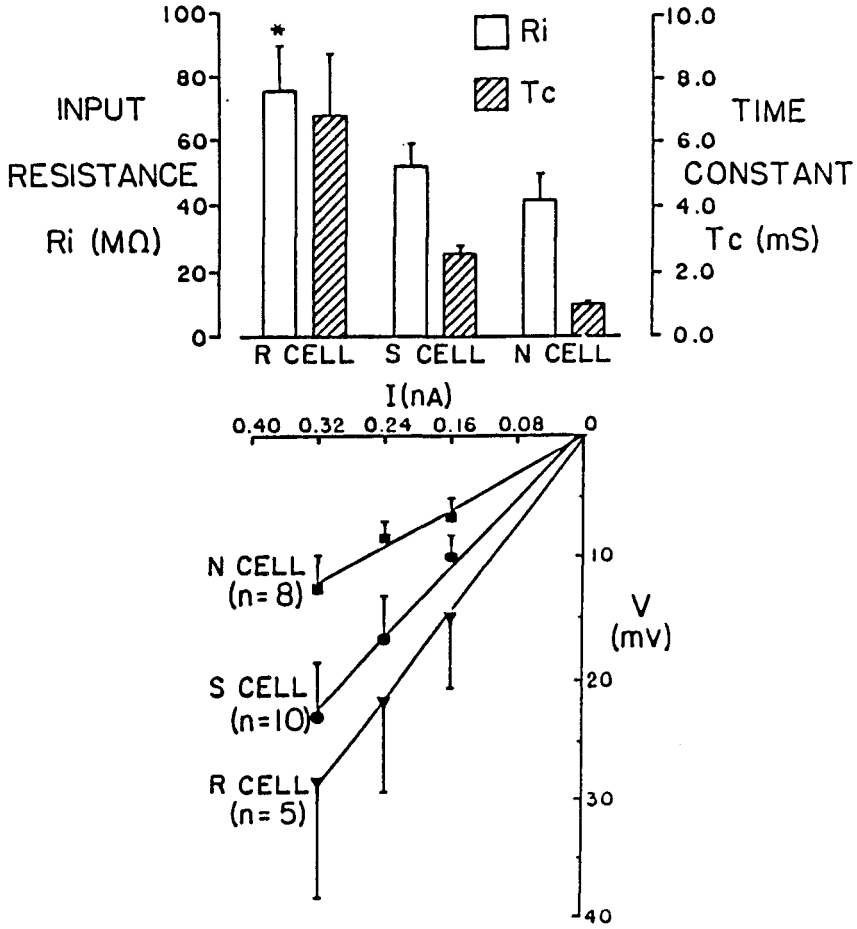
Input resistance estimation and time constant characteristics of R-, S-, and N-cells (see text and Table 5-2 for details). Statistical significant differences are indicated by * (P <0.05). The current-voltage relationship is plotted below. The slopes for the current-voltage relationship for R-, S- and N-cells are statistically different (84.4, 65.6 and 40.6 MΩ, respectively).

TABLE 5-2

ELECTRICAL MEMBRANE PROPERTIES OF R-, S- AND N-CELLS

| | PASSIVE PROPERTIES | | | ACTIVE PROPERTIES | | | |
| | | | | ACTION POTENTIAL* | | AHP | |
	RESTING POTENTIAL mV	INPUT RESISTANCE MΩ	TIME CONSTENT ms	AMPLITUDE mV	THRESHOLD -mV	AMPLITUDE mV	DURATION ms
R-CELL	52.5 ±1.8	75.3 ±14.8	6.8 ±2.0	76.8 ±1.1	32.1 ±1.0	14.1 ±0.3	76.2 ±3.4
	(41 - 77)	(9.3 - 210)	(1.1 - 13)	(60 - 95)	(21 - 52)	(8 - 21)	(18 -190)
	n = 30	n = 30	n = 30	n = 54	n = 65	n = 95	n = 89
S-CELL	58.8 ±1.5	52.0 ±7.2	2.6 ±0.2	75.4 ±4.0	32.2 ±3.8	14.4 ±0.8	68.9 ±5.7
	(42 - 87)	(6.7 - 144)	(1.0 - 4.5)	(54 - 84)	(22 - 39)	(6 - 24)	(14 - 168)
	n = 57	n = 30	n = 30	n = 47	n = 47	n = 30	n = 36
N-CELL	77.3 ±2.2	41.9 ±7.9	1.0 ±0.1	-	-	-	-
	(53 - 96)	(3.3 - 100)	(0.7 - 1.9)	-	-	-	-
	n = 23	n = 15	n = 15	-	-	-	-
P	<0.05 #	<0.05 ##	NS	NS	NS	NS	NS

Values represent mean ±standard error of the mean. Statistical analysis was done using one way ANOVA. NS =no statistical difference (P >0.05)
* orthodromic action potential # Among all three groups ## R-cell vs S- and N-cells

The mean time constant for R-cells (n = 16) was longer than for S-cells (n = 30) which was longer for N-cells (n = 15), but no statistical significance was reached (top of Fig. 5-8). The input resistance was significantly larger for R-cells (n = 16) than S- (n = 30) or N-cells (n = 15) (P < 0.05). When voltage changes were plotted as a function of injected currents (bottom of Fig. 5-8), a nearly linear relationship existed between current and voltage for all 3 types of cells. Input resistance calculations based upon the slope of this current-voltage relationship revealed that statistically significant differences existed between all 3 types of cells with R-cells > S-cells > N-cells.

The active properties of S- and R-cells are compared in Table 5-2. There were no significant differences in action potential amplitude, threshold and AHP amplitude of S- and R-cells. The AHP duration for S-cells was slightly shorter than for R-cells (68.9 $\pm$ 5.7 vs 76.2 $\pm$ 3.4), but was not statistically, significantly different (P > 0.05).

4. Mechanisms for Membrane Potentials:

The mechanisms involved in the resting membrane potential, the action potential and the AHP were investigated in both S- and R-cells. Unless otherwise mentioned, the following studies represent the responses of both groups.

a. Increased extracellular potassium ions. The influence of extracellular K^+ concentration on the resting membrane potential of canine intracardiac neurons was tested. After the extracellular K^+ concentration of Krebs solution was increased from 4.7 to 15 mM, the membrane potential was lowered 18 mV in the neuron tested. Theoretically, the dependence of the transmembrane potential (V_m) on the intracellular and extracellular concentrations of K^+ and Na^+ and on the conductances (g_K and g_{Na}) of

these ions is described by the chord conductance equition [27]: $V_m = [g_K/(g_K + g_{Na})] \times E_k$ + $[g_{Na}/(g_K + g_{Na})] \times E_{Na}$. In the resting nerve cell, equilibrium potentials (E_k and E_{Na}) could be expressed by the Nernst equation -60 $\log_{10} [(K^+)_i/(K^+)_o]$ and -60 $\log_{10}$ $[(Na^+)_i/(Na^+)_o]$, respectively, and g_K is about 20 times greater than g_{Na} [27]. When the $(K^+)_i/(K^+)_o$ was decreased in this experiment, the measured value of transmembrane potential decrease (18 mV) approximated that predicted by the Nernst equation. Therefore, the transmembrane potentials of these neurons are essentially affected by potassium. Similar observations (17.3 $\pm$ 1.2 mV) were made in another 5 cells. The amplitude of the action potential was slightly reduced due to the depolarized resting potential. Hyperpolarizing the resting potential to control level could restore the amplitude of the action potential.

b. Sensitivity to TTX. In Fig. 5-9 the ionic mechanisms involved in S- and R-cells' action potentials are compared. As demonstrated above, S- and R-cells were identified by their discharge responses to prolonged depolarizing currents. Using a short duration, suprathreshold depolarizing current, S- and R-cell action potentials have a similar appearance (Fig. 5-9, control). With a superfusion containing 3×10^{-7} M TTX solution, the R-cell action potential had a higher threshold and longer duration while the S-cell action potential was unaffected. A low Ca^{2+}/high Mg^{2+} solution with 3×10^{-7} M TTX (not depicted in figure) was able to block the R-cell but not the S-cell action potential. To block the S-cell action potential, a 10^{-6} M TTX solution with low Ca^{2+}/high Mg^{2+} solution was required. Hence, the R-cell action potential was more sensitive to TTX blockade than the S-cell. Similar responses were observed in 8 cells.

FIGURE 5-9

SENSITIVITIES OF S- AND R-CELLS TO TETRODOTOXIN
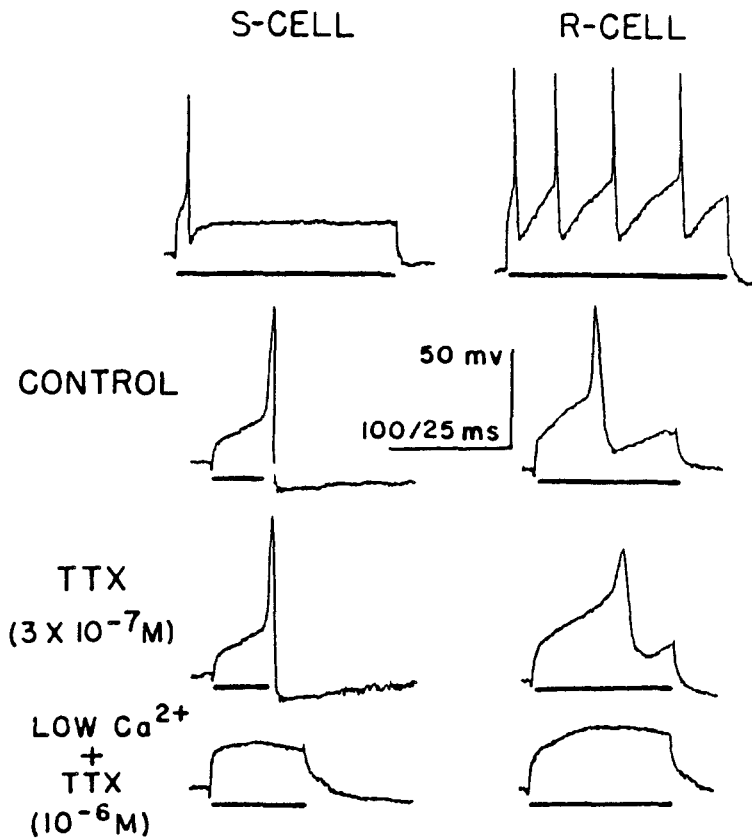
Relative sensitivities of S- and R-cells to tetrodotoxin (TTX) and low Ca^{2+} solutions are shown.   Upper panels show identification of S- and R-cells to a prolonged depolarizing current (time calibration = 100 ms). Lower panels show responses of these cells to a short depolarizing pulse (time calibration = 25 ms) during control superfusion with control perfusion (CONTROL), TTX (3×10^{-7}M) and combined low Ca^{2+} and TTX (10^{-6}m). S-cell required a higher TTX concentration than R-cell to block the fast action potential. Both cells required low Ca^{2+}/high Mg^{2+} to block the remaining slow action potential.

c. Low Ca^{2+}/high Mg^{2+} solutions on membrane and action potentials. Superfusion with a low Ca^{2+}/high Mg^{2+} solution caused the resting membrane potential to depolarize gradually. In 5 cells the resting membrane potential was significantly lowered by 10.6 $\pm$ 2.3 mV (18.4%, P < 0.01) from -57.77 $\pm$ 3.1 mV to -47.1 $\pm$ 3.6 mV. The amplitude of the action potential overshoot was sometimes slightly diminished. The mean overshoot was lowered by 9.2 $\pm$ 4.2 mV (33.4%) but was not statistically significant (n = 5, P > 0.05).

d. Mechanisms involved in the AHP. In addition to changes in resting membrane potential for the above 5 cells, the low Ca^{2+}/high Mg^{2+} solution caused the average peak amplitude of AHP to be reduced by 6.3 $\pm$ 2.8 mV (39.3%) from 16.1 $\pm$ 0.7 mV to 9.8 $\pm$ 2.5 mV , but this difference was not statistically significant (n = 5, P > 0.05). On the other hand, the duration of AHP was significantly diminished from 55.5 $\pm$ 6.0 ms to 22.9 $\pm$ 6.6 ms (58.7%, n = 5, P < 0.01). To eliminate the possible effects that resting membrane potential changes might have on the AHP, these studies were repeated with the resting membrane potential maintained constant by injecting a steady hyperpolarizing current (Fig. 5-10 A). The amplitude of the AHP was again slightly diminished and the duration of the AHP was greatly reduced in a low Ca^{2+}/high Mg^{2+} solution. This suggests that calcium ions play an important role in the later portion of AHP.

To further elucidate the ionic mechanism of AHP, the effects of membrane potential on the amplitude of AHP were studied. In summated AHP, AHP amplitude was linearly related to membrane potential between -50 and -110 mV (Fig. 5-11).

FIGURE 5-10

MECHANISMS INVOLVED IN AFTERHYPERPOLARIZATION
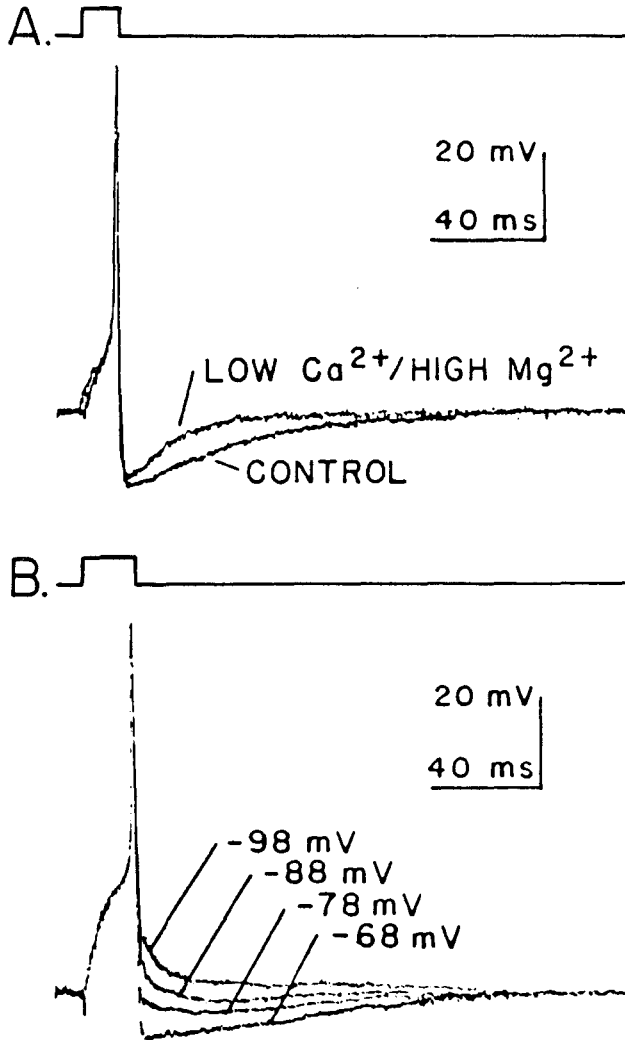
Factors determining the afterhyperpolarization (AHP) following an action potential induced by a depolarizing current. A. AHPs with control and low Ca^{2+}/high Mg^{2+} superfusion while maintaining resting membrane potential constant. B. The effects of resting membrane potential changes upon AHPs. Tracings at 5 different resting membrane potentials were superimposed (see text for details).

FIGURE 5-11

VOLTAGE DEPENDENCY OF AFTERHYPERPOLARIZATION
FOLLOWING MULTIPLE ACTION POTENTIALS
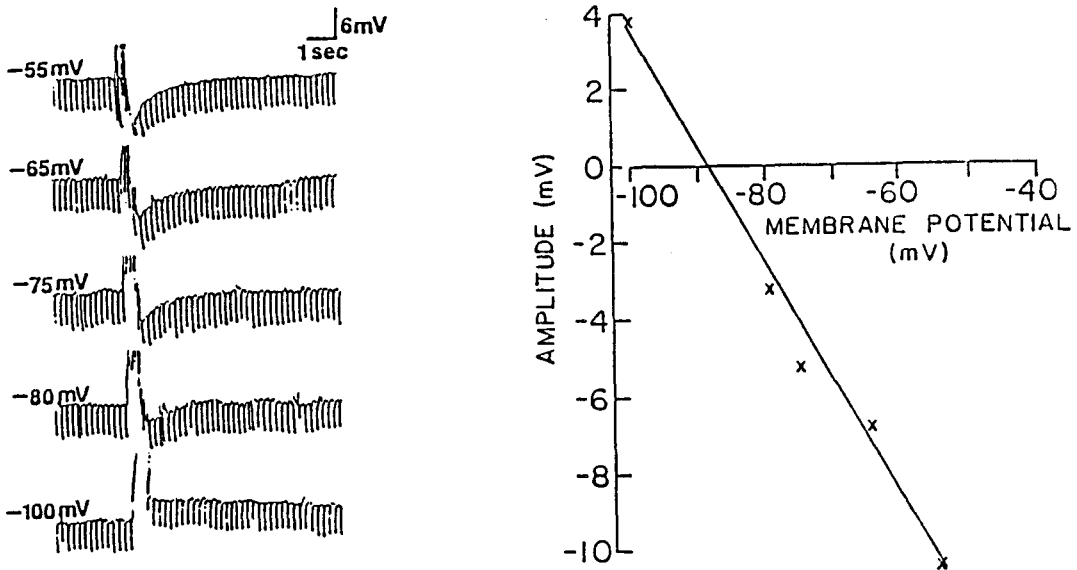
Left: the amplitude of AHP in a R-cell (resting potential -55 mV) at different membrane potential as indicated. Action potentials were evoked by antidromic stimulation (0.6 s, 25 Hz, 20 V, 0.1 ms pulse) in the presence of hexamethonium (10^{-4} M). Action potentials were truncated. Downward deflections are the result of passing brief 40 ms duration constant hyperpolarizing current pulses (0.2 nA) in order to monitor changes in membrane input resistance. Note a slight decrease of input resistance during the AHP. Right: a plot of amplitude against membrane potential for the cell shown in top panel. The amplitude was linearly related to the membrane potential over the range -55 to -110 mV and reversed at a membrane potential of -88.1 mV. This evidence suggests that the AHP probably results from an increase in potassium conductance.

Membrane potential hyperpolarization reduced the amplitude of AHP with the reversal

occurring at -88.1 mV. Similar results were observed in another 5 neuron. In single

spike AHP (Fig. 5-10 B) as well, the amplitude of AHP diminished at -78 mV, nearly

completely disappeared at -88 mV and resulted in a reverse or hypopolarization at

-98 mV. This also suggests an reversal potential to be between -88 and -98 mV, which

is close to the one of the summated AHP.

D. DISCUSSION

1. Passive Membrane Properties

Stable transmembrane potentials were recorded intracellularly from canine intracardiac ganglion cells *in vitro* with intact synaptic inputs. These ganglia receive vagal preganglionic fibers and send postganglionic fibers to control the sinoatrial node [6,41]. In general, the basic electrical characteristics - the mean resting membrane potential (-61 mV), input resistance (55 MΩ) and time constant (3 ms) are similar to that of other autonomic ganglia. However, their input resistances were about half of those reported for *in situ*, neonatal rat [45] and cultured guinea-pig intracardiac ganglion cells [1]. This may be related to differences in the size of the soma and dendritic network related to differences in species, to morphological maturation and possibly to damage of the cultured cells following dissociation utilizing enzymatic and mechanical separation.

The input resistance was estimated using voltage changes induced by hyperpolarizing currents. A linear relationship was observed over a narrow range of voltage changes (-50 to -110 mV). In sympathetic ganglion studies, Chirst and Nishi [10] and later Brown and Adams [7] observed a similar linear relationship in this voltage range. Comparable results were also reported from cultured guinea-pig intracardiac neurons [1]. However, larger hyperpolarizations may result in anomalous rectification which is abolished by barium or strontium ions. On the other hand, depolarizations above the resting membrane potential may also cause rectification due to activation of voltage sensitive channels.

2. Cell Types

Based upon their responses to prolonged depolarizing intracellular current pulses, these cells were categorized into three groups in the present study: N-cells (not excitable), S-cells type (single action potential), and R-cells (repetitive firing). The activity patterns of these cell types were inversely related to the order of the resting membrane potentials (N-cells > S-cells > R-cells). The order of the input resistance was also reversed, R-cells > S-cells > N-cells. The low excitability may in part due to the greater resting conductance which tend to prevent these cells depolarized. With a low input resistance and high resting membrane potential, it is unlikely that the N- or S-cells were damaged or that the recordings were made from dendritic processes.

From the time constant measurements and estimations of total capacitance, other properties of these cells can be surmised. No significant differences were found in the time constants for these three groups. The time constant is equal to the input resistance times the total capacitance. Thus, the order of estimated total capacitance appears to be N-cells > S-cells > R-cells. Because the capacitance per unit area of membrane is relatively constant for most nerves, the surface area of the cell would be related to the total capacitance. Therefore, the order of the estimated cell surface area is N-cells > S-cells > R-cells. As Xi et al. described previously [49] and in Chapter IV, intracellularly labeled these ganglion cells following functional identification of cell types, allowing direct measurements of the area of the soma profile. The order of soma area was N-cells > S-cells > R-cells, in agreement with the present estimation of cell size. Thus, the functional characteristics of these cell types were related, in part, to their morphological

characteristics.

Intracardiac ganglion cells from other animals are compared to canine cells. However, only one functional type of amphibian intracardiac ganglion cells has been recorded [43], which had a narrower range of resting membrane potentials than canine intracardiac ganglion cells (-45 to -66 mV vs. -35 to -95 mV). On the other hand, on cultured guinea-pig intracardiac ganglion cells, Allen and Burnstock [1] described three different cell types: multiple discharging cells with and without post-spike AHPs and single discharging cells with AHPs. Blockade of a Ca^{2+}-mediated K^+ current eliminated this AHP and converted single discharging cells into multiple discharging cells. However, in the canine intracardiac ganglion cells, almost all cells have AHP of various length. The mean duration of AHP following single spike is much shorter than Allen and Burnstock's report [1] and the presence of AHP did not significantly distinguish S-cells from R-cells. Therefore, species differences in electrical properties of intracardiac ganglion neurons may exist.

Three cell types similar to R-, S- and N-cells have been described also in sympathetic ganglia [4,5,11,16], other parasympathetic ganglia [21] and in the enteric nervous system [23,33]. Furukawa et al.[18] noted statistical differences in the resting membrane potentials between the multiple and single discharging types of enteric neurons. In the guinea-pig inferior mesenteric [11], these cell types had the same order of resting membrane potentials, input resistances and AHPs as canine intracardiac ganglion cell types. They considered the single responding and non-responding cells to be possibly small intensely fluorescent cells and glial or supportive cells, respectively. However,

Hodgkiss and Lees [24] and Erde et al.[15] also compared morphological and functional properties. They failed to find any useful relationship among the three morphological categories described by Dogiel [13] based upon the length of processes and whether the axon left the ganglion plexus. In cat vesical pelvic ganglia, no differences in resting membrane potential, input resistance or time constant were found in these cells types, except that the non-responding cells had a higher resting membrane potential [21]. These non-responding or "silent cells" were also assumed to be glial cells, interneurons or satellite cells similar to those described by Blackman et al.[5], Dennis and Gerschenfled [12] and Gallego and Eyrzguirre [20]. Nevertheless, Xi et al.[48] noted that intracellularly labeled canine intracardiac N-cells had clearly the morphological characteristics of large neuronal cell bodies with axons leaving the ganglion, not SIF or supportive cells.

In general, there seems to be considerable similarity between the classification of canine intracardiac ganglion cells and other autonomic ganglia or plexuses. The physiological role for these different types is not understood. McLachlin and co-investigators have noted intriguing differences between phasic and tonic discharging cells in the guinea pig and cat lumbar paravertebral ganglia and prevertebral sympathetic ganglia [8,31]. They noted that the phasic cells receive predominantly control from spinal preganglionic neurons. On the other hand, the tonic cells receive considerable excitation from afferent fibers, forming peripheral reflex arcs not requiring CNS connections. The possibility of peripheral reflexes, i.e. cardio-cardiac reflexes were proposed by Nozdrachev and Pogorelov [35], Priola et al.[38] and Gagliardi et al.[19], among others. Is it

possible that S-type cells in the cardiac ganglia receive predominantly vagal preganglionic input while the R-type cells might participate in cardio-cardiac reflexes analogous to the intestino-intestinal reflexes [46]?

3. Ionic mechanisms

Due to the dependency of the resting membrane potential upon the K^+ conductance, increased superfusate K^+ concentration expectedly decreased the resting membrane potential without greatly affecting the action potential of the canine intracardiac ganglion cells. Decreased extracellular Ca^{2+} concentration also lowered the resting membrane potential. This is unlikely due to the direct contribution of Ca^{2+} currents on the resting membrane potential but rather secondarily due to the effects of Ca^{2+} on the inward Na^+ current or diminished outward K^+ current.

The S- and R-cells of the canine intracardiac ganglion had different sensitivities to the effects of TTX - a fast, voltage-sensitive Na^+ channel blocker [9]. The action potentials of the R-cells were more sensitive to TTX than the S-cells. After blockade of the fast action potential, the remaining slow action potential was blocked by lowering the extracellular Ca^{2+} concentration. These observations support the notion that voltage-sensitive Na^+ and Ca^{2+} channels may contribute to the action potentials in these ganglion cells. However, a delayed outward K^+ current probably follows the normal fast action potential causing repolarization before very much of the slow Ca^{2+} current is usually initiated. Allen and Burnstock [1] reported that action potentials in some guinea-pig intracardiac ganglion cells were also insensitive to TTX alone but were blocked by TTX plus low extracellular Ca^{2+} concentration. Similar observations have been made on

sympathetic ganglion cells [20] and enteric neurons [23,33,47].

Afterhyperpolarizations following the action potentials were observed in all excitable cells. Although both duration and amplitude were affected by low Ca^{2+}/high Mg^{2+} solution, mainly the duration, but not the amplitude, of the AHP was found to be more sensitive to changes in extracellular calcium ion concentrations. Since changes in resting membrane potential accompanied these ion changes, these experiments were repeated with the resting membrane potential being held constant; and once again the low Ca^{2+}/high Mg^{2+} solution caused a significant reduction in the duration and less decrease in the peak amplitude of the AHP. The reversal potential of AHP was near -90 mV which is the potassium equilibrium potential. In addition, a small decrease of input resistance was usually observed during AHP. These observations suggest that an increase in potassium conductance was responsible for the AHP [1]. There seems to be different components which make up the AHP - a later component involving both Ca^{2+} and K^+ and an earlier and a larger component involving K^+ but not much Ca^{2+}. The earlier component is probably due to delayed or voltage - sensitive K^+ channels, and the later component is probably due to Ca^{2+} - sensitive K^+ channels. Similar currents have been demonstrated in many excitable membranes including the sympathetic and enteric ganglion cells [32,34]. These AHPs are important for they would increase the safety factor of synaptic transmission with repetitive activation and decrease the probability of repetitive action potentials. Similar observations on AHP of guinea-pig intracardiac neurons was reported by Allen and Burnstock [1]. Furthermore, they also found that both repetitive and single discharge cells had these Ca^{2+}-sensitive K^+-AHP.

In the present studies, the differences between S- and R-cells can not be explained on the basis of solely Ca^{2+}-sensitive K^+-currents. The differences may instead be related to other K^+ - mediated hyperpolarizations such as the A- and M-currents seen in sympathetic cells [7]. Similar explanation for differences between phasic and tonic sympathetic neurons has been proposed by Cassel et al.[8]. Possible M-currents are inhibited via muscarinic receptors; hence, the properties of the canine intracardiac ganglion cells may be altered by acetylcholine released from vagal preganglionic activity.

In summary, vagal control of heart rate is mediated by intracardiac ganglion cells located in a fat pad on the right atrium. After removal of the fat pad from the heart and placement in a superfused tissue bath, 151 intracardiac ganglion cells with intact synaptic inputs from 34 dogs were studied *in vitro* using intracellular recording techniques. These neurons were classified according to discharge responses to a depolarizing current: R-cells, S-cells and N-cells. These functional cell types correspond to different passive electrical (membrane potential, input resistance, time constant and calculated capacitance) characteristics and to differences in cell body size. R-cells were more sensitive to blockade of the fast, Na^+-mediated action potential by tetrodotoxin than S-cells. Following this block, both R- and S-cells had a remaining slow-Ca^{2+} dependent action potential. Afterhyperpolarizations of about 15 mV lasting 68 ms were characteristic of both R- and S-cells. A low Ca^{2+} solution greatly reduced the length but not the amplitude of these afterhyperpolarizations. In general, the characteristics of these cells are similar to other *in vitro* mammalian sympathetic, parasympathetic and enteric neurons.

E. REFERENCES

1 Allen, T.G.J. and Burnstock, G., Intracellular studies of the electrophysiological properties of cultured intracardiac neurons of the guinea-pig, *J. Physiol. (Lond.)*, 388 (1987) 349-366.

2 Armour, J.A. and Hopkins, D.A., Activity of canine in situ left atrial ganglion neurons, *Am. J. Physiol.*, 259 (1990) H1207-H1215.

3 Armour, J.A. and Hopkins, D.A., Activity of *in vivo* canine ventricular neurons, *Am. J. Physiol.*, 258 (1990) H326-H336.

4 Blackman, J.G., Crowcroft, P.J., Devine, C.E., Holman, M.E. and Yonemura, K., Transmission from preganglionic fibres in the hypogastric nerve to peripheral ganglia of male guinea-pigs, *J. Physiol. (Lond.)*, 201 (1969) 723-743.

5 Blackman, J.G. and Purves, R.D., Intracellular recording from ganglia of the thoracic sympathetic chain of the guinea-pig, *J. Physiol. (Lond.)*, 203 (1969) 173-198.

6 Bluemel, K.M., Wurster, R.D., Randall, W.C., Duff, M.J. and O'Tool, M.F., Parasympathetic postganglionic pathways to the sinoatrial node, *Am. J. Physiol.*, 259 (1990) H1504-H1510.

7 Brown, D.A. and Adams, P.R., Muscarinic suppression of a noval voltage-sensitive K-current in a vertebrate neurone, *Nature*, 283 (1980) 673-676.

8 Cassel, J.F., Clark, A.L. and McLachlan, E.M., Characteristics of phasic and tonic sympathetic ganglion cells of the guinea-pig, *J. Physiol. (Lond.)*, 372 (1986) 457-483.

9 Catterall, W.A., Neurotoxins that act on voltage-sensitive sodium channels in excitable membranes, *Ann. Rev. Pharmacol. Toxicol.*, 20 (1980) 15-43.

10 Christ, D.D. and Nishi, S., Anomalous rectification of mammalian sympathetic ganglion cells, *Exp. Neurol.*, 40 (1973) 806-815.

11 Crowcroft, P.J. and Szurszewski, J.H., A study of the inferior mesenteric and pelvic ganglia of guinea-pigs with intracellular electrodes, *J. Physiol. (Lond.)*, 219 (1971) 421-441.

12 Dennis, M.J. and Gerschenfeld, H.M., Some physiological properties of identified mammalian neuroglial cells, *J. Physiol. (Lond.)*, 203 (1969) 211-222.

13 Dogiel, A.S., Ueber den Bau der Ganglien in den Geflechten des Darmes und der Gallenblase des Menschen un der Saeugethiere, *Arch. Anat. Physiol. Anat. Abt.*, (1899) 130-158.

14   Ehinger, B., Falck, B., Persson, H. and Sporrong, B., Adrenergic and cholinesterase-containing neurons of the heart, *Histochemistry*, 16 (1968) 197-205.

15   Erde, S.M., Gershon, M.D. and Wood, J.D., Morphologically and eletrophysiologically identified types of myenteric neurons by intracellular recording and injection of lucifer yellow in the guinea-pig small bowel, *Soc. Neurosci. Abs.*, 6 (1980) 274.(Abstract)

16 Erulkar, S.D. and Woodward, J.K., Intracellular recordings from mammalian superior cervical ganglion in situ, *J. Physiol. (Lond.)*, 199 (1968) 189-203.

17 Fee, J.D., Randall, W.C., Wurster, R.D. and Ardell, J.L., Selective ganglionic blockade of vagal inputs to sinoatrial and /or atrioventricular regions, *J. Pharmacol. Exp. Ther.*, 242 (1987) 1006-1012.

18 Furukawa, K., Taylor, G.S. and Bywater, R.A.R., An intracellular study of myenteric neurons in the mouse colon, *J. Neurophysiol.*, 55 (1986) 1395-1406.

19 Gagliardi, M., Randall, W.C., Bieger, D., Wurster, R.D., Hopkins, D.A. and Armour, J.A., Activity of *in vivo* canine cardiac plexus neurons, *Am. J. Physiol.*, 255 (1988) 789-800.

20 Gallego, R. and Eyzaguirre, C., Membrane and action potential characteristics of A and C nodose ganglion cells studied in whole ganglia and in tissue slices, *J. Neurophysiol.*, 41 (1978) 1217-1232.

21   Griffith, W.H.III, Gallagher, J.P. and Shinnick-Gallagher, P., An intracellular investigation of cat vesicle pelvic ganglia, *J. Neurophysiol.*, 143 (1980) 343-354.

22 Hartzell, H.C., Kuffler, S.W., Stickgold, R. and Yoshikami, D., Synaptic excitation and inhibition resulting from direct action of acetylcholine on two type of chemoreceptors on individual parasympathetic neurons, *J. Physiol. (Lond.)*, 271 (1977) 817-846.

23   Hirst, G.D.S., Holman, M.E. and Spence, I., Two types of neurones in the myenteric plexus of duodenium in the guinea-pig, *J. Physiol. (Lond.)*, 236 (1974) 303-326.

24 Hodgkin, J.P. and Lees, G.M., Morphological features of guinea-pig myenteric plexus neurones. In J. Christnsen (Ed.), *Gastrointestinal motility*, Raven Press, New York, 1980, pp. 111-117.

25 Julé, Y., Krier, J. and Szurszewski, J.H., Patterns of innervation of neurones in the inferior mesenteric ganglion of the cat, *J. Physiol. (Lond.)*, 344 (1983) 293-304.

26 king, T.S. and Coakley, J.B., The intrinsic nerve cells of the cardiac atria of mammals and man, *J. Anat.*, 92 (1958) 353-376.

27 Koester, J., Resting membrane potential and action potential. In E.R. Kandel and J.H. Schwartz (Eds.), *Principles of Neural Science*, Elsevier Science Publishing Co.,Inc., New York, 1985, pp. 49-57.

28 Konishi, S., Okamoto, T. and Otsuka, M., Synaptic transmission and effects of substance P and somatoatatin on the guinea-pig cardiac ganglia, *IUPHAR Proc.*, (1984) 1604p-1604p.(Abstract)

29 Malor, R., Taylor, S., Chesher, G.B. and Griffin, C.J., The intramural ganglia and chromaffin cells in guinea pig atria: an ultrastructural study, *Cardiovasc. Res.*, 8 (1974) 731-744.

30 McMahan, M.N. and Purves, D., Visual identification of two kinds of nerve cells and their synaptic contacts in a living autonomic ganglion of the mudpuppy (necturus maculosus), *J. Physiol. (Lond.)*, 254 (1976) 405-425.

31 Meckler, R.L. and McLachlan, E.M., Axons of peripheral origin preferentially synapse with tonic neurones in the guinea-pig coeliac ganglion, *Neurosci. Lett.*, 86 (1988) 189-194.

32 Minota, S., Calcium ions and the posttetanic hyperpolorization of bullfrog sympathetic ganglion cells, *Jpn. J. Physiol.*, 24 (1974) 501-512.

33 Nishi, S. and North, R.A., Intracellular recording from the myenteric plexus of the guinea-pig ileum, *J. Physiol. (Lond.)*, 231 (1973) 471-491.

34 North, R.A., The calcium-dependent slow after-hyperpolarization in myenteric plexus neurons with tetrodotoxin-resistant action potentials, *Br. J. Pharmacol.*, 49 (1973) 709-711.

35 Nozdrachev, A.D. and Pogorelov, A.G., Extracellular recording of neuronal activity of the cat heart ganglia, *J. Auton. Nerv. Syst.*, 6 (1982) 73-81.

36 Osborne, L.W. and Silva, D.G., Histological, acetylcholinesterase, and fluorescence histochemical studies on the atrial ganglia of the monkey heart, *Exp. Neurol.*, 27 (1970) 497-511.

37 Perri, V., Sacchi, O. and Casella, C., Synaptically mediated potentials elicited by the stimulation of post-ganglionic trunks in the guinea-pig superior cervical ganglion, *Pflugers. Arch.*, 314 (1970) 55-67.

38 Priola, D.V., Intrinsic innervation of the canine heart, *Circ. Res.*, 47 (1980) 74-79.

39 Randall, W.C. and Ardell, J.L., Differential innervation of the heart. In D. Zipes and J. Jalife (Eds.), *Cardiac Electrophysiology and Arrhythmias*, Grune & Stratton, New York, 1985, pp. 137-144.

40 Randall, W.C., Ardell, J.L., Calderwood, D., Milosavljevic, M. and Goyal, S.C., Parasympathetic ganglia innervating the canine atrioventricular nodal region, *J. Auton. Nerv. Syst.*, 16 (1986) 311-323.

41 Randall, W.C., Ardell, J.L., Wurster, R.D. and Milosavljevic, M., Vagal postganglionic innervation of the canine sinoatrial node, *J. Auton. Nerv. Syst.*, 20 (1987) 13-23.

42 Randall, W.C., Milosavljevic, M., Wurster, R.D., Geis, G.S. and Ardell, J.L., Selective vagal innervation of the heart, *Ann. Clin. Lab. Sci.*, 16 (1986) 198-208.

43 Roper, S., An electrophysiological study of chemical and electrical synapses on neurons in the parasympathetic cardiac ganglion of the mudpuppy ,necturus maculosus: evidence for intrinsic ganglionic innervation, *J. Physiol. (Lond.)*, 254 (1976) 427-454.

44 Roper, S., The acetylcholine sensitivity of the surface membrane of multiply-innervated parasympathetic ganglion cells in the mudpuppy before and after partial denervation, *J. Physiol. (Lond.)*, 254 (1976) 455-473.

45 Seabrook, G.R., Fieber, L.A. and Adams, D.J., Neurotransmission in neonatal rat cardiac ganglion in situ, *Am. J. Physiol.*, 259 (1990) H997-H1005.

46 Szurszewski, J.H., Physiology of mammalian prevertebral ganglia, *Ann. Rev. Physiol.*, 43 (1981) 53-68.

47 Wade, P.R. and Wood, J.D., Electrical behavior of myenteric neurons in guinea pig distal colon, *Am. J. Physiol.*, 254 (1988) G522-G530.

48 Xi, X., Randall, W.C. and Wurster, R.D., Morphology of canine intracardiac ganglion cells, *J. Comp. Neurol.*, (1991) (submitted)

49 Xi, X., Thomas, J.X., Randall, W.C. and Wurster, R.D., Intracellular recordings from canine intracardiac ganglion cells, *J. Auton. Nerv. Syst.*, 32 (1991) 177-182.

CHAPTER VI

SYNAPTIC POTENTIALS AND MECHANISMS

IN CANINE INTRACARDIAC GANGLION CELLS

A.   INTRODUCTION

Since the early work of Langley and Dickinson [57,58], autonomic ganglionic transmission has been considered to be monosynaptic, as a one-to-one relay station [89]. A more complex view of ganglionic transmission was introduced by Eccles and libet [29] when they reported the muscarinic nature of a slow postganglionic response in sympathetic ganglion.   Today, the autonomic ganglionic transmission is no longer just a synaptic relay station involving a simple excitatory monosynaptic transmission. Preganglionic signals are conveyed to the postganglionic neurons by a variety of synaptic events subserving the integrative functions of the ganglia [51].

Generally, ganglionic transmission can be divided into nicotinic cholinergic, muscarinic cholinergic and noncholinergic events.   Acetylcholine released from preganglionic terminals unequivocally induces nicotinic transmission - the fast excitatory postsynaptic potential (f-EPSP), since it is depressed by nicotinic blocking agents [9,28] and is augmented by anticholinesterase agents.   The peak amplitude of the f-EPSP is, in general, large enough to initiate action potentials in the postganglionic neuron.   Thus, the nicotinic transmission mediated by f-EPSP is the main synaptic pathway in autonomic ganglia [56] and is responsible for eliciting the largest portion of end-organ response [87].

The muscarinic transmission in the rabbit superior cervical ganglion was clearly observed when Eccles and Libet [29] recorded a series of synaptic potentials: an initial negative potential was followed by a positive potential (P) and later by a prolonged late negative potential (LN). The P and LN potentials could be blocked by low concentrations of atropine [29,59,60] and mimicked by iontophoresis of ACh on a curarized neuron (see Chapter II for detail). The muscarinic slow potentials are characterized in contradistinction to the f-EPSP by their complex ionic mechanisms and by their species and preparation specificity [3]. The functional role of the slow potentials mainly constitutes the modulation of nicotinic outputs [3].

The noncholinergic synaptic transmission has only been studied since the late 1960's. A slow depolarization resistant to cholinergic antagonists was first recorded in bullfrog sympathetic ganglia by Nishi and Koketsu [71]. Several neuropeptides [24-26,43] and ionic mechanisms [47] are involved (see Chapter II).

The ganglionic spontaneous activity was first described by Nishi and Koketsu [70] in frog sympathetic ganglion. The characteristics of the spontaneous depolarization greatly resembled that of miniature end plate potentials in the neuro-muscular junction [70], suggesting spontaneous ACh release from preganglionic nerve terminals. Another synaptic mediated spontaneous activity was recorded only when the connections to the central nerve system are intact [65,67]. Some pacemaker-like neurons are also reported in a small group of ganglia [6,32,36,52-54,91]. These cells fire action potentials spontaneously, which are not likely mediated by ACh release [36,52,53].

Unlike the sympathetic ganglia which have long been used for synaptic

transmission investigations, parasympathetic ganglia have been less frequently studied because they are more difficult to localize in the walls of the organ they innervate. Therefore, most of our understanding of ganglionic transmission has been from sympathetic ganglia, and far less is known about the physiology and pharmacology of parasympathetic synaptic transmission.

The parasympathetic ganglion plexuses innervating mammalian heart are located in different areas of the walls of the heart [79,80]. These ganglia receive input from efferent vagal fibers, which originate in the medulla oblongata [78]. The intracardiac neurons, in turn, innervate the sinoatrial and atrioventricular nodes and the cardiac musculature [7,13,80,81]. These nerve cells are important because they are responsible for the control of heart rate [30]. Recently, some investigators recorded f-EPSP [88] and muscarinic agonist- mediated responses [5,66] from *in situ* or primary cultured mammalian intracardiac neurons. These results are consistent with previous studies on the cardiac ganglia of the frog [22] and the mudpuppy [83,84], which demonstrated the presence of nicotinic transmission and muscarinic receptor on the ganglionic somata. However, no direct evidence of neurally evoked slow synaptic potential has been reported. In terms of spontaneous activity, only a miniature EPSP-like activity was described in neonatal rat intracardiac ganglia [88], which may not exactly represent the situation in fully developed mammalian ganglia. Taken together, the specific objectives of the present study were:

1. To characterize the synaptic transmission in canine intracardiac ganglion plexus. The advantages of using canine preparation compared to using the intracardiac ganglia from other mammals [66,88] are that vagal control of canine heart rate has been well

established and the functional role of this plexus, innervating sinoatrial node, has been clearly identified [80].

2. To examine the possible presence of spontaneous neuronal activities and their derivations.

3. To analyze the general features, the receptor and ionic mechanisms of both neurally evoked f-EPSP and ACh evoked response.

4. To investigate the possible existence of muscarinic mediated synaptic potentials, the possible subtypes of muscarinic receptor and the ionic mechanism of both neurally evoked slow synaptic potentials and bethanechol, a muscarinic agonist, evoked responses.

Since the nicotinic f-EPSP has been well characterized in autonomic ganglia [34,56] including the intracardiac ganglia [22,83,88], more attention would be paid to the muscarinic transmission.

B. METHODS

Following induction of α-chloralose (80 - 100 mg/kg,iv) anesthesia and a right

thoracotomy, the entire pulmonary vein fat pad (PVFP) was removed form mongrel

dogs. The whole mount tissue was then quickly immersed into cold (0-5 °C) Krebs

solution (See Section G of Chapter III) continuously aerated with 95% O_2 and 5% CO_2.

The PVFP region was carefully dissected under a dissecting microscope (40x). An

approximate 3 mm x 2 mm x 1 mm portion of the tissue containing one to several

surface-cleaned ganglia and their interganglionic nerves overlying a thin layer of fatty

tissue and cardiac muscle was then pinned down to the tissue bath. Special care was

taken not to damage either the ganglia or the interganglionic nerves. The tissue and the

superfusion fluids were maintained at 34.0 $\pm$ 0.5 °C [24,26,62] throughout the experiment.

Glass microelectrodes (40-70 MΩ) were made from pipettes (FHC) and filled with

3 M KCl. The intracellular recording system was essentially the same as described in

Chapter III. Briefly, the microelectrode was connected to a microelectrode holder (FHC)

then an amplifier probe and a micromanipulator (ENCO, Model 360). The amplifier

probe consisted of a high impedance preamplifier (WP Instruments, Model 701)

connected to an amplifier system providing capacitance neutralization, current injection

and a virtual bridge circuit. The tissue bath was grounded by a Ag-Ag/Cl electrode.

The membrane potentials and voltages proportional to applied currents were displayed

on a digital oscilloscope (Nicolet, Model 4094) and stored on a floppy disk recorder

(Nicolet, XF-44) for later plotting on a digital plotter (HP,7475A). Slow membrane

potential and current changes were also simultaneously recorded on a two channel chart

recorder (Grass, Model 79C).

Standard intracellular recording and stimulation techniques were used to record transmembrane potentials (also see Chapter III). Direct intrasomal stimulation was performed via a recording microelectrode and a stimulator (Grass, model S44) with a stimulus isolation unit. Pulses of hyperpolarizing or depolarizing current (0.2 nA, 20-30 ms, 1.0 Hz) were injected via recording microelectrode using the bridge circuit which was previously balanced outside the cell. The balance was checked again on withdrawal of the microelectrode. Input resistance was estimated by the amplitude of electrotonic potentials caused by hyperpolarizing current pulses (0.1 - 0.2 nA, 50 ms). According to the electrical properties from Chapter V, the criteria used to accept cells for these experiments were 1) the cell had a resting membrane potential more negative than -40 mV, or 2) the cell had an action potential overshoot above 5 mV.

Orthodromic or antidromic responses were elicited by using suction electrodes to stimulate interganglionic nerves. Unless otherwise mentioned, the pulse duration was 0.1 ms; the pulse frequency was 1.0 Hz. During repetitive stimulation, the train duration was usually less than 1.0 sec with a pulse frequency of 10 - 30 Hz. The stimulus intensity varied between preparations but usually was less than 15-20 volts. The suction electrode method involved the application of a negative pressure which draws the nerve into the end of a polyethylene tube (PE-10) containing a concentric bipolar electrode. A Grass S48 stimulator with a stimulus isolation unit was used for extracellular stimulation.

As mentioned before, because of the complexity and heterogeneity of

interganglionic nerves, it was not always possible, under our condition, to stimulate only pre- or postganglionic fibers. Antidromic and orthodromic spikes were distinguished by these established criteria [20,45,77]: 1) Orthodromic f-EPSPs possess a longer delay time. If action potential evoked, the spike is induced by an initial gradual rising phase (f-EPSP); antidromic action potentials have shorter delay time and usually have no initial slow rising phase; 2) An antidromic action potential could be separated into two components, initial segment (IS) and soma-dendrite (SD) spikes.   During a hyperpolarizing current pulse (20-30 mV) or increased stimulation frequency (up to 30 Hz), the SD spike is blocked. Therefore, the full action potential is converted into a short, fast-rising IS spike (Fig. 3-5).   3) Identified antidromic action potentials are completely unaffected by hexamethonium (10^{-4} M), while orthodromic f-EPSPs and spikes are consistently blocked.

Pharmacological agents dissolved in Krebs solution and applied to the ganglia in known concentrations by superfusion were: hexamethonium bromide (C_6, Sigma) 10^{-5} to 10^{-4} M, atropine (Sigma) 10^{-6} or 10^{-7} M, pirenzepine dihydrochloride (Sigma) 10^{-8} M, 4-DAMP (Sigma) 10^{-7} or 5×10^{-7} M, phentolamine hydrochloride (Regitine, CIBA Pharmaceutical Co.) 10^{-6} M,l-propranolol (Sigma) 10^{-6} M and physostigmine sulfate (Sigma) 10^{-7} M. A low Ca^{2+}/high Mg^{2+} solution (See Chapter III) was used to diminish the transmitter release in certain experiments. Acetylcholine chloride (ACh, Sigma) and bethanechol chloride (Sigma) were introduced by pressure ejection (see below). Drug concentrations in the ejection microelectrode (3-10 tip diameter) [5] were 10^{-2} - 10^{-3} M [44].

The pressure micro-ejection system consisted of ejecting very small quantities of

agents in a microelectrode in close proximity to the recording cell [68], using high pressure

nitrogen (1700 mmHg) and a very fast solenoid valve controlled by a stimulator (Grass,

model S4). Although the exact concentration of drugs on the recording cell is unknown,

the amount of ejected drug could be proportionally altered by varying the open duration

of the valve (up to hundreds milliseconds). Compared to the method of continuous

superfusion which may cause receptor desensitization [35], pressure microejection is a more

convenient and reliable method to evoke consistent postsynaptic cholinergic responses.

Group results are expressed as Mean $\pm$ SEM. Statistical analysis was done using

a paired Student's t-test to distinguish between mean values. A p value of 0.05 or less

was considered significant.

C. RESULTS AND DISCUSSION

1. Spontaneous Activity

Spontaneous activity was referred to as electrical potential changes that were not induced by the investigators or by apparent injury. Spontaneous neuronal activity was investigated from totally 381 intracardiac neurons throughout the 124 experiments. All cells were from PVFP region and had intact synaptic connections. Amongst the 381 neurons studied with stable resting membrane potentials, 52% (n = 198) demonstrated well-maintained spontaneous activity. Spontaneous activity was observed in 59% of the R-cells (94/159 R-cells), in 50% of the S-cells (61/121 S-cells) and only in 10% of the N-cells (2/21 N-cells).

Based on their different electrophysiological and pharmacological characteristics, spontaneous activity could be classified into four groups:

a. Spontaneous miniature EPSP-like depolarizations with or without action potentials. About 90% of the spontaneous activity consisted of miniature EPSPs-like depolarizations which occurred with or without action potentials (Fig. 6-1A), depending on the amplitude of the miniature EPSP-like depolarizations and thresholds. This type of spontaneous activity was observed in all cell types (R-, S- and N-cells). The frequency of the miniature EPSP-like depolarization was 9.3 ± 2.4/min (n = 49). Their occurrence could persist for hours. Most of these neurons (82%, n = 40) had a very low frequency of 2.5 ± 0.4 min (range 0.8 to 4.7/min). Similar frequency of appearance of miniature EPSPs was also reported from other autonomic ganglia cells [11,27,36]. In a small group (18%, n = 9), the frequency was higher (38.8 ± 13/min,

FIGURE 6-1

DIFFERENT TYPES OF SPONTANEOUS ACTIVITY (1)
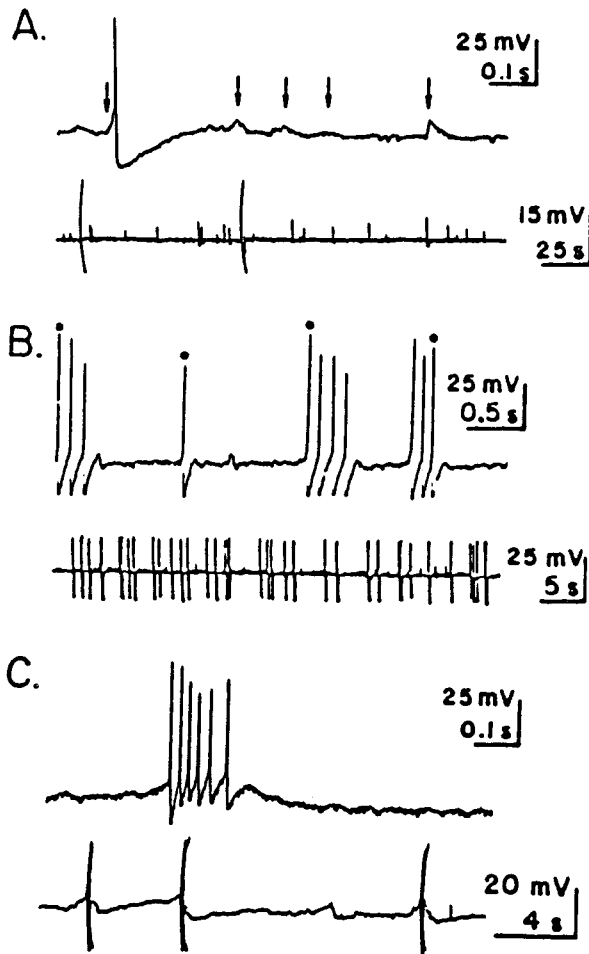
Spontaneous miniature EPSPs and action potentials recorded from canine intracardiac ganglion cells. A. Top. Digital oscilloscope recording of a R-cell with spontaneous EPSPs (arrows) which occasionally initiate an action potential. Below. Slow oscillograph recording of the same cell showing the variations in EPSP amplitude. The larger spikes are the action potentials which are attenuated due to slow frequency response of chart recorder. B. Top. Digital oscilloscope recording of a spontaneous bursting R-cell. Action potentials with solid dots above have been induced by intrasomal depolarizing current injections. No systematic differences in spontaneous and intrasomal stimulated action potentials were observed. Below. Slow oscillograph recording of same cell showing burst activity. C. Spontaneous activity induced by spontaneous slow depolarizations. Top: Digital oscilloscope recording in an S-cell. Bottom. Slow oscillograph recording of same cell.

range 13 to 66/min). The mean amplitude and duration of the miniature EPSP-like depolarization was 4.4 ± 0.5 mV (n = 36) and 36.5 ± 2.3 ms (n = 36).

Spontaneous miniature EPSPs-like depolarizations usually induced action potentials. The firing pattern of these cells was irregular and sometimes in bursts. Some cells fired continuously (Fig. 6-1A), while other cells fired only occasionally. In Fig. 6-1B single action potentials or sporadic bursts of action potentials were observed in addition to subthreshold miniature EPSP-like depolarizations. Action potential responses to intracellularly injected depolarizing currents are also shown. The frequency of the bursts was usually low although the interspike intervals within a burst might have an equivalent frequency approaching 50 impulses per second.

b. Spontaneous action potentials evoked by a slow depolarization. Occasionally, cells (n = 6) displayed burst activity superimposed upon triangular-shaped, irregularly occurring slow depolarizations (Fig. 6-1C). The amplitude and duration of slow depolarizations were 8.2 ± 0.6 mV and 0.3 to approximately 2.0 sec., respectively. This significantly distinguished them from miniature EPSPs-like depolarization. The number of spikes in each slow depolarization were usually varied between 4 and 8. Some cells with this type of spontaneous activity became quiescent after 20 to 30 minutes of activity.

c. Rhythmically firing action potentials. A small group of cells (n = 3) showed continuously rhythmic depolarizations upon which one or two action potentials were superimposed (Fig. 6-2A, B). This activity could persists for more than 40 minutes. Yet, these cells were also excitable with intercellular applied depolarizing currents,

FIGURE 6-2

DIFFERENT TYPES OF SPONTANEOUS ACTIVITY (2)
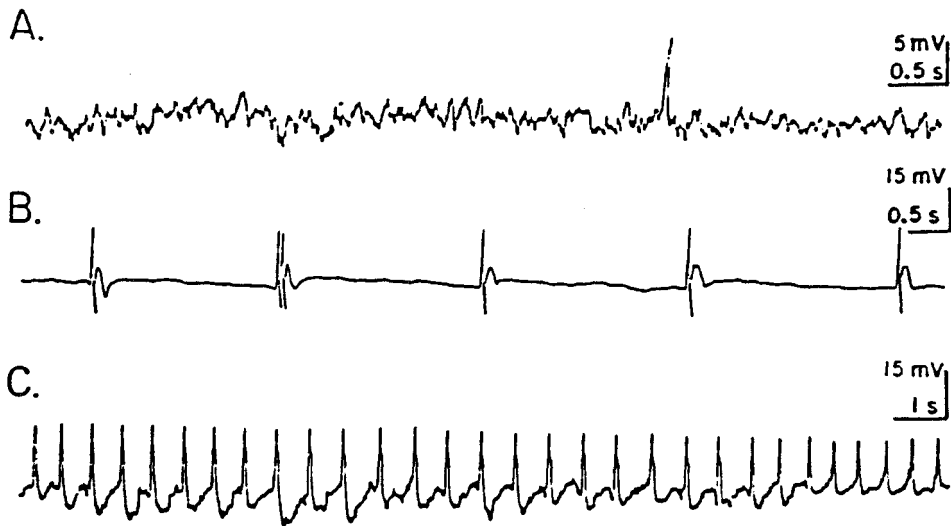
A. Continuous membrane potential fluctuations which occur at a frequency > 6/s. Although most of these fluctuations are a few mV, on rare occasions larger fluctuations of 5-10 mV were observed as depicted in this recording. B and C. Rhythmic spontaneous activity consisting of action potentials which seem to be associated with muscle contraction-induced movements (B and C are S- and R-cells, respectively).

producing normally appearing direct action potentials. Through the microscope, visible contractions of the cardiac muscle fibers in this isolated tissue were observed, which had a similar frequencies (2-3/s) to the recorded electrical activity. In fact, the movements from the contractions made it difficult to record these cells for long durations. However, it is not known if this type of spontaneous activity is directly related to the mechanical activity of myocytes or not.

d. Small membrane potential fluctuations. Occasionally, some cells (26/302 cells) showed continuously, small, irregular potential fluctuations (Fig. 6-2C). The appearance of this activity differed from the above monophasic miniature EPSP-like depolarizations for they were often biphasic or triphasic (amplitudes of 1 to 3 mV) and had a higher frequency of occurrence (> 3/s). This spontaneous fluctuation could also be distinguished from miniature EPSPs-like depolarization by hyperpolarizing the membrane which usually decreased the amplitude of these small membrane potential fluctuations.

Because of the rare occurrence of cells with slow depolarization evoked action potentials and rhythmic action potentials, no systematic investigations of their mechanisms were conducted.

Experiments were performed to determine if the spontaneous miniature EPSPs-like depolarization were synaptic in origin and required release of a neurotransmitter. A low Ca^{2+}/high Mg^{2+} solution was superfused (Fig. 6-3A) following the recording of control spontaneous activity. This solution blocked the spontaneous miniature EPSP-like activity and also caused a small resting membrane depolarization (4 mV). Upon returning to the Krebs solution, the spontaneous activity returned. Similar results were made in 12 cells.

FIGURE 6-3

EFFECTS OF NICOTINIC BLOCKING SOLUTION
ON THE SPONTANEOUS ACTIVITY
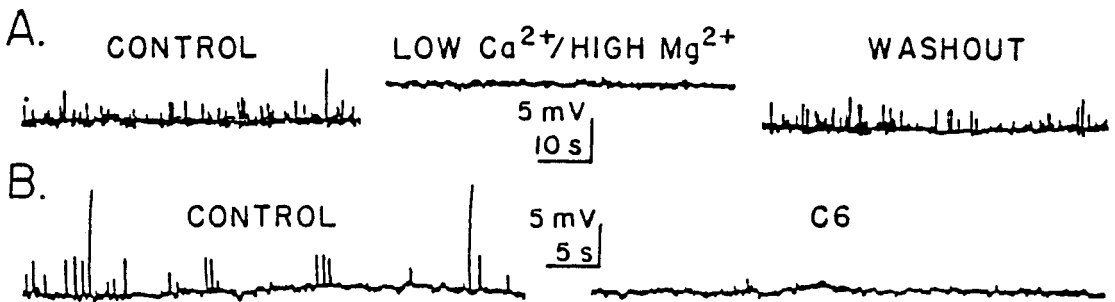
A. Slow oscillograph tracing of spontaneous miniature EPSP-like activity before, during and following washout of a low Ca^{2+}/high Mg^{2+} synaptic blocking solution. In addition to a small resting membrane depolarization, most of the spontaneous miniature EPSP-like activity was blocked in the presence of the synaptic blocking solution. B. Slow oscillograph recording of spontaneous miniature EPSP-like activity before and during the application of the nicotinic blocking agent hexamethonium (C_6) (10^{-4} M).

To test if these miniature EPSPs required presynaptic action potentials and to determine if the spontaneous postsynaptic action potentials had a similar sensitivity to tetrodotoxin (TTX) as intrasomal action potential, the sodium channel blocker, TTX (3.3×10^{-6} M) was administered while recording from 5 cells with spontaneous EPSPs. Although both the intrasomal action potentials and spontaneous EPSP evoked action potentials were blocked, the spontaneous EPSP activity persisted. Even TTX doses as high as 3.3×10^{-3} M did not curtail the spontaneous miniature EPSPs. Thus, the spontaneous EPSPs did not require presynaptic action potentials to occur. Both spontaneous and intrasomal action potentials were dependent on voltage sensitive sodium channel.

The role of nicotinic receptors in mediating spontaneous activity was tested by the addition of hexamethonium (C_6 10^{-4} M) (Fig. 6-3B). This obliterated the spontaneous EPSPs-like depolarizations and spontaneous action potentials, suggesting the importance of nicotinic receptors and the release of acetylcholine in mediating the spontaneous activity. Similar observations were made on 11 preparations. However, the cells which had spontaneous, small membrane potential fluctuations were not blocked by either low Ca^{2+}/high Mg^{2+} or hexamethonium. Similar phenomena were observed in cells in other types of ganglia [36,39], but the mechanism remains unknown.

In 5 cells the characteristics of the spontaneous and intrasomal evoked action potentials were compared (e.g. Fig.6-1B). The threshold voltage for the spontaneous and evoked action potentials were not significantly different (-33.7 $\pm$ 3.3 mV and -32.7 $\pm$ 7.0 mV, respectively. P > 0.05). The action potential overshoots for spontaneous and

evoked action potentials were also not significantly different (19.9 $\pm$ 3.3 mV and 24.8 $\pm$ 1.6 mV; P > 0.05). Likewise, the duration of the action potentials for spontaneous and evoked action potentials were almost the same (3.5 $\pm$ 0.9 ms and 3.2 $\pm$ 0.9 ms). In another 5 cells, the orthodromic action potentials produced by stimulation of a intracardiac nerve with a suction electrode were compared to the spontaneous action potentials. The amplitude, duration and threshold of the orthodromic action potentials were 78 $\pm$ 2.3 mV, 3.0 $\pm$ 0.3 ms and -36.8 $\pm$ 0.8 mV, respectively. These values were not statistically significantly different (P > 0.05) from the amplitude, duration and threshold of the spontaneous action potentials which were 80.3 $\pm$ 4.5 mV, 3.1 $\pm$ 0.4 ms and -31.4 $\pm$ 0.7 mV, respectively. Thus, the spontaneous, orthodromic and intrasomal evoked action potentials were comparable.

Spontaneous miniature EPSP-like depolarizations were first reported by Nishi and Koketsu [70] in frog sympathetic ganglion cells. These spontaneous depolarizing potentials resembled the fast EPSP and were decreased in amplitude by nicotinic receptor antagonists [10,70]. These potentials are thought to be similar to the miniature end-plate potentials caused by quantal release of ACh at the neuromuscular junction [31]. Similar spontaneous activity has now been reported in other sympathetic [9-11,15,85], parasympathetic [36,88] and myenteric ganglia [72].

About 50% of canine intracardiac ganglion cells with intact synaptic connections displayed four types of spontaneous activities in the present study. This differs from other intracellular studies of mammalian intracardiac ganglia. In neonatal rat cardiac ganglia cells *in situ*, Seabrook et al. [88] recorded no spontaneous action potentials although

they did report spontaneous EPSPs. The frequency (<2/min) and amplitude (1.3 mV) of miniature EPSPs in the neonatal rat were much smaller than those observed in the adult dog. Allen and Burnstock [4] did not report spontaneous activity in cultured guinea pig intracardiac neurons which have lost their processes and synaptic connections due to enzymatic and mechanical dissociation. These observations suggest that perhaps mature and intact synaptic connections are required to observe this spontaneous activity or that the presence of this activity varies in different mammalian species.

In the canine intracardiac ganglia, the spontaneous activity in the form of miniature EPSPs either with or without action potentials was recorded in all physiological types of neurons, i.e. R-, S- and N-cells [99]. As the spontaneous activity could be usually recorded for many hours, and as tetrodotoxin which blocks sodium-mediated action potentials, failed to block the spontaneous miniature EPSPs, it is unlikely that these EPSPs are due to injury-induced action potentials of cut presynaptic fibers [86]. Because most of this spontaneous activity was consistently blocked by nicotinic antagonist and low Ca^{2+}/high Mg^{2+} solution, this activity was not due to non-synaptic pacemaker activity of spontaneously firing neurons. Rather, this is most likely due to spontaneous vesicular release at the presynaptic nerve terminals [31]. The threshold voltages, amplitudes and durations of the spontaneous action potentials were similar to those induced by intrasomal depolarizing current injections or orthodromic stimulation. Thus, a similar site was probably involved in the initiation of spontaneous, orthodromically-activated and intrasomal-induced action potentials. Apparently, the spontaneous miniature EPSP-like activity and associated action potentials are synaptically-mediated.

This activity involves acetylcholine and nicotinic receptors.

Recently, Gagliardi et al.[33] reported spontaneous neuronal activity from presumably the same group of canine intracardiac neurons with intact nerve connection, using *in vivo* extracellular recording techniques. They provided evidence that ganglion neurons could be activated independently of central nervous system, which was consistent with the present result. Forty-seven percent of the neurons in their study displayed spontaneous activity correlated with cardiovascular or respiratory cycles. Some neurons (14%) respond with action potentials to mechanical stimulation on different areas of the heart and lung, suggesting an afferent input. The majority of spontaneous neurons (208 or 53%) exhibited intermittent, short bursts or dispersed activity that was not correlated with cardiovascular or respiratory cycles. This type of spontaneous activity could persist even after acute decentralization. Notwithstanding some notable facts, e.g. the mechanical movement of the pumping heart may distort the ganglion cells and cause similar "spontaneous" activity and, particularly, this spontaneous activity was not readily blocked by hexamethonium, these observations appear to be comparable to the present miniature EPSP mediated action potentials. However, the majority of the spontaneous activity (more than 90%) in present report was synaptic and nicotinic in origin while most of the spontaneous activity recorded extracellularly [33] was not nicotinic receptor mediated. Some other discrepancies were also noted in the *in vivo* extracellular recording study, e.g. single pulse stimulation of preganglionic nerves failed to evoke responses of the postganglionic neurons although it consistently evoked f-EPSP and action potential in the present study. Furthermore, the extracellularly recorded spontaneous

activity occurred from ganglia primarily located in the middle portion of the PVFP [19] while, in the present study, spontaneous activity was found in ganglia taken from different portion of the fat pad. Although the cause of the discrepancy is currently not clear, it is likely that different nature of the preparations and recording techniques make the direct comparisons difficult.

Because of the low frequency of appearance, the mechanisms involved in the other three types of spontaneous activities were not fully investigated. Spontaneous membrane potential fluctuations were not blocked by either low Ca^{2+}/high Mg^{2+} or hexamethonium solutions, which is, therefore, not likely to be synaptically mediated. Spontaneous membrane potential fluctuations have been reported in Necturus cardiac ganglia [39] and in other autonomic ganglia, e.g. the pelvic ganglia [21,36].

The mechanisms of the rhythmic action potential and the slow potential evoked bursts were not elucidated in this study. Some of the possible explanations are: 1). Some non-synaptic action potentials have been reported in the myenteric plexus [94,96], vesical pelvic ganglia [36] and central nervous system [12,76]. Those neurons fire action potentials or bursts of action potentials spontaneously, which were not blocked with ganglionic blockade. Either the endogenous activation of the somata [36] or electrical coupling between neurons [8] has been reported as the responsible mechanism. Hence, these infrequent spontaneous activities in present study might be non-synaptic in origin and initiated by some intermittent firing pacemaker neurons. 2). Alternatively, it has been noted that mechanical distortion of the tissue is a potential source for some spontaneous activity. North and Williams [74] noted "spontaneous" extracellular electrical activity from

enteric neurons when mechanical distortion was induced by the suction recording electrode. Using extracellular recordings from the cat intracardiac ganglia *in vitro*, Nozdrachev and Pogorelov [75] also pointed out the importance of mechanical deformation of ganglion cells by the recording electrode for the recording of spontaneous discharges. In the present study, no electrodes movement existed in all experiments. However, a few preparations (n = 3) with rhythmic neuronal activity of unknown origin had visible movements which were due to rhythmic contractions of the thin layer of muscle adjoining the fat and intracardiac ganglia. In these few cells, rhythmic action potentials, sometimes hyperpolarization or biphasic membrane potential changes occurred, which seemed to correlate roughly with the contraction of the muscle fibers. However, the actual mechanism of possible coupling of contractions to these membrane potentials changes is not known. 3). Since the time course of the slow potential evoked bursts was in the range of a few seconds (Fig. 6-1 C), the presence of spontaneous muscarinic or some other noncholinergic excitation is possible. It has been reported [90] that a very small amount of ACh only sufficient to cause a miniature synaptic current via nicotinic receptor could activate muscarinic receptor, hence to suppress a potassium channel mediating excitatory response. Although direct evidences is still lacking, a transient activation of muscarinic receptor by ACh would lead to a long-lasting muscarinic excitation [73]. 4). Since the infrequency of their occurrence, the influence of injury potentials [86] should be considered as well. It has been reported that cutting postganglionic axons [86] or afferent fibers which connected to ganglion neuron [8] could in turn generate spontaneous spikes or bursts.

Julé et al. [45] noted that there were three types of neurons in the inferior mesenteric ganglion: non-spontaneous firing cells, irregular spontaneous discharging cells, and regular spontaneous discharging cells. The non-spontaneous firing and the irregular spontaneous discharging cells received preganglionic fibers as well as excitatory inputs from peripheral nerves and sent their axons to visceral structures. The regular spontaneous discharging cells did not send their axons out of the ganglion and received synaptic inputs mainly of preganglionic origins. Because of the lack of information about the synaptic input to the canine cardiac ganglion cells and the specific termination of their axons, the functional importance of cells with and without spontaneous activity is uncertain.

What is the physiological importance of the spontaneous activity in the PVFP ganglion plexus to cardiac function? Since the amount and rate of transmitter release from the postganglionic terminals is related to the amplitude, duration and the discharge frequency of the action potentials, respectively, the spontaneous activity, particularly spontaneous action potentials, may be responsible for supplying some of the "vagal tone", e.g. ongoing suppression of heart rate, which is blocked by muscarinic antagonist atropine [82].

2.   Fast Excitatory Postsynaptic Potentials (f-EPSP)

a. Responses to Single Stimuli on Interganglionic Nerve

Single or multiple orthodromic responses: In a total of 216 neurons tested from 71 experiments, a single pulse applied to the interganglionic nerve could almost always initiate orthodromic responses (Fig. 6-4) with various latencies between 2 and 7.2 ms . Typically, the response was subthreshold when using smaller stimulus intensity. When threshold stimulations were applied, the initial depolarization, f-EPSP, summated spatiotemporally to initiate an action potential (Fig. 6-4 A and B).   The afterhyperpolarization (AHP) was observed to follow these f-EPSP evoked action potentials. The mean amplitude and duration of neurally evoked f-EPSPs were 9.6 $\pm$ 0.5 mV (range 3.6 - 16.9 mV) and 29.2 $\pm$ 1.7 ms (range 12.7 - 46.3 ms) (n = 35), respectively. Although quantal release of ACh has not been proved in this preparation, the mean amplitude of neurally evoked f-EPSPs was higher than spontaneous miniature EPSPs (4.4 $\pm$ 0.5 mV).   A comparison of direct evoked and orthodromically evoked action potentials is shown in Table 5-1.   There was no significant difference in mean amplitude and duration of these two different action potentials. The synaptic origin of f-EPSP was demonstrated using low Ca^{2+}/high Mg^{2+} solution which abolished orthodromic nerve responses in all tested cells (n = 34).

Although most of the tested neurons in the present study showed single f-EPSP upon supramaximal stimulus strength, approximately 15% to 20% of the nerve cells received inputs from multiple fibers, as a single interganglionic nerve stimulation could evoke multiple f-EPSPs with differing latencies (Fig. 6-4 C, D, E, and F). The exact

FIGURE 6-4

FAST EPSP AND ORTHODROMIC ACTION POTENTIAL
IN CANINE INTRACARDIAC NEURONS
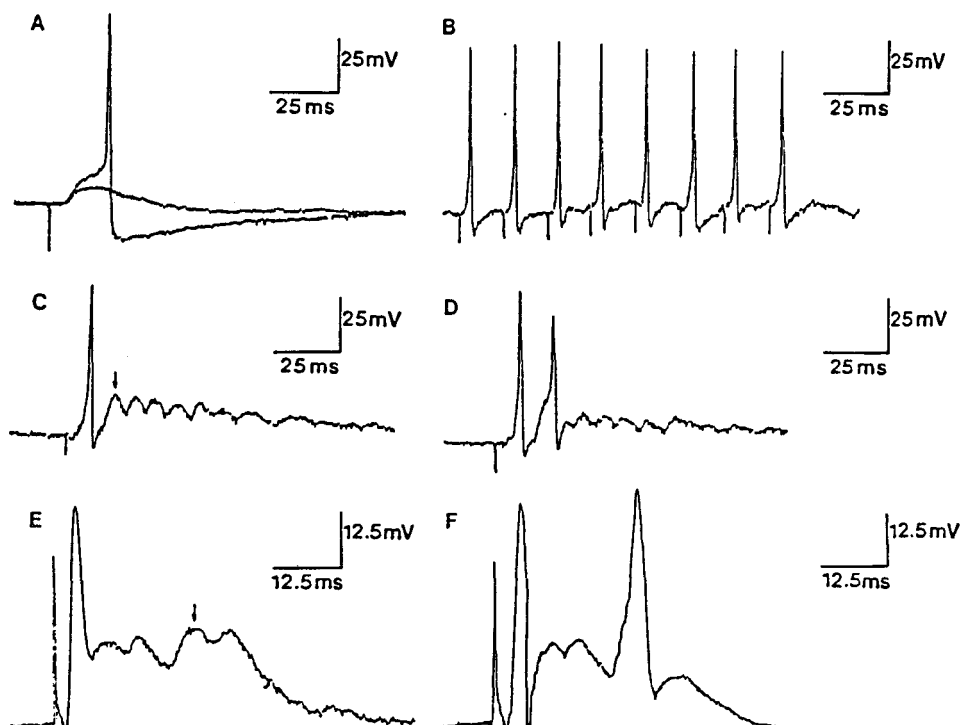
Orthodromic responses evoked by stimulating the interganglionic nerve fiber with either single or repetitive pulse. A. Two superimposed traces showing a typical f-EPSP response which initiated a spike when it reached the threshold. B. A representative orthodromic action potentials recorded from the same neuron as A. using repetitive stimulation. C. and D. Temporal and/or spatial summation of f-EPSPs associated with action potentials recorded from the same cell. After a single stimulation pulse, several f-EPSPs with different latencies occurred with the first one inducing an action potential (C.). When the stimulus strength was increased (D.), the second f-EPSP which is indicated by arrow in C. reached threshold also and evoked spike. E. and F. Another example of the temporal distribution of f-EPSPs recorded from an individual cell. Single stimulation mediated multiple f-EPSPs with differing latencies. More spikes were evoked by increasing stimulus strength (F.). Note the stimulation marker(s) as the first downward or upward deflection on each recordings.

ratio of nerve fibers to cells was not specifically determined but, as shown in Fig. 6-4 C, D, E and F, increased stimulus intensity recruited more interganglionic fibers and resulted in additional EPSPs and action potentials. This temporal distribution of f-EPSPs suggested that these neurons were innervated by multiple presynaptic fibers possessing a wide variety of conduction velocities and/or a wide spatial distribution of synaptic boutons [22,49]. The apparent percentage of multiple innervated neurons (15% - 20%) obtained by stimulating one of the connected interganglionic nerves may be an underestimation for these cells are likely to receive inputs from other interganglionic nerves which also supply each ganglion.

Antidromic response: In addition to orthodromic responses, stimulation of interganglionic nerve produced antidromic responses in about 30% of the tested neurons. In these cells, a single pulse delivered to one of the connecting interganglionic nerves evoked both orthodromic and antidromic responses (Fig. 6-5 B and C). Occasionally, only antidromic response was produced (Fig. 6-5 A).

Orthodromic responses of N-cells to interganglionic stimulation: Orthodromic responses, both f-EPSP and action potential, could be evoked from all three types of neurons (R-, S- and N-cells). However, a higher stimulus strength was usually required to evoke f-EPSP and orthodromic action potential from N-cells (Fig. 6-6). This is similar to other observations of a slow depolarization generated by single interganglionic nerve stimulation on unexcitable neurons [11,95].

Anatomical considerations: In a few experiments (n = 6), intracellular recordings were made sequentially from two serially arranged ganglia while the suction

FIGURE 6-5

ANTIDROMIC ACTION POTENTIAL
IN CANINE INTRACARDIAC NEURONS
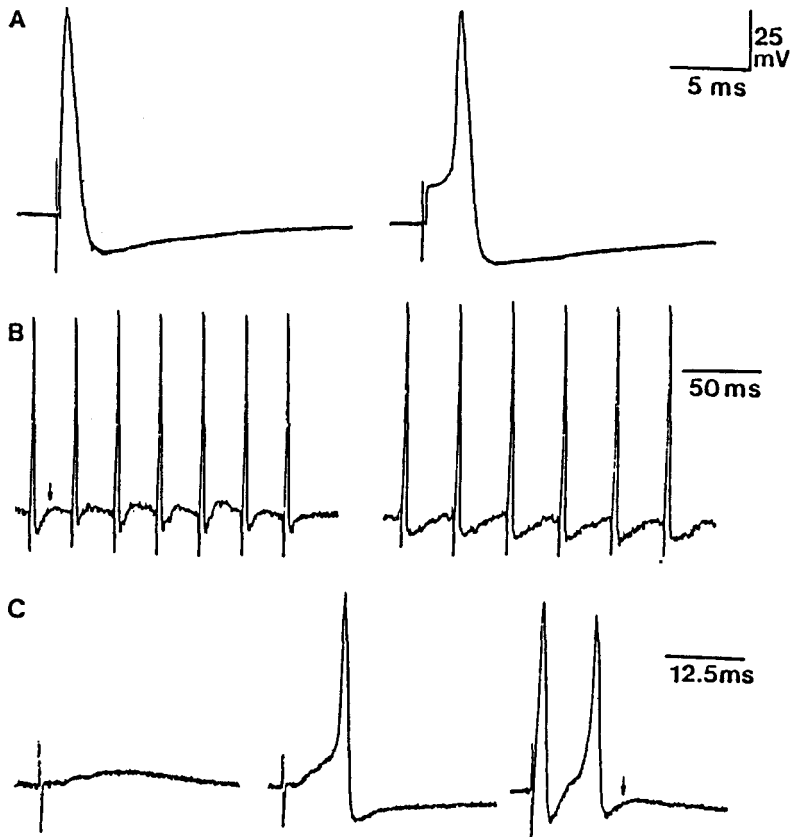
Antidromic responses evoked by interganglionic nerve stimulations. A. A typical antidromic action potential (left) which could be distinguished as initial segment and somadendritic segment (right) usually when the stimulating frequency was increased above 30 Hz. Two traces recorded from a single neuron. B. Nicotinic antagonist, hexamethonium (10^{-4} M), had no effects on antidromic response. Repetitive stimulation evoked both antidromic action potentials and orthodromic f-EPSPs (arrow) in the same neuron (left). Fifteen minutes after hexamethonium (10^{-4} M) superfusion (right), the f-EPSPs were blocked while the antidromic action potentials were not affected. C. A typical temporal pattern of antidromic and orthodromic responses recorded from a single neuron. All responses could be obtained by adjusting the stimulating strength. When the stimulating strength was increased from low to high, f-EPSP (left) was first elicited, and then was the orthodromic action potential (middle). Antidromic action potential (right, first spike) needed a higher stimulating strength and occurred prior to orthodromic responses (right, second spike), suggesting a shorter latency.

FIGURE 6-6

FAST EPSP AND ORTHODROMIC ACTION POTENTIAL OF N-CELLS
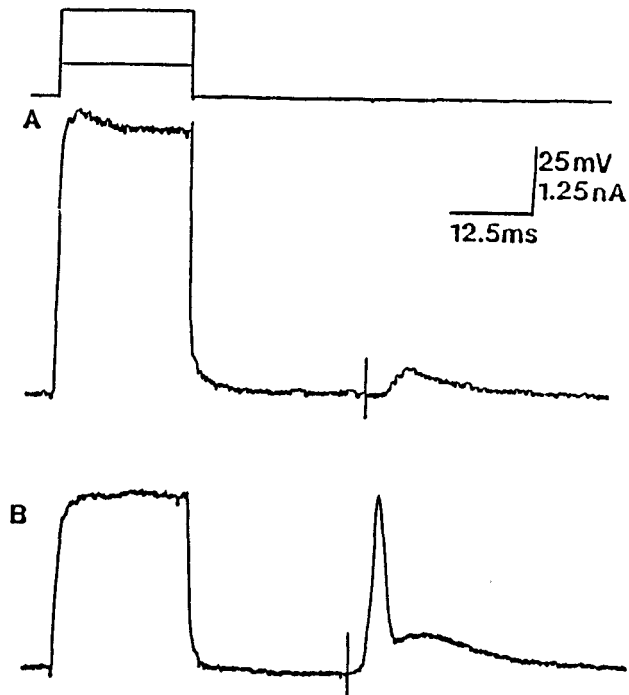
Orthodromic f-EPSP and/or action potential could be evoked from N-cells using a high stimulation strength. Top trace shows intracellular current injection pulses. Trace A and B were recorded from two different N-cells which exhibited no direct action potentials. Fast EPSP (A) and action potential (B) were obtained orthodromically.

electrode was first, placed in the interganglionic nerve connected to one of the ganglia (Fig. 6-7 A and B). The stimulation electrode was then moved to the nerve between the ganglia (Fig. 6-7 C and D). Stimulation at either site could evoked orthodromic responses in cells from both left and right ganglia. In the first case (Fig. 6-7 A and B), interganglionic fibers run to synapses on cells in the left ganglion and through the ganglion to synapse on cells in the right ganglion. An alternative hypothesis is that some neurons in the directly connected (left) ganglion act as *inter*ganglionic neurons [97,98] which may receive inputs from the stimulated interganglionic nerve and send their axons to contact neurons in the indirectly connected (right) ganglion. Regarding the second condition (Fig. 6-7 C and D), a given interganglionic nerve which located between two ganglia may include nerve fibers innervating both of the connected ganglia.

Usually, during stimulation of one of the connected interganglionic nerves, almost all tested cells responded orthodromically. A small portion of cells responded antidromically as well as orthodromically. This implies an anatomical arrangement wherein postganglionic axons depart the ganglion via different interganglionic pathways while each ganglion cell is receiving convergent inputs from different connecting nerves. Alternatively, another possible anatomical arrangement is that, as described in Chapter IV, there are some neurons with short axons or undistinguishable axons which never send their processes out of the ganglion but they may receive inputs from connecting interganglionic nerve fibers.

b. Responses to Repetitive Stimuli

Repetitive stimulation of the preganglionic fiber at frequencies lower than 40 Hz

FIGURE 6-7

ORTHODROMIC RESPONSE EVOKED BY STIMULATING
EITHER DIRECT OR INDIRECT CONNECTED NERVES
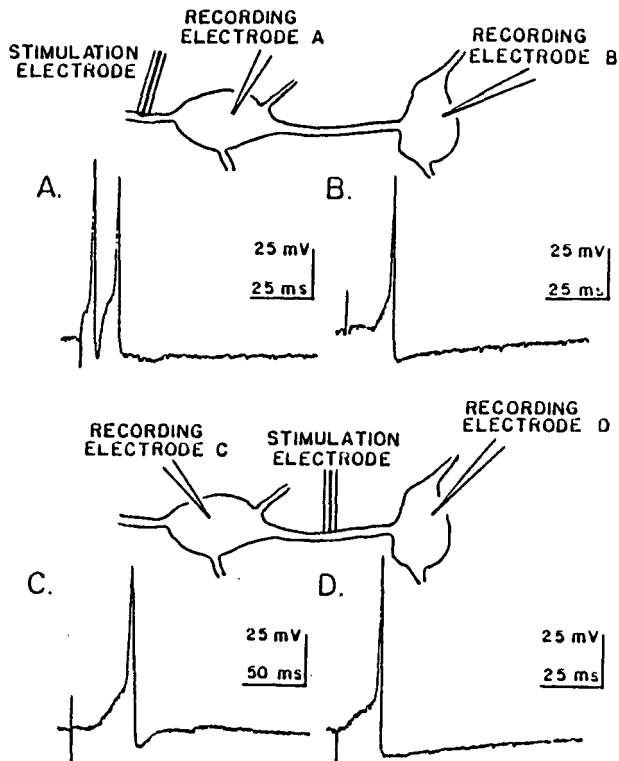
Intracellular recording traces and schematic drawings of the ganglia, interganglionic nerves and electrodes obtained from one experiment. The top schematic drawing shows the stimulation electrode placed in the interganglionic nerve directly connected to one of the two ganglia. Orthodromic action potentials, traces A and B, were obtained from both recording electrode A which recorded from the direct connected ganglion (left one) and electrode B which recorded from the indirect connected ganglion (right one), respectively. The recording electrode A also recorded an antidromic spike from the same neuron. The lower schematic drawing shows the stimulation electrode placed in the interganglionic nerve between those two ganglia. Orthodromic action potential could be recorded from both ganglia (traces C. and D.) via recording electrode C and D, respectively. Note trace A,B,C, and D were recorded from 4 different neurons.

can usually evoke a train of f-EPSPs which may induce action potentials. Stimulation of higher frequency resulted in an increased delay in triggering the action potentials, due to a decline in size of the f-EPSP. The f-EPSP eventually failed to reach threshold for initiating of an action potential. This may be attributed to a progressive reduction in the quantal release of neurotransmitter and, to a minor extent, the desensitization of postsynaptic receptors [22,72,83].

c. Effects of Cholinergic and Adrenergic Receptor Antagonists

In order to ascertain the neurotransmitter nature of the nerve stimulation evoked f-EPSP, cholinergic and adrenergic receptor antagonists were applied. Similar to central nervous system or autonomic ganglion studies [34,56], the nerve evoked f-EPSP could always be completely antagonized by the nicotinic receptor antagonist hexamethonium (10^{-5} to 10^{-4} M) (n = 41) or chlorisondamine (10^{-6} to 10^{-5} M) (n = 13). The effect sometimes was reversible after one to two hours of rinsing with Krebs solution alone. Representative experiments using hexamethonium (10^{-4} M) are shown in Fig. 6-8. Hexamethonium was chosen to antagonize the nicotinic responses in all appropriate situations in these experiments. The muscarinic receptor blocker atropine (10^{-6} or 10^{-7} M, n = 27), α-adrenergic receptor antagonist phentolamine (10^{-6} M, n = 7) and β-adrenergic receptor antagonist l-propranolol (n = 6 , 10^{-6} M) were also tested but had no effect on the f-EPSP. Therefore, as expected, nerve stimulation evoked f-EPSPs in canine intracardiac ganglion cells were mediated by ACh acting on nicotinic cholinergic receptors.

FIGURE 6-8

EFFECTS OF HEXAMETHONIUM (10^{-4} M) ON f-EPSP
AND ORTHODROMIC ACTION POTENTIAL
IN CANINE INTRACARDIAC NEURONS
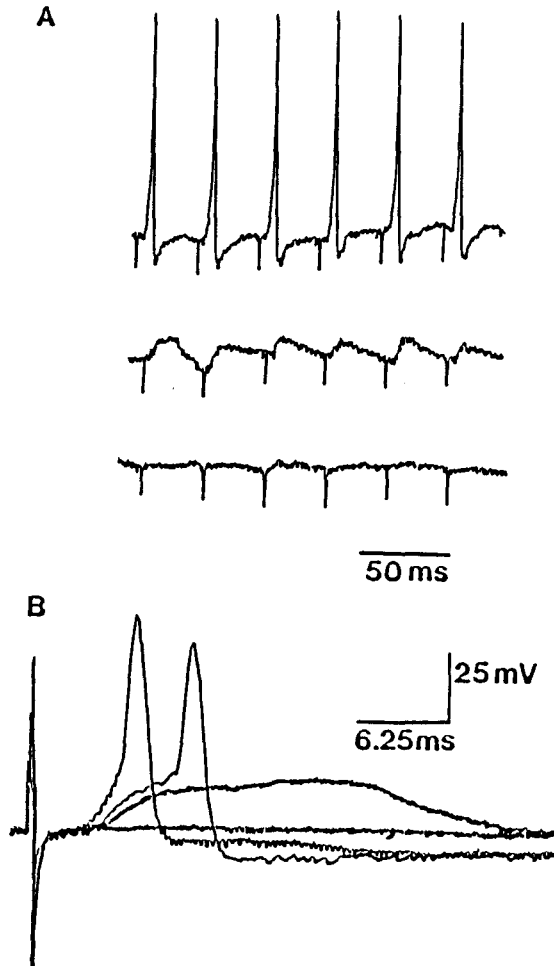
A. A train of orthodromic action potential was initiated by repetitive stimulation pulse (top trace), which was diminished (at the middle trace) 5 minutes after hexamethonium (10^{-4} M) superfusion, due to the decreased amplitude of the f-EPSPs. Ten minutes after, f-EPSPs were completely blocked by hexamethonium. B. The effects of hexamethonium recorded at higher speed from another cell. Superimposed traces, which show the control (first action potential), 3 minutes (second action potential), 5 minutes (no action potential, f-EPSP only) and 10 minutes (no f-EPSP) after hexamethonium superfusion.

d. Ionic Mechanism for the f-EPSP

The reversal potential for the f-EPSP was determined by passing continuous depolarizing or hyperpolarizing currents via the recording electrode to shift the membrane potential to a suitable level. Hyperpolarizing the membrane increased the amplitude of f-EPSP, while depolarizing the membrane decreased the amplitude as shown in Fig. 6-9. The amplitude of the f-EPSP was linearly related to the membrane potential. The extrapolated reversal potential was -7.1 $\pm$ 1.8 mV (n = 5). This reversal potential was between the equilibrium potential for Na^+ and K^+, suggesting the contribution of both these ions to the fast synaptic response [56].

e. Nicotinic Cholinergic Responses of Applied Ach on Intracardiac Neurons

In the presence of muscarinic receptor antagonist atropine (5 x 10^{-6} M), a depolarizing response could be induced by focal ejected ACh in all tested cells (n = 42). The amplitude and duration of the depolarization was related to the duration of ejection pulses. The depolarization from applied Ach could always be diminished by hexamethonium 10^{-6} M (n = 33); neither phentolamine (10^{-6} M, n = 5) nor

1-propranolol (10^{-6} M, n = 7) had any effects on the ACh induced depolarization. A low Ca^{2+} / high Mg^{2+} solution had no effect on the ACh depolarization (n = 5), indicating a direct postsynaptic effect of ACh on the nicotinic receptor of these ganglion cells.

The change in membrane conductance or input resistance was estimated by passing hyperpolarizing pulses through the recording electrode during response to applied ACh (Fig. 6-10). During the ACh induced depolarization, a decrease in the

FIGURE 6-9

EFFECTS OF MEMBRANE POTENTIAL ON THE AMPLITUDE OF f-EPSP

A

B
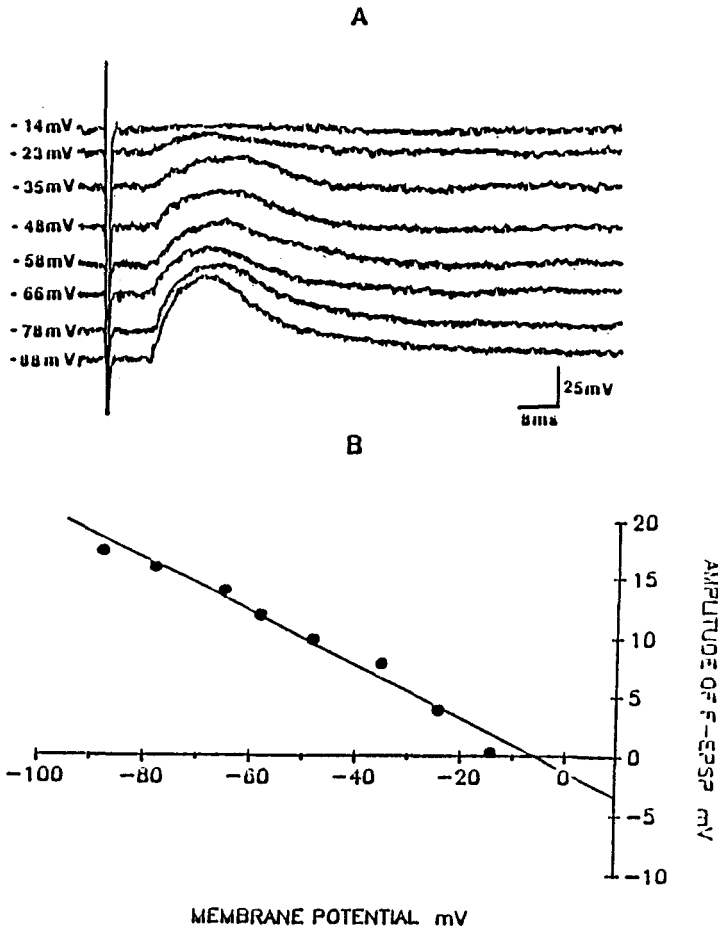
A. The f-EPSP was recorded from a canine intracardiac neuron (resting potential -48 mV) while its membrane potential was manipulated by a constant, intracellular current injection. The amplitude of the f-EPSP was increased during hyperpolarization and decreased during depolarization. B. Graph of the responses shown in A. A linear response of the amplitude of the f-EPSP was obtained as the function of membrane potential. The extrapolated reversal potential in this case was -7.2 mV.

FIGURE 6-10

EFFECTS OF MEMBRANE POTENTIAL ON THE ACh
EVOKED NICOTINIC DEPOLARIZATION
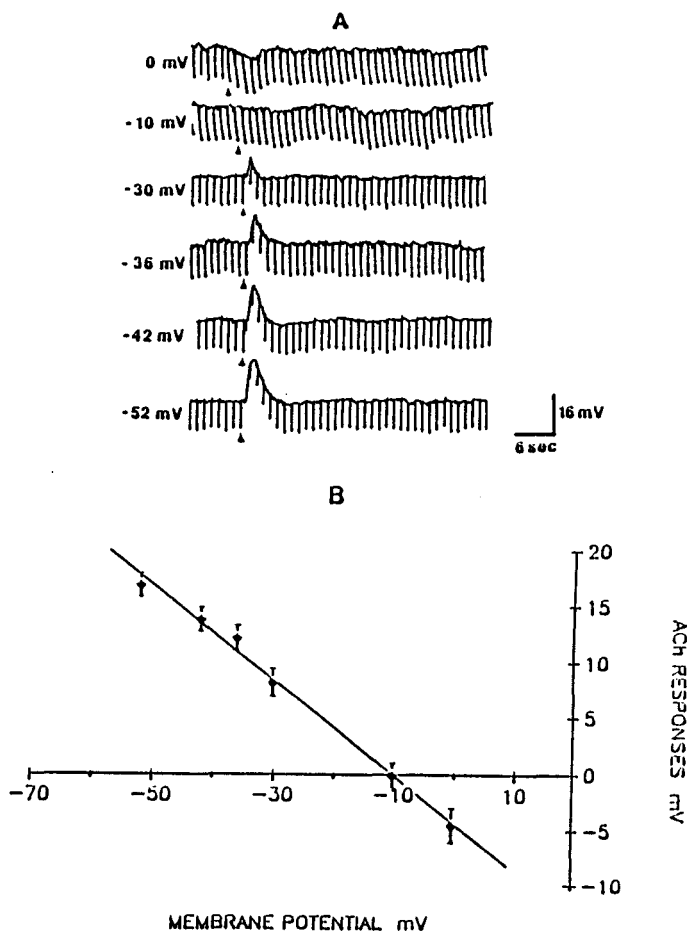
A. Acetylcholine was applied to an canine intracardiac neuron (resting potential -42 mV) by microejection techniques in the presence of atropine (10^{-6} M). Both membrane potential depolarization and input resistance decreased during the ACh action. While the membrane potential was manipulated via a constant, intracellular current injection, the amplitude of the nicotinic depolarization was increased during the hyperpolarization and decreased or even reversed during the depolarization. Arrow heads indicate the onset of microejection (50 ms pulse). Downward deflections were electrotonic potentials caused by intracellular hyperpolarization pulses injection (0.15 nA, 50 ms), which were used as an estimation of input resistance. B. The amplitude of the nicotinic depolarization in 4 neurons (including the one showing in A) was plotted as the function of membrane potential. The linear relationship between the amplitude and membrane potential was observed with a reversal potential at -10.0 $\pm$ 1.9 mV.

hyperpolarizing pulse amplitude was observed, indicating an increased membrane conductance. A 34.4 ± 9.8 % (range 13 - 55%) reduction in membrane resistance was observed in 33 cells tested (Fig. 6-10).

The reversal potential for the ACh response was examined (Fig. 6-10) and compared to that for the neurally evoked f-EPSP (Fig. 6-9). In 4 experiments the mean extrapolated reversal potential for the ACh responses was 10.0 ± 1.9 mV which is close to the reversal potential for the f-EPSP responses. Thus, both the neurotransmitter candidate and the ionic mechanism of the f-EPSP in the canine intracardiac ganglion are very similar to those of the f-EPSP in other peripheral nerve systems [22,34,56,83,88].

The release of ACh by an action potential in preganglionic terminals generates a f-EPSP at the subsynaptic membrane of a postganglionic neuron. The neurally evoked f-EPSP in canine intracardiac ganglia are similar in many respects to that of other ganglia and the central nervous system [22,36,39,56]. In this study single or repetitive pulses evoked f-EPSP(s) could be observed in almost all neurons tested (Fig. 6-4). Temporal dispersion of f-EPSPs in a subgroup of neurons was readily observed. Therefore, nicotinic synaptic transmission in canine intracardiac ganglia involves a convergent-type of synapses that require coincidental activation of several preganglionic fibers for the generation of an action potential in the postganglionic neuron. Evidently, nicotinic transmission is the most effective synaptic pathway in this preparation. Temporal dispersion of the f-EPSP may also be due to the location of synapses. As in other ganglia [36,56], the f-EPSP could be consistently blocked by the nicotinic receptor antagonist, hexamethonium (Figs. 6-5, 6-8), but not by atropine and adrenergic receptor antagonists. In the presence of

muscarinic blockade, applied ACh evoked a nicotinic depolarizing response with decreased input resistance which makes it different from the ACh evoked muscarinic depolarization. The extrapolated reversal potentials (around -10 mV) of both the f-EPSP and the ACh evoked depolarization were close to that observed in sympathetic ganglia [56] and in parasympathetic ganglia, including amphibian intracardiac ganglia [22,36,39]. Previously reported [56], the reversal potential of f-EPSP becomes more negative when the extracellular sodium or potassium concentration is reduced, while it shifts to a less negative value with increasing potassium concentration. Thus, the f-EPSP appears to be generated by concomitant increase in the membrane conductance for sodium and potassium.

3.   Slow Synaptic Potentials

In addition to f-EPSPs, slow synaptic potentials were also examined in 85 canine intracardiac neurons. Slow synaptic potentials were produced following trains of repetitive, orthodromic stimulation of an interganglionic nerve (train duration < 1.0 s, pulse 0.1 ms, frequency < 40 Hz). Neurons which responded antidromically were not included in these studies. To diminish the influence of f-EPSPs, most experiments were performed in the presence of nicotinic receptor antagonist hexamethonium (10^{-4} M). Previously, this concentration has been demonstrated to block completely both f-EPSP and ACh nicotinic responses. Since sometimes the amplitude of slow potentials was too low to analyze adequately, a cholinesterase inhibitor physostigmine (10^{-7} M) was employed. Similar to previous reports [35], physostigmine at this concentration had no

direct membrane effects, e.g. hyperpolarizing or depolarizing the membrane potential or other non-specific effects [46].

a. Categories of slow potentials

In the presence of hexamethonium, repetitive orthodromic stimulation evoked both the slow excitatory postsynaptic potential (s-EPSP) and the slow inhibitory postsynaptic potential (s-IPSP) in canine intracardiac neurons. These slow potentials can sometimes be clearly observed following a train of fast responses even without the administration of a nicotinic receptor antagonist (Fig. 6-11). This indicates that the synaptically released neurotransmitter could initiate both fast and slow synaptic potentials in the same neurons.

In 35 of 85 neurons (41.2 %), only s-EPSPs were recorded (Figs. 6-12 and 6-14). The amplitude and duration of these s-EPSPs varied from cell to cell with the shortest latency being less than 1 second. The mean amplitude and duration of s-EPSPs were 3.8 $\pm$ 1.2 mV (range 1.8 - 8.6 mV) and 4.2 $\pm$ 1.1 sec (range 2.5 - 5.8 sec.), respectively (n = 35). A burst of action potentials usually occurred during the s-EPSP, suggesting an increased excitability (Fig. 6-12). Physostigmine (10^{-7} M) consistently enhanced s-EPSPs (Fig. 6-13). The membrane conductance, defined as the reciprocal of input resistance estimated by hyperpolarization current pulses, was decreased during the neurally evoked s-EPSPs (Fig. 6-14). In the presence of physostigmine (10^7 M), some cells (n = 5) exhibited multiple or oscillating s-EPSPs following a single orthodromic stimulation train (Fig. 6-13). The typical pattern of these oscillating s-EPSPs was that 2 to 5 slow depolarizations occurred for 6 to 7 seconds after one orthodromic stimulation

FIGURE 6-11

AN REPRESENTATIVE RECORDING OF f-EPSP, s-IPSP
AND s-EPSP IN A CANINE INTRACARDIAC NEURON
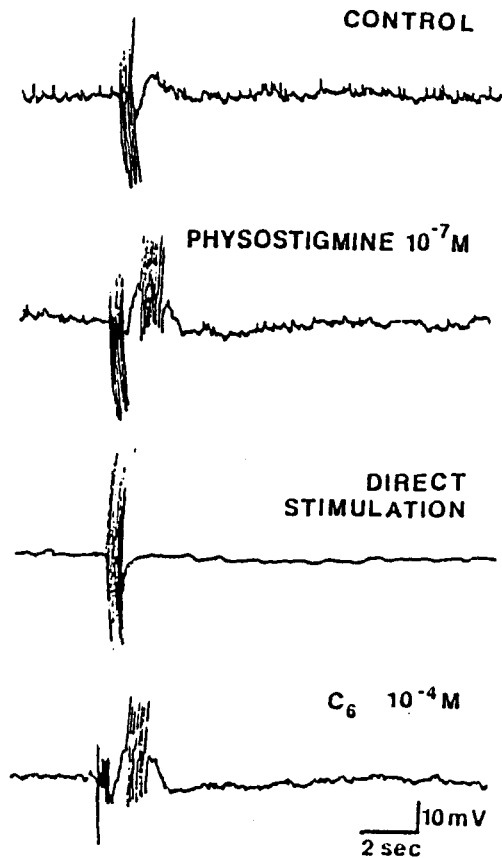
In the control tracing, a train stimulation (30 Hz for 0.9 sec.) evoked orthodromic action potentials (initial spikes) which was followed by a slow hyperpolarization (s-IPSP) and then a depolarization (s-EPSP). The s-EPSP was significantly enhanced by cholinesterase inhibitor, physostigmine (10^{-7} M), and induced action potentials (second tracing). The intracellularly induced action potentials (the initial spikes of the third tracing) were not followed by s-IPSP and s-EPSP, indicating the distinction between slow potentials and spike induced potential changes, such as afterhyperpolarization. Addition of hexamethonium (C_6 10^{-4} M) in the last tracing blocked the orthodromic action potentials, indicated as the diminishment of the initial spikes, but had no effect on both s-IPSP and s-EPSP.

FIGURE 6-12

DIFFERENT SLOW MUSCARINIC POTENTIALS EVOKED
BY REPETITIVE ORTHODROMIC STIMULATION
IN CANINE INTRACARDIAC NEURONS
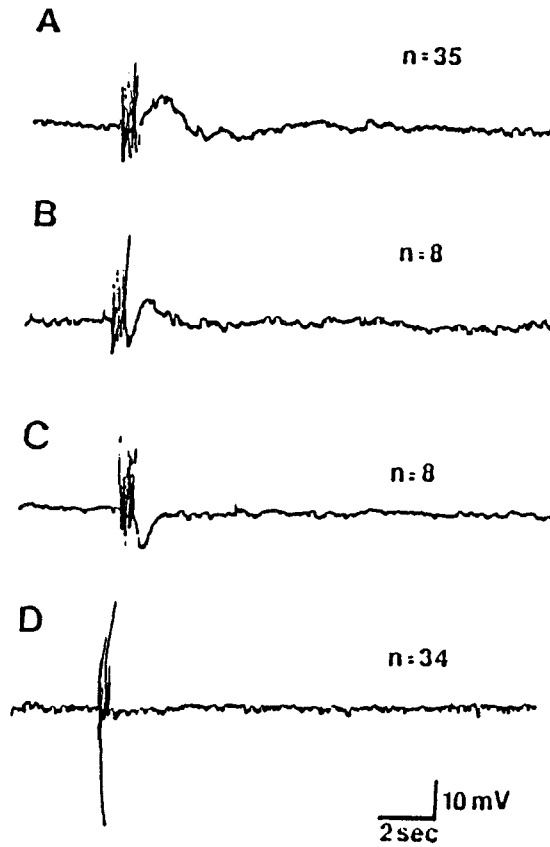
In the presence of hexamethonium (10^{-4} M), repetitive stimulation revealed s-EPSP (A), s-IPSP followed by s-EPSP (B), s-IPSP (C) and no muscarinic slow potentials (D) in different neurons tested. The orthodromic stimulation is indicated as the initial stimulation artifacts.

FIGURE 6-13

OSCILLATING s-EPSP EVOKED BY A SINGLE
ORTHODROMIC TRAIN STIMULATION
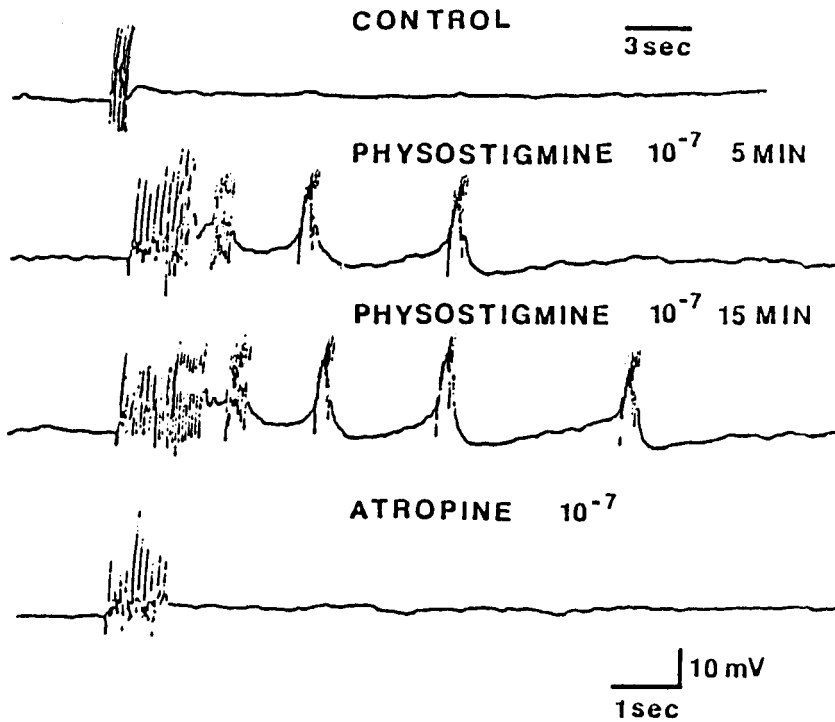
In the presence of hexamethonium, a small s-EPSP was evoked by a train orthodromic stimulation (30 Hz, 0.3 sec.) from an canine intracardiac neuron (control tracing). After the administration of physostigmine (10^{-7} M), the original s-EPSP was enhanced and associated with spikes. Additionally, multiple slow depolarization pulses (s-EPSPs) occurred after the original one and induced burst of spikes as well. The amplitudes of the s-EPSPs were declined as a function of time. All s-EPSPs were blocked by atropine (10^{-7} M).

FIGURE 6-14

EFFECTS OF ADRENERGIC AND MUSCARINIC CHOLINERGIC
ANTAGONISTS ON THE s-EPSP AND s-IPSP
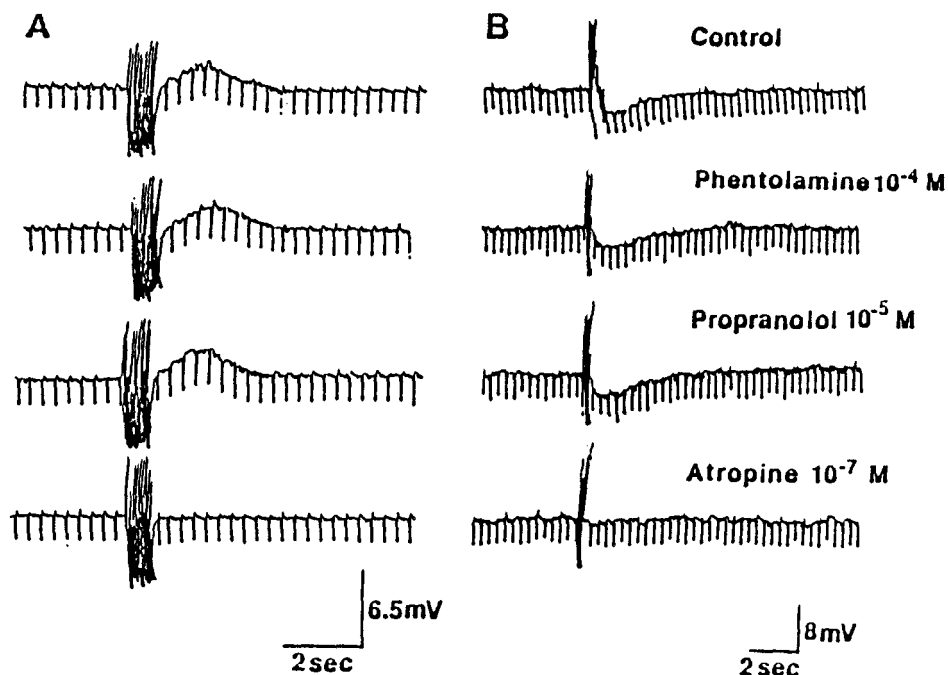
Trace A was recorded from a neuron exhibited s-EPSP and a slightly increased input resistance after a repetitive orthodromic stimulation (30 Hz, 0.9 sec.). Trace B was obtained from a neuron with s-IPSP and a small decrease in input resistance after a orthodromic stimulation (30 Hz, 0.3 sec.). Both the s-EPSP and s-IPSP were blocked by atropine (10^{-7} M), but not affected by α-adrenergic antagonist, phentolamine (10^{-4} M) and β-adrenergic antagonist, propranolol (10^{-5} M). Orthodromic stimulation was indicated as the initial stimulation artifacts. Downward deflections were electrotonic potentials induced by hyperpolarizing pulse injection (0.15 nA, 50 ms), and were used to monitor input resistance changes.

train. The mean amplitude and duration of the first depolarizing oscillation were 9.7 ± 1.8 mV and 2.8 ± 0.6 sec., respectively. Then the amplitudes of the succeeding s-EPSPs were gradually decreased while the intervals between them were gradually increased. Action potentials sometimes fired on these oscillating s-EPSPs. The latency of the first s-EPSP was less than 1 second.

In 9.4 % of these neurons (n = 8), only a s-IPSP was observed (Fig. 6-12). The mean amplitude of the s-IPSPs was 6.2 ± 1.8 mV with a range of 4.4 - 7.5 mV. The mean duration was 4.3 ± 1.1 sec. with a range of 2.0 - 4.5 sec. (n = 8). The latency of s-IPSPs was less than 1 second. Physostigmine (10^{-7} M) increased the size of s-IPSP as well. The membrane conductance was increased during the s-IPSPs (Fig. 6-14).

In 9.4 % of the neurons (n = 8), both s-IPSP and s-EPSP were recorded after a single orthodromic stimulation train (Fig. 6-12). The s-EPSP followed the s-IPSP and sometimes initiated action potentials. The amplitude and duration of these s-IPSPs were 4.3 ± 1.0 mV and 1.8 ± 0.6 sec. (n = 8), respectively. The amplitude and duration of these s-EPSPs were 3.7 ± 1.3 mV and 2.5 ± 1.2 sec.(n = 8), respectively. In all 8 cells, a s-IPSP can be observed without physostigmine. However, in some neurons (n = 5), the s-EPSP was masked by the preceding s-IPSP. In these cases, a clear observation of the small s-EPSP can only be obtained with physostigmine (10^{-7} M), causing the size of s-EPSP to be augmented more than that of the s-IPSP.

Generally, in the cells which exhibited slow synaptic responses, physostigmine (10^{-7} M) more dramatically increased the amplitude of depolarization than that of hyperpolarization. These observations may indicate that the s-EPSP requires a higher

concentration of ACh. Similar evidence was reported in cat vesical pelvic ganglion [35].

It is important to note that the apparent distribution of s-EPSP and s-IPSP in the tested neurons may not necessarily represent the distribution of the receptors which mediate the s-EPSP or s-IPSP. It has been found in some other ganglia [50] that the s-IPSP is usually superimposed on the s-EPSP. It was also occasionally observed in the present study that the small s-IPSP was masked by a physostigmine-enhanced s-EPSP. Therefore, in some cases, the recorded slow potential may be the balance between changes of the s-EPSP and the s-IPSP, although the exact percentage of this occurrence is uncertain.

In the remaining 34 neurons (40.0 %), no slow potentials were observed (Fig. 6-12) even when the orthodromic stimulation duration was gradually increased from less than 1 sec. up to 8 sec. Some of these observations (n = 21) were also confirmed in the presence of physostigmine (10^{-7} M). Since these cells had a normal range resting potentials and fast orthodromic responses, they are not likely to be damaged neurons. It is not clear if these neurons represent a subtype of canine intracardiac neurons. Previously, using autoradiographic techniques, Hassall et al. [40] have shown that in a cell culture preparation of guinea-pig atria, muscarinic receptors are present in all intracardiac neurons. Exogenously applied muscarinic agonist initiates depolarizing and/or hyperpolarizing responses in almost all of the canine (see result 3 - d.) and guinea-pig tested [5,66] intracardiac neurons. Moreover, neurons with no slow potentials could sometimes be depolarized by directly microejected bethanechol. Therefore, the relative large population (40%) of neurons without neurally evoked slow potential may suggest that some of these neurons are actually responsive to muscarinic agonist if the

concentration of the agonist is high enough. Similar evidence that a certain subpopulation of ganglion neurons exhibited no slow potentials has been reported in other sympathetic [61] and parasympathetic ganglia [37].

b. Effects of Cholinergic and Adrenergic Receptor Antagonists on the Slow Potentials

In different ganglia, slow postsynaptic potentials have been suggested to be mediated by adrenergic [59] or muscarinic receptors [37]. In order to elucidate the neurotransmitter and receptor mechanisms responsible for the slow postsynaptic potentials in canine intracardiac neurons, the effects of α- and β-adrenergic receptor antagonists (phentolamine and l-propranolol, respectively) and muscarinic receptor antagonist (atropine) were studied on the s-IPSP and s-EPSP responses. The nicotinic cholinergic antagonist, hexamethonium (10^{-4} M) was superfused throughout the experiments to inhibit f-EPSPs. Phentolamine (10^{-6} M) and l-propranolol (10^{-6} M) had no effects on either the s-EPSP (n = 7) or the s-IPSP (n = 5)(Fig. 6-14). However, atropine (10^{-7} or 10^{-6} M) completely blocked both the s-EPSP and s-IPSP in all tested neurons (n = 28) (Fig. 6-14). In two experiments, stable recordings were maintained for more than two hours after washout of atropine and a partial recovery of slow synaptic responses was observed. Therefore, the muscarinic receptor plays an important role in the induction of slow synaptic responses in canine intracardiac neurons.

c. Effects of M_1 and M_2 Receptor Antagonists on the Slow Potentials

The muscarinic cholinergic receptors consist of at least two subtypes: the M_1 and M_2 receptors which are distinguished by their high and low affinity, respectively, to a

selective antagonist pirenzepine [38]. M_2 receptor could be further discriminate into two subdivisions: the M_2 receptor on smooth muscle/gland cells which has a high affinity to 4-DAMP; the cardiac myocytes M_2 receptor which shows a low affinity to 4-DAMP [14]. All subtypes of muscarinic receptor have the same affinity to atropine.

The s-EPSP and s-IPSP were mediated by different subtypes of muscarinic receptor. Thus, the effects of M_1 receptor antagonist pirenzepine and M_2 receptor antagonists 4-DAMP were studied upon the s-EPSP and s-IPSP. Pirenzepine (10^{-8} M) reversibly blocked the s-EPSP in all tested cells with either single or oscillated depolarization responses (n = 10) (Fig. 6-15). On the other hand, ten fold higher concentration of 4-DAMP (10^{-7} M) had no effect on s-EPSPs (n = 5) (Fig. 6-15) even with a prolonged superfusion. Since s-IPSPs are infrequent, the effects of pirenzepine on the s-IPSP were tested on only 2 cells. A seven fold higher concentration of pirenzepine (7×10^{-8} M) caused no change of either the amplitude or duration of the s-IPSP. Accordingly, these results indicate that different muscarinic receptors are involved in s-EPSP and s-IPSP in canine intracardiac ganglion. Neurally evoked slow EPSPs are predominantly mediated via one of the muscarinic receptor subtypes, M_1 receptor.

d. Muscarinic Cholinergic Responses of Applied Bethanechol on Intracardiac Neurons

From the previous physiological studies, muscarinic mechanisms play an important role in synaptic transmission in canine intracardiac ganglia. To further elucidate the candidate neurotransmitter and receptor for slow postsynaptic potentials, a

FIGURE 6-15

EFFECTS OF M_1 AND M_2 MUSCARINIC RECEPTOR
ANTAGONISTS ON NEURALLY EVOKED s-EPSP
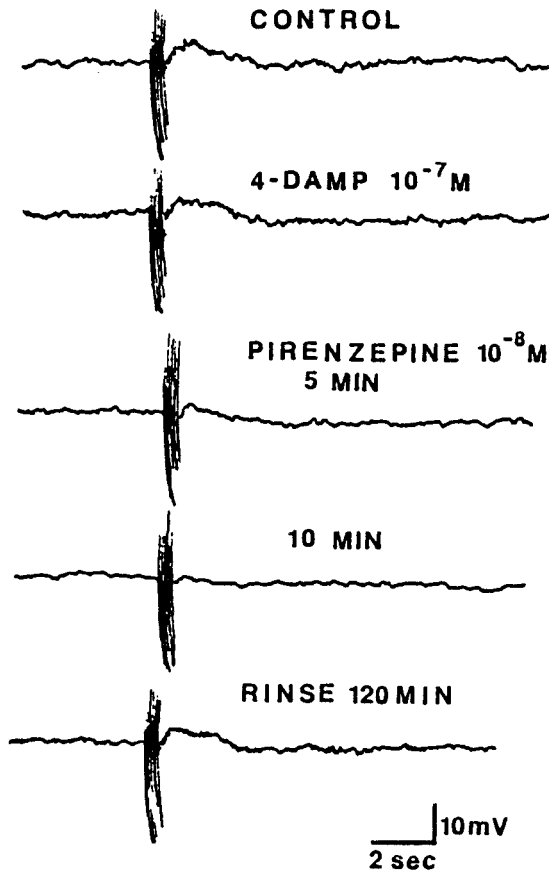
In the control tracing, repetitive stimulation (25 Hz, 0.5 sec.) evoked s-EPSP in an intracardiac neuron in the presence of hexamethonium (10^{-4} M). M_2 receptor antagonists 4-DAMP (10^{-7} M) had no effect on the s-EPSP. However, the M_1 receptor antagonist, pirenzepine (10^{-8} M) reversibly blocked the s-EPSP. Note the orthodromic stimulation was indicated as the initial stimulation artifacts.

selective muscarinic receptor agonist, bethanechol, was applied exogenously to canine intracardiac neurons, using pressure microejection technique. The specific aim of these experiments was to compare the bethanechol induced responses with neurally evoked responses in terms of alterations in membrane potential and conductance. This group of experiments was performed on a total of 36 cells.

Focal application of muscarinic agonist, bethanechol (micropipette concentration 10^{-2} or 10^{-3} M), produced a depolarization in the majority of neurons tested (30/36, 83%). Most commonly, the membrane potential rose fast and then slowly declined with various durations (Figs. 6-16 and 6-17). The amplitude and duration of the bethanechol evoked depolarization on a given cell were dependent on the duration of ejection. The amplitude and duration of the depolarization varied significantly from cells to cells. A decreased membrane conductance (27 ± 6 %) was consistently recorded in all cells (Fig. 6-16 D). Thus, an enhanced excitability was generally associated with the decreased membrane conductance. During the depolarization, cells usually fired spontaneously or following the termination of hyperpolarizing current pulses (Fig. 6-16). The spontaneous action potentials exhibited either a continuous or a burst pattern (Fig. 6-16). Three neurons had a small hyperpolarization with a increased membrane conductance to the bethanechol ejection. However, because of their very rare appearance, no systematic study was performed in the present experiment. Finally, three neurons exhibited no changes of either the resting membrane potential or membrane conductance although they had a stable resting membrane potential and fast orthodromic responses.

FIGURE 6-16

INCREASED EXCITABILITY OF INTRACARDIAC NEURONS DURING BETHANECHOL INDUCED DEPOLARIZATION RESPONSE
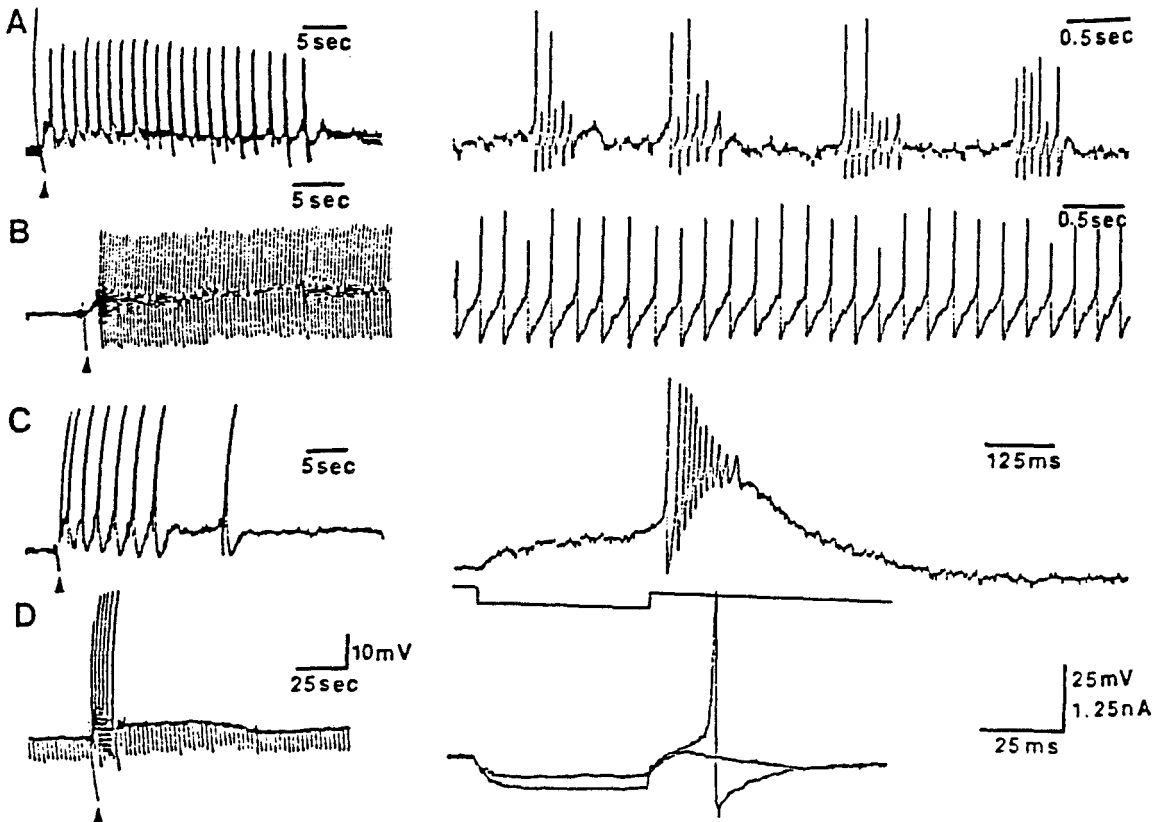
Each trace of the figure was recorded from an individual cell with two different speeds. Arrow heads indicate the onset of bethanechol microejection (30 - 90 ms, 1700 mmHg). A. In addition to membrane depolarization, bethanechol induced spontaneous bursts of spikes. B. Bethanechol caused the membrane depolarization and a long-lasting spontaneous firing in a rhythmic pattern. C. Spikes were evoked by slow spontaneous depolarizing potentials after the bethanechol ejection. D. Bethanechol initiated the depolarization of membrane potential, the increase in input resistance as indicated by the downward deflections, and the off-set spikes which were observed at the cessation of the hyperpolarizing pulse.

FIGURE 6-17

EFFECTS OF CHOLINERGIC ANTAGONISTS ON BETHANECHOL INDUCED DEPOLARIZATION RESPONSE
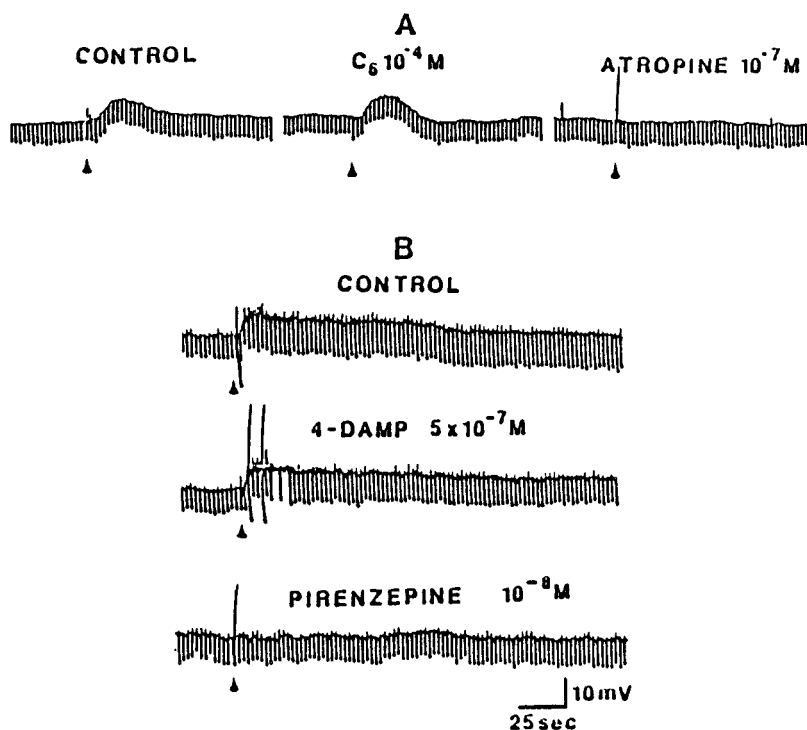
A. In the control tracing, bethanechol (50 ms, at arrow head) initiated membrane depolarization with an slightly increased input resistance (downward deflections). The depolarizing responses were not affected by hexamethonium (C_6 10^{-4} M) but were blocked by atropine (10^{-7} M). B. Bethanechol induced depolarization was not affected by 4-DAMP (5 x 10^{-7} M) but blocked by the M_1 receptor antagonist pirenzepine (10^{-8} M). Arrow heads indicate the onset of bethanechol microejections.

The bethanechol evoked depolarizations were completely abolished by atropine (10^{-7} or 10^{-6} M) (n = 27) (Fig. 6-17 A) but were resistant to hexamethonium (10^{-4} M) (n = 5) (Fig. 6-17 A). The blocking effect of atropine (10^{-7} M) on bethanechol hyperpolarization was tested and observed in only one cell. These confirmed a muscarinic mechanism in the depolarization and, possibly, the hyperpolarization responses. A low Ca^{2+} / high Mg^{2+} solution which diminishes neurotransmitter release, failed to block the bethanechol depolarizing responses (n = 5). This observation suggests a direct effect of bethanechol on the postsynaptic muscarinic receptor of the recorded somata. The M_1 receptor antagonist pirenzepine (10^{-8} M) blocked the depolarization in all cells tested (n = 16) (Fig. 6-17 B). However, the M_2 receptor antagonist 4-DAMP (5×10^{-7}) had no detectable effects (n = 7) (Fig. 6-17 B). This evidence indicates that the M_1 receptor plays a significant role in the muscarinic depolarizing response, which correlates with the function of M_1 receptor in nerve evoked s-EPSPs.

e. Ionic Mechanisms for the s-EPSP and Bethanechol Evoked Depolarization

In order to establish the ion(s) responsible for a particular response, it is necessary to determine the membrane potential at which a response reverses its polarity and then to study the effects of different ion concentrations on that reversal potential. In terms of determination of a neurotransmitter candidate, the established standard is that there should be similar reversal potentials present for both the responses to the exogenous compound and to the nerve stimulation.

The ionic mechanisms involved in the s-EPSP and bethanechol induced

depolarizations were established by experiments similar to those used to determine the reversal potential for the f-EPSP. Because of the rare occurrence of the s-IPSP and bethanechol evoked hyperpolarizations, the ionic mechanisms were not studied. The amplitudes of the nerve evoked s-EPSP and bethanechol induced depolarizations were altered with the variation of membrane potential. Both of these amplitudes were decreased when the membrane potential was hyperpolarized and were increased when the membrane potential was depolarized (Fig. 6-18 A and B). For the neurally evoked response, the s-EPSP disappeared when the membrane potential was hyperpolarized more negative than -80 mV (n = 5) (Fig. 6-18 A). Similarly, the polarity of the bethanechol induced depolarization was reversed at the same voltage range with the extrapolated reversal potential of -83 $\pm$ 3.9 mV (n = 4) (Fig. 6-18 B and C). Both of these estimated reversal potentials are close to the equilibrium potential for potassium.

Attempts were made to determine the effect of extracellular potassium concentration on the reversal potential. If potassium is the ion responsible, changing the extracellular potassium concentration would shift the reversal potential of the s-EPSP or bethanechol depolarization to the value predicted by the Nernst equation:

$E_k = 61 \log ([K]_o / [K]_i)$. In two neurons examined, when the potassium concentration of the Krebs solution was increased from 4.7 to 15 mM, the reversal potentials of bethanechol depolarizations were shifted 18 and 20 mV more positive, respectively (Fig. 6-18 C). These reversal potentials were very close or identical to the estimated E_k value from the Nernst equation. Therefore, s-EPSP and bethanechol depolarizations are primarily the result of a decreased potassium conductance.

FIGURE 6-18

EFFECTS OF MEMBRANE POTENTIAL ON THE AMPLITUDE
OF s-EPSP AND BETHANECHOL EVOKED DEPOLARIZATION
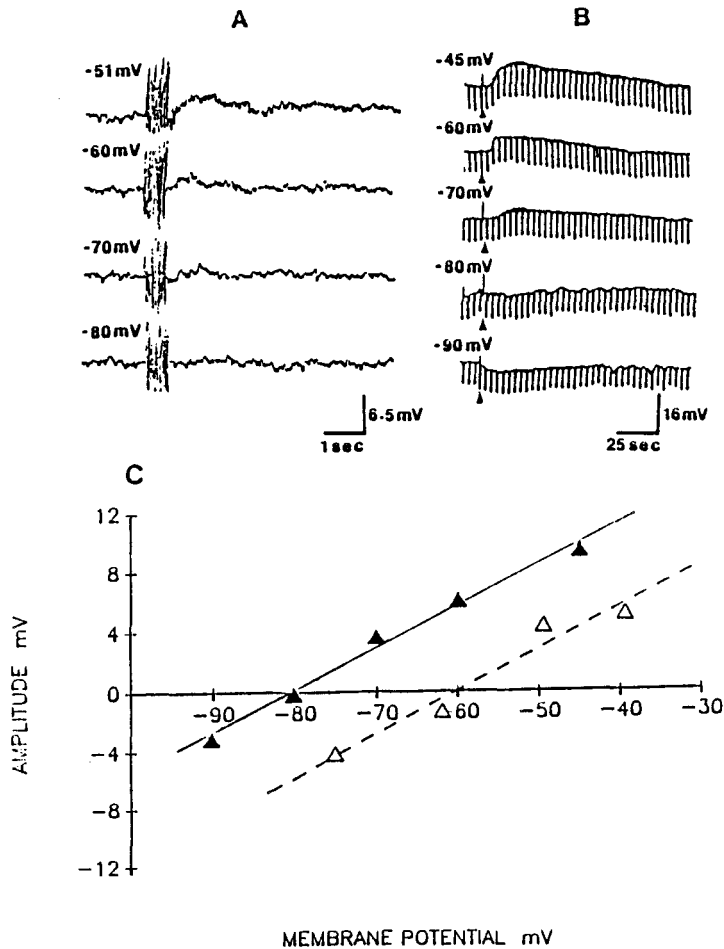
A. Repetitive orthodromic stimulation (40 Hz, 0.9 sec.) induced s-EPSP in an intracardiac neuron. The amplitude of the s-EPSP was decreased during hyperpolarizing the membrane potential and increased with the depolarization. The s-EPSP disappeared at membrane potential of -80 mV. B. The amplitude of bethanechol induced depolarization was decreased with the membrane hyperpolarization and increased with the membrane depolarization. As well, the response reversed its polarity at about -80 mV. C. The amplitudes of B. was plotted as the function of membrane potential (solid triangle). A linear relationship was obtained with the reversal potential of -80 mV. When the potassium concentration of Krebs solution was increased from 4.7 to 15 mM in the same neuron, the reversal potential shifted 20 mV more positive (opened triangle).

Since the resting conductance and intracellular concentration of chloride ions in the intracardiac neurons is not known, the above data do not exclude the possibility of the involvement of inactivation of chloride conductance [3,66] whose reversal potential is close to that of potassium.

Repetitive stimulation releases ACh from interganglionic nerve terminals. Then, in turn, ACh activates postsynaptic nicotinic and muscarinic receptors in the recorded cell. One of the findings in this study was that, in addition to the f-EPSP, both neurally evoked s-IPSP and s-EPSP were directly recorded in intracardiac neurons. This triphasic evidence has not been previously obtained in intracardiac ganglia. Other related findings of this study include:

i). General characteristics of neurally evoked slow potentials: in the majority of tested neurons (60 %), repetitive stimulation (< 40 Hz, < 1 sec.) initiated s-EPSPs and/or s-IPSPs. The temporal sequence of neurally evoked membrane potential changes is f-EPSP, s-IPSP and s-EPSP, if both slow potentials were observed in the same neuron (Fig. 6-11). The amplitude of slow potentials was usually a few millivolts, and the time course varied a few seconds. The s-EPSP requires a higher concentration of ACh than the s-IPSP since the s-EPSP was more readily observed after a low concentration of cholinesterase inhibitor, physostigmine.

ii). The transmitter candidate for the s-EPSP and s-IPSP is ACh in the following reasons. First, the cholinesterase inhibitor physostigmine can enhance both the s-EPSP and s-IPSP; second, exogenously applied ACh, in the presence of nicotinic antagonists, evoked similar membrane potential responses; and third, a low Ca^{2+}/high Mg^{2+} solution

which diminishes ACh release also reduced s-EPSP and s-IPSP.

iii). Both the s-EPSP and the s-IPSP are muscarinic cholinergic receptor mediated, since they were consistently blocked by low concentrations of atropine but not by the nicotinic receptor antagonist hexamethonium and adrenergic receptor antagonists, l-propranolol and phentolamine. Additionally, the muscarinic receptor agonist bethanechol can mimic the neurally evoked responses, which was not blocked by a low Ca^{2+}/high Mg^{2+} solution, suggesting a direct effect on the muscarinic receptor.

iv). The s-EPSP is mediated by the M_1 muscarinic receptor which had a higher affinity to the selective M_1 receptor antagonist, pirenzepine, than to the selective M_2 receptor antagonist, 4-DAMP. On the other hand, the s-IPSP is not mediated by the M_1 receptor since it was not affected by a higher concentration of pirenzepine. It is presumably induced by a different subtype of muscarinic receptor.

v). The ionic mechanism for the s-EPSP is a decreased potassium conductance, because first, the s-EPSP is associated with an increased input resistance; second, the estimated reversal potential of s-EPSP was close to the potassium equilibrium potential; and third, the bethanechol induced depolarization had a similar extrapolated reversal potential which shifted to the predicted value of the Nernst equation in a high potassium concentration.

Hartzell et al.[39] have previously described in detail a dual action of nerve released ACh on cells at the cardiac ganglia of the mudpuppy. A brief repetitive stimulation produced two distinct post-synaptic responses in individual principal cells: a rapid EPSP resembling f-EPSP within milliseconds range and a slow hyperpolarization that lasts for

several seconds. On the basis of three criteria, namely, exogenous agonist, receptor antagonist and ionic mechanism, they reported that the f-EPSP and s-IPSP result from the direct action of ACh on the nicotinic and muscarinic receptors, respectively. More recently, after the initiation of the present study, the existence of differential muscarinic receptors and muscarinic potentials in intracardiac neurons were also suggested [5,55,66]. In the mudpuppy cardiac neurons, exogenous bethanechol evoked predominantly a hyperpolarization which was readily blocked by atropine and 4-DAMP but not by pirenzepine[55].

The results from guinea-pig intracardiac neurons are controversial [5,66]. In cultured intracardiac neurons from the newborn guinea-pig atrium, autoradiographic techniques showed the presence of muscarinic receptors [40]; applied muscarine mediated depolarization and/or hyperpolarization via M_1 and M_2 receptor, respectively [5]. On the other hand, Mihara et al.[66] found that, in isolated adult guinea-pig intracardiac ganglia, muscarinic depolarization was likely mediated via a M_2 receptor. Nicotinic EPSP and muscarinic EPSP and IPSP could all be induced by endogenous ACh in individual intracardiac neurons. This provides a more direct or physiological view on the actual pattern of nicotinic and M_1 and M_2 muscarinic transmissions in the intracardiac ganglia.

The slow synaptic potentials and muscarinic responses in the present study have a number of similarities to those previously described in other autonomic ganglionic neurons. In addition to intracardiac ganglia [5,39], the slow muscarinic potentials or synaptic potentials mediated via muscarinic receptor have been reported in the amphibian and mammalian sympathetic ganglion [16,18,23,42] and parasympathetic cat vesical (bladder)

pelvic ganglion [37].

In canine intracardiac ganglia, the s-EPSP and muscarinic depolarization with both similar increased input resistance changes and voltage dependency is best explained by a decrease or inactivation of resting potassium conductance. Since the resting membrane potential is maintained in part by an outward potassium current [41,48], synaptic inactivation of this potassium conductance would cause i) an increase in the membrane resistance; ii) the shifting of the membrane potential away from the potassium equilibrium potential and toward to the equilibrium potential of other resting conductances [41,48]; and iii) the induction of a depolarization - the s-EPSP. Electrical depolarization of the membrane may increase the electrochemical gradient for potassium which increases the outward potassium current. Synaptic inactivation of this outward potassium current would generate a larger s-EPSP. Electrical hyperpolarization, on the other hand, may decrease the potassium electrochemical gradient which would decrease the size of the s-EPSP. At the potassium equilibrium potential, there is no net potassium current, hence there is no s-EPSP initiated. If the membrane potential is hyperpolarized below the potassium equilibrium potential, the electrochemical gradient for potassium is reversed, producing a net inward potassium current. In this case, inactivation of the potassium conductance would result in a hyperpolarization potential [93]. The present experimental observations were consistent with the hypothesis that inhibition of potassium current was responsible for the s-EPSP.

Several types of voltage sensitive potassium currents have been demonstrated to exist in various vertebrate neurons: namely, the rectifying potassium current (I_K)[2,18], the

Ca-dependent potassium current (I_C)[1,18,63], the voltage dependent potassium current (I_M)[2,17,18], the transient outward potassium current (I_A)[2,18] and the potassium current underlying a train of spike potentials (I_{AHP})[63,69]. Synaptic s-EPSPs and muscarinic depolarization have been shown to be mediated predominantly via I_M in sympathetic [16,18] as well as parasympathetic ganglion cells [5]. I_M is a time and voltage-dependent potassium current which is partly activated at resting membrane potentials and becomes more strongly activated as the cell is depolarized. It forms the dominant outward component of membrane current over the range -70 to -25 mV. Hence, inhibition of I_M produces a net inward (depolarization) current which increases in magnitude as the cell is depolarized. This accounts for the peculiar dependence of the muscarinic depolarization on cell membrane potential [18]. Although no direct study on I_M was performed in the present report, the estimated reversal potential suggested that the most possible channel candidate responsible for s-EPSP is likely to be the muscarinic agonist inhibited potassium channel. The lack of influences of a low calcium solution on bethanechol depolarization suggested little involvement of I_C in the s-EPSP which are synaptically activated in ganglion neurons [5].

Taken together, in canine intracardiac ganglia spontaneous membrane potential changes consisting primarily of miniature EPSP-like depolarizations, suggesting a potentially important contribution to tonic neural control of SA nodal function. Acetylcholine released from preganglionic nerve terminals directly activates both the nicotinic and different muscarinic cholinergic receptors on individual postganglionic neurons. The activated receptors, in turn, cause alteration of different ion conductances

and result in f-EPSP, s-IPSP and s-IPSP in a fixed temporal pattern.

The presence of both nicotinic and muscarinic receptors and spontaneous activities in the canine intracardiac ganglia provides the basis for integrative capabilities. Since this ganglion plexus directly innervates the SA node in the canine heart, the ganglion cells constitute the last integrative stations for vagal output to the SA node. The temporal and/or spatial summation of f-EPSPs occur in the canine intracardiac ganglia (Fig. 6-4) as in many other ganglia [56]. The time course of the slow potentials was hundreds of times longer than the fast synaptic potentials. The relative long duration of slow potentials could provide long-lasting modulation of synaptic transmission [92]. The s-EPSP has been shown to mediate excitation (Figs. 6-12, 6-14) and/or facilitate spontaneous firing in the present preparation and in other peripheral and central nervous system neurons [35,64,92,96]. The mechanism is likely related to both the membrane potential depolarization and the decreased conductance. On the other hand, s-IPSP has been shown to depress spontaneous firing and directly activated action potentials, suggesting an inhibition of ganglion transmission [35,64]. This comprehensive knowledge of the complex synaptic mechanism in the intracardiac neurons and their interactions is an important step toward a better understanding of the vagal control of SA nodal function.

D. REFERENCES

1 Adams, P.R., Brown, D.A. and Clark, R.B., Intracellular Ca++ activates a fast voltage-sensitive K+ current in vertibrate sympathetic neurones, *Nature*, 296 (1982) 746-749.

2 Adams, P.R., Constanti, A. and Brown, D.A., Effects of divalent cations on outward currents of voltage clamped bullfrog sympathetic neurons, *Fed. Proc.*, 39 (1980) 2063-2063.

3 Akasu, T. and Koketsu, K., Muscarinic transmission. In A.G. Karczmar, K. Koketsu and S. Nishi (Eds.), *Autonomic and Enteric Ganglia*, Plenum Press, New York and London, 1986, pp. 161-179.

4 Allen, T.G.J. and Burnstock, G., Intracellular studies of the electrophysiological properties of cultured intracardiac neurons of the guinea-pig, *J. Physiol. (Lond.)*, 388 (1987) 349-366.

5 Allen, T.G.J. and Burnstock, G., M_1 and M_2 muscarinic receptors mediate excitation and inhibition of guinea-pig intracardiac neurons in culture, *J. Physiol. (Lond.)*, 422 (1990) 463-480.

6 Alving, B., Spontaneous activity in isolated somata of Aplysia pacemaker neurons, *J. Gen. Physiol.*, 51 (1968) 29-45.

7 Ardell, J.L. and Randall, W.C., Selective vagal innervation of sinoatrial and atrioventricular nodes in canine heart, *Am. J. Physiol.*, 251 (1986) H764-H773.

8 Baker, R. and Llinas, R., Electrical coupling between neurons in the rat mesencephalic nucleus, *J. Physiol. (Lond.)*, 203 (1971) 550-570.

9 Blackman, J.G., Ginsborg, B.L. and Ray, C., Synaptic transmission in the sympathetic ganglion of the frog, *J. Physiol. (Lond.)*, 167 (1963) 355-373.

10 Blackman, J.G., Ginsborg, B.L. and Ray, C., Spontaneous synaptic activity in sympathetic ganglion cells of the frog, *J. Physiol. (Lond.)*, 167 (1963) 389-401.

11 Blackman, J.G. and Purves, R.D., Intracellular recording from ganglia of the thoracic sympathetic chain of the guinea-pig, *J. Physiol. (Lond.)*, 203 (1969) 173-198.

12 Bloom, F.E., Costa, E. and Salmoiraghi, G.C., Anesthesia and the responsiveness of individual neurons of the caudate nucleus of the cat to acetylcholine,norepinephrine and dopamine administered by microelectrophoresis, *J. Pharmacol. Exp. Ther.*, 150 (1965) 244-252.

13 Bluemel, K.M., Wurster, R.D., Randall, W.C., Duff, M.J. and O'Tool, M.F., Parasympathetic postganglionic pathways to the sinoatrial node, *Am. J. Physiol.*, 259 (1990) H1504-H1510.

14 Bonner, T.I., The molecular basis of muscarinic receptor diversity, *TINS*, 12 (1989) 148-151.

15 Bornstain, J.C., Multiquantal release of acetylcholine in mammalian ganglia, *Nature*, 248 (1974) 529-531.

16 Brown, D.A., M-currents: an update, *TINS*, 11 (1988) 294-299.

17 Brown, D.A. and Adams, P.R., Muscarinic suppression of a novel voltage-sensitive K current in a vertebrate neurone, *Nature*, 283 (1980) 673-676.

18 Brown, D.A., Adams, P.R. and Constanti, A., Voltage-sensitive K-currents in sympathetic neurons and their modulation by neurotranmitters, *J. Auton. Nerv. Syst.*, 6 (1982) 23-35.

19 Butler, C.K., Smith, F.M., Cardinal, R., Murphy, D.A., Hopkins, D.A. and Armour, J.A., Cardiac responses to electrical stimulation of discrete loci in canine atrial and ventricular ganglionated plexi, *Am. J. Physiol.*, 259 (1990) H1365-H1373.

20 Crowcroft, P.J. and Szurszewski, J.H., A study of the inferior mesenteric and pelvic ganglia of guinea-pigs with intracellular electrodes, *J. Physiol. (Lond.)*, 219 (1971) 421-441.

21 De Groat, W.C., Booth, A.M. and Krier, J., Interaction between sacral parasympathetic and lumbar sympathetic inputs to pelvic ganglia. In C.McC. Brooks, K. Koizumi and A. Sato (Eds.), *Integrative Functions of the Autonomic Nervous System*, Elseveir/North-Holland Biomedical Press, Amsterdam, 1979, pp. 234-247.

22 Dennis, M.J., Harris, A.J. and Kuffler, S.W., Synaptic transmission and its duplication by focally applied acetylcholine in parasympathetic neurons of the frog, *Proc. Roy. Soc. Lond.*, 177 (1971) 509-539.

23 Dodd, J. and Horn, R.P., Muscarinic inhibition of sympathetic neurons in the bullfrog, *J. Physiol. (Lond.)*, 334 (1983) 271-291.

24 Dun, N.J. and Jiang, Z, G., Non-cholinergic excitatory transmission in inferior mesenteric ganglia of the guinea-pig: Possible mediation by substance P, *J. Physiol. (Lond.)*, 325 (1982) 145-159.

25   Dun, N.J., Kiraly, M. and Ma, R.C., Evidence for a serotonin-mediated slow excitatory potential in the guinea pig coeliac ganglia, *J. Physiol. (Lond.)*, 351 (1984) 61-76.

26   Dun, N.J. and Ma, R.C., Slow non-cholinergic excitatory potentials in neurones of the guinea-pig coeliac ganglia, *J. Physiol. (Lond.)*, 351 (1984) 47-60.

27   Dun, N.J. and Nishi, S., Effects of dopamine on the superior cervical ganglion of the rabbit, *J. Physiol. (Lond.)*, 239 (1974) 155-164.

28   Eccles, R.M., Orthodromic activation of single ganglion cells, *J. Physiol. (Lond.)*, 165 (1963) 387-391.

29   Eccles, R.M. and Libet, B., Origin and blockade of the synaptic responses of curarized sympathetic ganglia, *J. Physiol. (Lond.)*, 157 (1961) 484-503.

30   Evans, J.M., Randall, D.C., Funk, J.N. and Knapp, C.F., Influence of cardiac innervation on intrinsic heart rate in dogs, *Am. J. Physiol.*, 258 (1990) H1132-H1137.

31   Fatt, P. and Katz, B., Spontaneous subthreshold activity at motor nerve-endings, *J. Physiol. (Lond.)*, 117 (1952) 109-128.

32   Frazier, W.T., Kandel, E.R., Kupfermann, I., Waziri, R. and Coggeshall, R.E., Morphological and functional properties of identified neurons in the abdominal ganglion of Aolysia Californica, *J. Neurophysiol.*, 30 (1967) 1288-1351.

33   Gagliardi, M., Randall, W.C., Bieger, D., Wurster, R.D., Hopkins, D.A. and Armour, J.A., Activity of *in vivo* canine cardiac plexus neurons, *Am. J. Physiol.*, 255 (1988) 789-800.

34   Gallagher, J.P. and Shinnick-Gallagher, P., Excitatory transmission in parasympathetic ganglia. In A.G. Karczmar, K. Koketsu and S. Nishi (Eds.), *Autonomic and Enteric Ganglia*, Plenum Press, New York and London, 1986, pp. 341-351.

35   Griffith, W.H.III, The physiology and pharmacology of a mammalian parasympathetic ganglion. Dissertation. University of Texas Graduate School of Biomedical Science at Galveston, 1980.

36   Griffith, W.H.III, Gallagher, J.P. and Shinnick-Gallagher, P., An intracellular investigation of cat vesicle pelvic ganglia, *J. Neurophysiol.*, 143 (1980) 343-354.

37   Griffith, W.H.III, Gallagher, J.P. and Shinnick-Gallagher, P., Cholinergic slow potentials influence parasympathetic ganglionic transmission, *Soc. Neurosci. Abs.*, 6 (1980) 68-68.

38 Hammer, R., Berrie, E.P., birdsall, N.J.M., Burgen, A.S.V. and Hulme, E.E.C., Pirenzepine distinguishes between different subclasses of muscarinic receptors, *Nature*, 283 (1980) 90-92.

39 Hartzell, H.C., Kuffler, S.W., Stickgold, R. and Yoshikami, D., Synaptic excitation and inhibition resulting from direct action of acetylcholine on two type of chemoreceptors on individual parasympathetic neurons, *J. Physiol. (Lond.)*, 271 (1977) 817-846.

40 Hassall, C.J.S., Buckley, N.J. and Burnstock, G., Autoradiographic localization of muscarinic receptors on guinea-pig intracardiac neurons and atrial myocytes in culture, *Neurosci. Lett.*, 74 (1987) 145-150.

41 Hodgkin, A.L., *The Conduction of the Nervous Impulse*, Thomas, Springfield, 1964.

42 Horn, J.P. and Dodd, J., Monosynaptic muscarinic activation of K conductance underlies the slow inhibitory postsynaptic potential in sympathetic ganglia, *Nature*, 292 (1981) 625-627.

43 Jan, L.Y. and Jan, Y.N., Peptidergic transmission in sympathetic ganglia of the frog, *J. Physiol. (Lond.)*, 327 (1982) 219-246.

44 Jiang, Z.G. and Dun, N.J., Facilitation of nicotinic response in the guinea pig prevertebral neurons by substance P, *Brain Res.*, 363 (1986) 196-198.

45 Julé, Y., Krier, J. and Szurszewski, J.H., Patterns of innervation of neurones in the inferior mesenteric ganglion of the cat, *J. Physiol. (Lond.)*, 344 (1983) 293-304.

46 Karczmar, A.G., Pharmacological, toxicological, and therapeutic properties of anticholinesterase agents. In Root and Hofmann (Eds.), *Physiological Pharmacology*, , New York, 1967, pp. 163-322.

47 Katayama, Y. and Nishi, S., Peptidergic transmission. In A.G. Karczmar, K. Koketsu and S. Nishi (Eds.), *Autonomic and Enteric Ganglia*, Plenum Press, New York and London, 1986, pp. 181-199.

48 Katz, B., *Muscle and Synapse*, McGraw-Hill, New York, 1966.

49 King, B.F. and Szurszewski, J.H., An electrophysiological study of inferior mesenteric ganglion of the dog, *J. Neurophysiol.*, 51 (1984) 607-615.

50 Koketsu, K., Inhibitory transmission: Slow inhibitory postsynaptic potential. In A.G. Karczmar, K. Koketsu and S. Nishi (Eds.), *Autonomic and Enteric Ganglia*, Plenum Press, New York and London, 1986, pp. 201-223.

51 Koketsu, K. and Karczmar, A.G., General concepts of ganglionic transmission and modulation. In A.G. Karczmar, K. Koketsu and S. Nishi (Eds.), *Autonomic and Enteric Ganglia*, Plenum Press, New York and London, 1986, pp. 63-77.

52 Kononenbo, N.I., Modulation of the endogenous electrical activity of the bursting neuorn in the snail Helix promatia: III. A factor modulating the endogenous electrical activity of the bursting neuron, *Neuroscience*, 4 (1979) 2055-2059.

53 Kononenbo, N.I., Modulation of the endogenous electrical activity of the bursting neuron in the snail Helix promatia: II. The membrane characteristics of the neuron, *Neuroscience*, 4 (1979) 2047-2054.

54 Kononenbo, N.I., Modulation of the endogenous electrical activity of the bursting neuron in the snail Helix promatia: I. The generator of the slow rhythms, *Neuroscience*, 14 (1979) 2037-2045.

55 Konopka, L.M. and Parsons, R.L., The muscarinic agonist bethanechol initiates hyperpolarization and depolarization of mudpuppy intracardiac neurons, *Soc. Neurosci. Abs.*, 16 (1990) 1055.(Abstract)

56 Kuba, K. and Minota, S., General characteristics and mechanisms of nicotinic transmission in sympathetic ganglia. In A.G. Karczmar, K. Koketsu and S. Nishi (Eds.), *Autonomic and Enteric Ganglia*, Plenum Press, New York and London, 1986, pp. 107-135.

57 Langley, J.N. and Dickinson, W.L., Actions of various poisons upon nerve fibers and peripheral nerve cells, *J. Physiol. (Lond.)*, 11 (1880) 509-527.

58 Langley, J.N. and Dickinson, W.L., In the local paralysis of the peripheral ganglia and on the connexion of different classes of nerve fibers with them, *Proc. Roy. Soc. Lond.*, 46 (1889) 423-431.

59 Libet, B., Slow synaptic responses and excitatory changes in sympathetic ganglia, *J. Physiol. (Lond.)*, 174 (1964) 1-25.

60 Libet, B., Long latent periods and further analysis of slow synaptic responses in sympathetic ganglia, *J. Neurophysiol.*, 30 (1967) 494-514.

61 Libet, B. and Tosaka, T., Dopamine as a synaptic transmitter and modulator in sympathetic ganglia: A different mode of synaptic action, *Proc. Natl. Acad. Sci. USA*, 67 (1970) 667-673.

62 Ma, R.C. and Dun, N.J., Excitation of lateral horn neurons of the neonatal rat spinal cord by 5-hydroxytryptamine, *Dev. Brain Res.*, 24 (1986) 89-98.

63 McAfee, D.A. and Yarowsky, P.J., Calcium-dependent potentials in the mammalian sympathetic neurone, *J. Physiol. (Lond.)*, 290 (1979) 507-523.

64 McGeer, P.L., Eccles, J.C. and McGeer, E.G., *Molecular Neurobiology of the Mammalian Brain*, Plenum press, New York, 1978.

65 Melnichenko, L.V. and Skok, V.I., Natural electrical activity in mammlian parasympathetic ganglion neurons, *Brain Res.*, 23 (1970) 277-279.

66 Mihara, S., Ikeda, K. and Nishi, S., Muscarinic M_2 receptors on cardiac ganglion neurons of the guinea-pig heart, *Kurume Med. J.*, 35 (1988) 183-192.

67 Mirgorodsky, V.N. and Skok, V.I., Intracellular potentials recorded from a tonically active mammalian sympathetic ganglion, *Brain Res.*, 15 (1969) 570-572.

68 Mo, N. and Dun, N.J., Is glycine an inhibitory transmitter in rat lateral horn cells?, *Brain Res.*, 400 (1987) 139-144.

69 Monota, S., Calcium ions and the post-tetanic hyperpolarization of bullfrog sympathetic ganglion cells, *Jpn. J. Physiol.*, 24 (1974) 501-512.

70 Nishi, S. and Koketsu, K., Electrical properties and activities of single sympathetic neurons in frogs, *J. Cell. Comp. Physiol.*, 55 (1960) 15-30.

71 Nishi, S. and Koketsu, K., Early and late after-discharges of amphibian sympathetic ganglion cells, *J. Neurophysiol.*, 31 (1968) 109-121.

72 Nishi, S. and North, R.A., Intracellular recording from the myenteric plexus of the guinea-pig ileum, *J. Physiol. (Lond.)*, 231 (1973) 471-491.

73 North, R.A. and Tokimasa, T., The time course of muscarinic depolarization of guinea-pig myenteric neurones, *Br. J. Pharmacol.*, 82 (1984) 85-92.

74 North, R.A. and Williams, J.T., Extracellular recordings from the guinea pig myenteric plexus and the action of morphine, *Eur. J. Pharmacol.*, 45 (1977) 23-33.

75 Nozdrachev, A.D. and Pogorelov, A.G., Extracellular recording of neuronal activity of the cat heart ganglia, *J. Auton. Nerv. Syst.*, 6 (1982) 73-81.

76 Okamato, K. and Quastel, J.H., Spontaneous action potentials in isolated guinea-pig cerebellar slices: effects of amino acids and conditions affecting sodium and water uptake, *Proc. Roy. Soc. Lond.*, 184 (1973) 83-90.

77 Perri, V., Sacchi, O. and Casella, C., Synaptically mediated potentials elecited by the stimulation of post-ganglionic trunks in the guinea-pig superior cervical ganglion, *Pflugers. Arch.*, 314 (1970) 55-67.

78 Plecha, D.M., Randall, W.C., Geis, G.S. and Wurster, R.D., Localization of vagal preganglionic somata controlling sinoatrial and atrioventricular nodes, *Am. J. Physiol.*, 255 (1988) R703-R708.

79 Randall, W.C., Ardell, J.L., Calderwood, D., Milosavljevic, M. and Goyal, S.C., Parasympathetic ganglia innervating the canine atrioventricular nodal region, *J. Auton. Nerv. Syst.*, 16 (1986) 311-323.

80 Randall, W.C., Ardell, J.L., Wurster, R.D. and Milosavljevic, M., Vagal postganglionic innervation of the canine sinoatrial node, *J. Auton. Nerv. Syst.*, 20 (1987) 13-23.

81 Randall, W.C., Milosavljevic, M., Wurster, R.D., Geis, G.S. and Ardell, J.L., Selective vagal innervation of the heart, *Ann. Clin. Lab. Sci.*, 16 (1986) 198-208.

82 Rigel, D.F., Lipson, D. and Katona, P.G., Excess tachycardiac: heart rate after antimuscarinic agents in conscious dogs, *Am. J. Physiol.*, 15 (1984) H168-H173.

83 Roper, S., An electrophysiological study of chemical and electrical synapses on neurons in the parasympathetic cardiac ganglion of the mudpuppy ,necturus maculosus: evidence for intrinsic ganglionic innervation, *J. Physiol. (Lond.)*, 254 (1976) 427-454.

84 Roper, S., The acetylcholine sensitivity of the surface membrane of multiply-innervated parasympathetic ganglion cells in the mudpuppy before and after partial denervation, *J. Physiol. (Lond.)*, 254 (1976) 455-473.

85 Sacchi, O. and Perri, V., Quantal release of acetylcholine from the nerve endings of the guinea-pig superior cervical ganglion, *Pflugers. Arch.*, 329 (1971) 207-219.

86 Sacchi, O., Prigioni, I. and Perri, V., Post-tetanic spontaneous spike activity in rat sympathetic neurons exposed to low potassium ion concentration, *Brain Res.*, 123 (1977) 287-299.

87 Saum, W.R., The neural control of the urinary bladder of the cat. Dissertation. University of Pittsburg. 234 pp, 1973.

88 Seabrook, G.R., Fieber, L.A. and Adams, D.J., Neurotransmission in neonatal rat cardiac ganglion in situ, *Am. J. Physiol.*, 259 (1990) H997-H1005.

89 Sherrington, C.S., *Integrative Action of the Nervous System*, Yale University Press, New Haven, 1906.

90 Tokimasa, T., Spontaneous muscarinic suppression of the Ca-activated K-current in bullfrog sympathetic neurons, *Brain Res.*, 344 (1985) 134-141.

91 Treistman, S., Duplication of a spontaneous active neuron in Aplysia: electrical coupling and effects of a phosphodiesterase inhibitor, *J. Neurobiol.*, 10 (1979) 325-330.

92 Weight, F.F., Schulman, J.A., Smith, P.A. and Busis, N.A., Long-lasting synaptic potentials and the modulation of synaptic transmission, *Fed. Proc.*, 38 (1979) 2084-2094.

93 Weight, F.F. and Votava, J., Slow synaptic excitation in sympathetic ganglion cells: Evidence for synaptic inactivation of potassium conductance, *Science*, 170 (1970) 755-758.

94 Wood, J.D., Neurophysiology of Auerbach's plexus and control of intestinal motility, *Physiol. Rev.*, 55 (1975) 307-324.

95 Wood, J.D. and Mayer, C.J., Intracellular study of electrical activity of Auerbach's plexus in guinea-pig small intestine, *Pflugers. Arch.*, 374 (1978) 265-275.

96 Wood, J.D. and Mayer, C.J., Slow synaptic excitation mediated by serotonin in Auerbach's pelux, *Nature*, 276 (1978) 386-837.

97 Wurster, R.D., Xi, X., Webber, M. and Randall, W.C., Morphological organization of ganglion cells and small intensely fluorescent (SIF) cells of the canine intracardiac ganglia, *Soc. Neurosci. Abs.*, 16 (1990) 860.(Abstract)

98 Xi, X., Randall, W.C. and Wurster, R.D., Morphology of canine intracardiac ganglion cells, *J. Comp. Neurol.*, (1991) (submitted)

99 Xi, X., Thomas, J.X., Randall, W.C. and Wurster, R.D., Intracellular recordings from canine intracardiac ganglion cells, *J. Auton. Nerv. Syst.*, 32 (1991) 177-182.

CHAPTER VII

SUMMARY

1.   The physiology and morphology of neurons from the canine intracardiac ganglia innervating SA nodal region were investigated using intracellular microelectrode techniques.

2.   An intracellular HRP staining study demonstrated that canine intracardiac neurons were multipolar cells with oval-shaped soma and several processes. The principal neurons had one long axon exited the ganglion. The *intra*ganglionic neurons had a short or undistinguishable axon; all the processes were restricted in the ganglionic profile.

3.   Various numbers of SIF cells were found in different ganglia. These cells were smaller and in close proximity to non-monoaminergic neurons.

4.   Intracellular injection of depolarizing current (200 ms) evoked repetitive action potentials from the R-cells, a single action potential from the S-cells and no action potential from the N-cells. These cell types had different passive membrane properties, somata sizes and TTX and extracellular Ca^{2+} sensitivities.

5. Spontaneous activity was recorded from many intracardiac neurons. The majority of the spontaneous activity was miniature EPSP-like depolarizations which were blocked by hexamethonium and a low Ca^{2+}/ high Mg^{2+} solution but not by TTX.

6. Fast EPSPs were evoked on all type of cells by single orthodromic stimulation. The f-EPSPs were blocked by hexamethonium and low Ca^{2+}/ high Mg^{2+} solution but not by muscarinic and adrenergic antagonists. Depolarizing the membrane decreased the amplitude of the f-EPSP with a reversal potential close to -10 mV. Pressure microejection of ACh in the presence of atropine induced a depolarizing response with increased membrane conductance and a similar reversal potential.

7. Repetitive orthodromic stimulation induced s-EPSP, s-IPSP or s-IPSP followed by s-EPSP in 60% of the cells tested. The slow potentials were blocked by atropine and a low Ca^{2+}/ high Mg^{2+} solution but not by hexamethonium or adrenergic antagonists. The size of the slow potentials was increased by physostigmine.

8. The s-EPSP was blocked by the M_1 receptor antagonist, pirenzepine, but not by the M_2 receptor antagonist. The s-IPSP was not blocked by the same concentration of pirenzepine.

9.   Both the s-EPSP and bethanechol induced depolarization were associated with a slightly decreased membrane conductance and an extrapolated reversal potential near the potassium equilibrium potential.   A high extracellular potassium concentration shifted the reversal potential of bethanechol depolarization to a level close to the predicted value.

CHAPTER VIII

CONCLUSIONS

This dissertation characterizes the morphological, electrophysiological, and synaptic transmission properties of intracardiac neurons which regulate SA nodal function in the canine heart.

A heterogeneous population of neurons has been established in the canine intracardiac ganglion. Based on electrophysiological characteristics of single neurons in the ganglion, three types of cells were identified (Chapter V). Upon applying a direct depolarizing current (200 ms), repetitive firing neurons were classified as R-cells, which had a relative low resting potential, high input resistance and small soma size. This direct depolarizing current caused no action potentials in N-cells although these cells could be activated by orthodromic stimulation. The N-cells had a relative high resting potential, low input resistance and large soma size. At the onset of a direct depolarizing current to S-cell activated only one or two action potentials. Their resting potential, input resistance and soma size were in between of those of R-cells and N-cells. The S-cells and R-cells also differ from their relatively sensitivity to a sodium channel blockade (TTX) and a low Ca^{2+}/ high Mg^{2+} solution (Chapter V).

Surprisingly, intracellular HRP staining elucidated two types of neurons (Chapter IV): one with long axon extending out of the ganglion (the principal neurons) and one with all its processes restricted within the ganglion, the *intra*ganglionic neurons. These

219

two types of cells also had different mean soma sizes and dendrite lengths. Although there was no ultrastructural conformation of synapse between *intra*ganglionic neurons and other neurons, it would appear that the *intra*ganglionic neurons may operate as endogenously active neurons or ganglionic interneurons. Similar type of neurons has been previously reported in sympathetic ganglia (Chapter II). The principal neurons projected to cardiac tissue as postganglionic neurons or may terminate upon neurons in other ganglia. However, this classification scheme is based upon HRP reaction product staining which may underestimate process lengths due to inadequate transport of HRP in very fine processes. Therefore, further confirmation by electron microscopy or other techniques will be appropriate.

In light of the neurohistochemical features (Chapter IV), cells could be clearly divided into a small group of monoaminergic cells and a large group of non-monoaminergic neurons. The monoaminergic cells were SIF cells which had a significantly smaller soma size. Hence, in addition to the electrophysiological cell types, neurons could also be classified into at least three morphologically different subgroups, namely principal neurons, *intra*ganglionic neurons and SIF cells (Fig. 8-1).

The nerves between ganglia, the interganglionic nerves, appeared to be composed of various kinds of nerve fibers (Fig. 8-1). It most likely included i) the preganglionic parasympathetic axons, ii) postganglionic axons from principal neurons or *inter*ganglionic neurons (Chapter IV), iii) fine and long monoamine-containing fibers which were probably sympathetic in origin (Chapter IV), and iv) possibly cardiac sensory nerves containing calcitonin gene-related peptide (unpublished data). No postganglionic axon

FIGURE 8-1   221

ORGANIZATION OF CELLS AND NERVE FIBERS

IN CANINE INTRACARDIAC GANGLIA
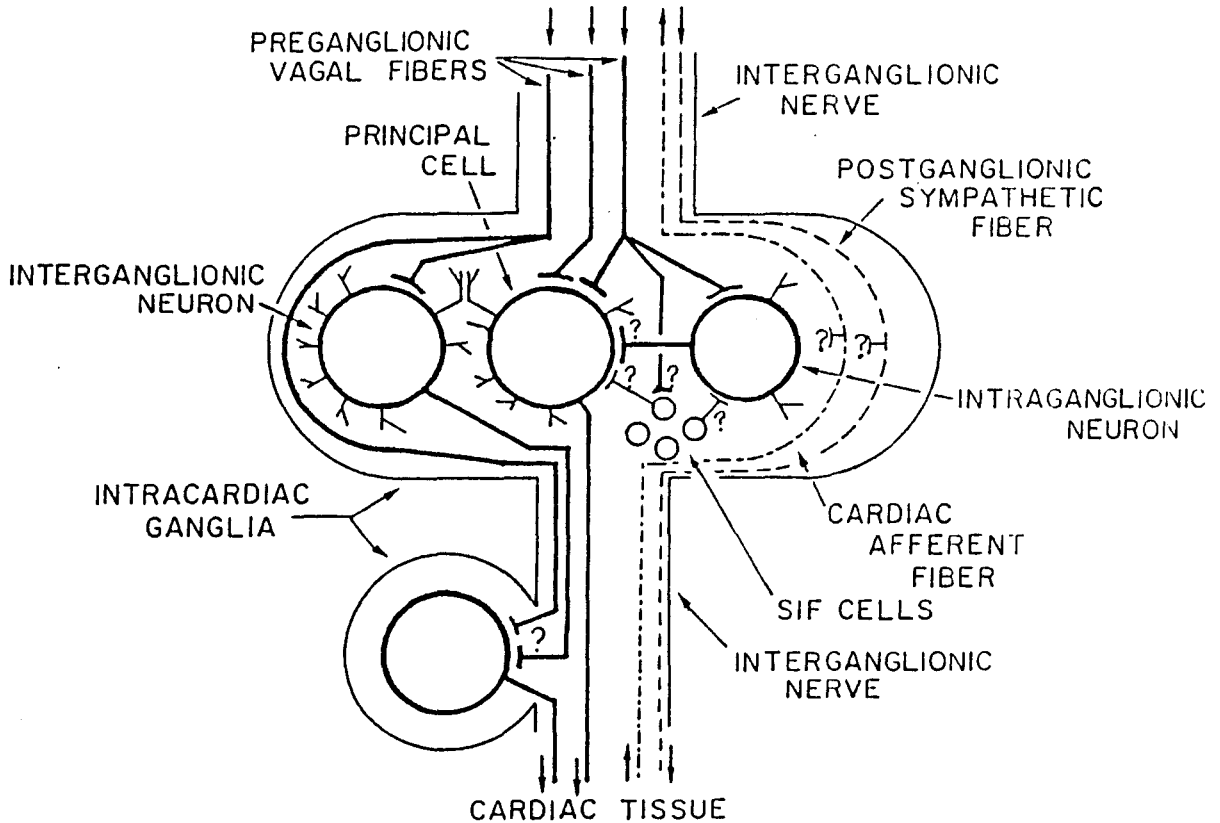
A schematic diagram summering the possible organization of cells and nerve fibers in two adjacent intracardiac ganglia. Based on the results of this dissertation, three different cell types are shown: principal neuron, *intra*ganglionic neuron and SIF cells. The *inter*ganglionic neuron can not be excluded. The preganglionic vagal fibers innervate neurons at both the ganglia. One neuron may receive innervation from different preganglionic fibers. Both sympathetic and afferent fibers are observed. The ? indicates indirect evidences for these possible synapses. See text for details.

collateral was found (Chapter IV) but some axons passed through one ganglion and synapsed with cell bodies in the neighboring ganglia. Taken together, each individual ganglion with its heterogenous cell types was connected by interganglionic nerves making a complex ganglionic plexus in the PVFP region.

In conclusion, the heterogeneous population of neurons in canine intracardiac ganglia are demonstrated electrophysiologically, morphologically, as well as histochemically. Based on above results, the possible organization of the canine intracardiac neurons is summarized schematically in Fig. 8-1. The electrophysiological cell types are morphologically different (Chapter IV). On the other hand, the morphological cell types did not correlate with the physiological classification (Chapter IV). Although a mixed population of cells would be expected in autonomic ganglia because of the complicated nature of their physiological function, the actual significance of different neuron types was not specifically examined in this dissertation.

One of the most important objectives of this dissertation was to determine the presence and mechanisms, both receptor and ionic, for the synaptic transmissions. The results show that intracardiac neurons have nicotinic and muscarinic receptors (Chapter VI). Evidences for muscarinic receptors in the canine intracardiac ganglia include: i) cholinergic responses are present after nicotinic receptor blockade; ii) neurally evoked s-EPSP can be mimicked by muscarinic receptor agonist, bethanechol; and iii) all responses are atropine-sensitive. Acetylcholine released from the nerve terminals activates both the receptors which in turn elicits different postsynaptic potentials via different ionic mechanisms. In canine intracardiac ganglia, the f-EPSP results most

likely from an increase of sodium and potassium conductance; the s-EPSP on the other hand is not due to an increase in conductance but rather a fall in membrane conductance (Chapter VI).

Generally speaking, the fast transmission in canine intracardiac ganglia (Chapter VI) resembled that in some other mammalian autonomic ganglia. Indirect evidence suggested convergence of multiple preganglionic fibers onto single neurons (Chapter VI). All cell types received orthodromic innervation and almost all cells respond to orthodromic stimulation. The possible transmitter, receptor and ionic mechanisms for the f-EPSP in these ganglia are basically indistinguishable from those for the other ganglia.

The slow excitatory and inhibitory postsynaptic potentials have been recorded in autonomic ganglia and central nervous system; but these potentials are usually believed to be associated with different neurotransmitter or with a transmitter releasing interneuron (Chapter II). In canine intracardiac ganglia, the slow potentials are blocked by atropine and a low Ca^{2+}/ high Mg^{2+} solution but not by hexamethonium or adrenergic antagonists (Chapter VI); therefore, a direct muscarinic effect of ACh on ganglionic neurons is highly suggested, which was essentially different from the bisynaptic model in sympathetic ganglia (Chapter II).

Since the evidence that the same neurotransmitter directly elicits different slow postsynaptic responses in the same cell, it is necessary to ascertain if different subtypes of muscarinic receptor exist. Experiments were performed to test the effects of M_1 receptor antagonist, pirenzepine and M_2 receptor antagonist, 4-DAMP on both neurally

evoked s-EPSP and bethanechol induced slow depolarization. The muscarinic depolarizations were completely blocked by the M_1 receptor antagonist but not by an equal concentration of the M_2 receptor antagonist (Chapter VI). Therefore, in canine intracardiac ganglia, the M_1 receptor is likely to be the subtype responsible for generating the s-EPSP. Additional experiments on s-IPSP provided further evidence that the slow muscarinic hyperpolarization on canine intracardiac ganglia is not mediated via the same subtype of muscarinic receptor as the one in muscarinic depolarization (Chapter VI). Regarding the slightly increased input resistance and a reversal potential near the equilibrium potential of potassium, the ionic mechanism underling s-EPSP and bethanechol induced depolarization appeared to be a decreased potassium conductance (Chapter VI). This ionic mechanism is different from the one underlying the fast nicotinic transmission but similar to that associated with the s-EPSP in sympathetic ganglia and the one related to the muscarinic agonist-induced depolarization in cultured guinea pig intracardiac neurons (Chapter II).

One should note that some neurons apparently responded with neither a s-EPSP nor a s-IPSP in the present experiments. Several possibilities exist: 1) the muscarinic receptors on these neurons require a higher concentration of ACh because in some cases they respond to a high concentration of bethanechol; 2) the s-EPSP and s-IPSP on these cells are temporally superimposed and completely mask each other, which was occasionally seen after physostigmine administration (Chapter VI); and 3) some of these neurons may represent a subpopulation which have no muscarinic receptors.

APPROVAL SHEET

The dissertation submitted by Xiaohe Xi has been read and approved by the following committee:

Dr. Robert D. Wurster, director
Professor, Department of Physiology
loyola University Medical Center

Dr. Walter C. Randall
Professor, Department of Physiology
Loyola University Medical Center

Dr. John X. Thomas, Jr.
Associate professor, Department of Physiology
Loyola University Medical Center

Dr. Nae J. Dun
Professor, Department of Anatomy
Medical College of Ohio

Dr. Zeljko J. Bosnjak
Professor, Department of Anesthesiology and Physiology
Medical College of Wisconsin

The final copies have been examined by the director of the dissertation and the signature which appears below verifies the fact that any necessary changes have been incorporated and that the dissertation is now given final approval by the Committee with reference to content and form.

The dissertation is therefore accepted in partial fulfillment of the requirements for the degree of Doctor of Philosophy.

June 13, 1991
Date

Robert D. Wurster, Ph.D
Director's Signature